

**Georg-August-Universität Göttingen**

**Hemispheric and region - specific effects of chronic  
stress in the rat prefrontal cortex**

Dissertation  
zur Erlangung des Doktorgrades  
der Mathematisch–naturwissenschaftlichen Fakultäten  
der Georg-August-Universität zu Göttingen

Vorgelegt von

**Claudia Perez-Cruz**

aus Mexico City, Mexico

Göttingen, 2007

**Georg - August Universität Göttingen**

**Hemispheric and region - specific effects of chronic  
stress in the rat prefrontal cortex**

Doctoral thesis  
in partial fulfillments of the requirements  
for the degree "Ph.D."  
in the Graduate Program  
Center for Systems Neuroscience  
at the Georg-August-Universität Göttingen, Faculty of Biology

Presented by

**Claudia Perez-Cruz**

Born in Mexico City, Mexico

Göttingen, 2007

**Members of Doctoral Committee:**

Thesis defense referees: Prof. Dr. Eberhard Fuchs, PD Dr. Frank Kirchhoff, PD Dr. Anastasia Stoykova

Dissertation thesis referees: JunProf. Dr. Ralf Heinrich, Prof. Dr. Walter Paulus, Prof. Dr. Hannelore Ehrenreich

Date of the thesis defense: 18. April 2007

**Declaration:**

I declare that this thesis has been written independently with no other sources and aids than required.

Claudia Perez-Cruz

Göttingen, 20.03.2007



# Table of Contents

<b>1</b>	<b>GENERAL INTRODUCTION.....</b>	<b>0</b>
1.1	STRESS CHANGES THE BRAIN.....	1
1.2	PLASTICITY OF THE BRAIN: ADAPTIVE OR MAL-ADAPTIVE CHANGES.....	2
1.3	PREFRONTAL CORTEX OF THE RAT: STRUCTURE AND FUNCTIONS.....	3
1.4	DIFFERENT ROLES OF THE PFC IN THE STRESS RESPONSE.....	4
1.5	LATERALIZED STRESS RESPONSE IN THE PREFRONTAL CORTEX.....	5
<b>2</b>	<b>HYPOTHESIS .....</b>	<b>8</b>
<b>3</b>	<b>AIM OF THE THESIS AND OBJECTIVES .....</b>	<b>8</b>
<b>4</b>	<b>PART I. DELINEATION OF BOUNDARIES IN SUB-AREAS OF THE RAT PREFRONTAL CORTEX.....</b>	<b>9</b>
	SUMMARY .....	10
4.1	RATIONALE.....	11
4.2	METHODS.....	11
4.2.1	<i>Animals.....</i>	<i>11</i>
4.2.2	<i>Perfusion and tissue preparation.....</i>	<i>11</i>
4.2.3	<i>Immunocytochemistry.....</i>	<i>12</i>
4.2.4	<i>Analysis of immunocytochemically stained sections.....</i>	<i>13</i>
4.3	RESULTS .....	14
4.4	CONCLUSION.....	15
<b>5</b>	<b>PART II. DENDRITIC MORPHOLOGY OF PYRAMIDAL NEURONS IN THE RAT PREFRONTAL CORTEX: LATERALIZED DENDRITIC REMODELING BY CHRONIC RESTRAINT STRESS.....</b>	<b>17</b>
	SUMMARY .....	18
5.1	RATIONALE.....	19
5.2	METHODS.....	20
5.2.1	<i>Animals.....</i>	<i>20</i>
5.2.2	<i>Chronic restraint stress.....</i>	<i>20</i>
5.2.3	<i>Prefrontal cortex slice preparation.....</i>	<i>21</i>
5.2.4	<i>Intracellular labeling and slice mounting.....</i>	<i>22</i>
5.2.5	<i>Neuronal reconstruction and morphometric analysis.....</i>	<i>23</i>
5.2.6	<i>Statistical analysis.....</i>	<i>25</i>
5.3	RESULTS .....	25
5.3.1	<i>Effects of chronic restraint stress on body and organ weights.....</i>	<i>25</i>
5.3.2	<i>Intracellular labeling with neurobiotin and dendritic reconstruction.....</i>	<i>26</i>
5.3.3	<i>Intrinsic morphological asymmetries.....</i>	<i>26</i>
5.3.4	<i>Stress effects on dendritic morphology.....</i>	<i>32</i>
5.4	DISCUSSION .....	35
5.5	CONCLUSIONS.....	39
<b>6</b>	<b>PART III. THE IMPACT OF THE DIURNAL LIGHT CYCLE ON THE MORPHOLOGY OF PYRAMIDAL NEURONS OF THE PRELIMBIC AREA .....</b>	<b>40</b>
6.1	EFFECTS OF STRESS APPLIED DURING THE LIGHT-PHASE OR DURING THE DARK-PHASE.....	41
	SUMMARY .....	41
6.1.1	<i>Rationale and hypothesis.....</i>	<i>42</i>
6.1.2	<i>Design and methods.....</i>	<i>43</i>
6.1.2.1	<i>Short-term restraint stress.....</i>	<i>43</i>
6.1.3	<i>Statistical analysis.....</i>	<i>46</i>
6.1.4	<i>Results.....</i>	<i>48</i>

6.1.4.1	<i>Effects of stress on body weight and adrenal glands</i> .....	48
6.1.4.2	<i>Effects of stress on the morphology of basal dendrites of pyramidal neurons in the prelimbic area</i> .....	50
6.1.4.2.1	<i>Stress during the light phase</i> .....	50
6.1.4.2.2	<i>Stress during the dark-phase</i> .....	54
6.1.5	<i>Discussion</i> .....	57
6.2	MORPHOLOGY OF BASAL DENDRITES OF PYRAMIDAL NEURONS IN THE PRELIMBIC AREA IN RELATION TO THE DIURNAL CYCLE.....	61
	SUMMARY.....	61
6.2.1	<i>Rationale</i> .....	62
6.2.2	<i>Design and methods</i> .....	62
6.2.3	<i>Results</i> .....	63
6.2.3.1	<i>Circadian variation in the morphology of pyramidal neurons in control rats</i> .....	63
6.2.3.2	<i>Circadian variation in the morphology of pyramidal neurons in stressed rats</i> .....	68
6.2.4	<i>Discussion</i> .....	68
<b>7</b>	<b>PART IV. EFFECTS OF THE ANTIDEPRESSANT TIANEPTINE ON STRESS-INDUCED MORPHOLOGICAL MODIFICATIONS IN PYRAMIDAL CELLS OF THE PRELIMBIC CORTEX</b> .....	<b>71</b>
	SUMMARY.....	72
7.1	RATIONALE.....	73
7.2	DESIGN AND METHODS.....	74
7.2.1	<i>Chronic restraint stress and antidepressant treatment</i> .....	74
7.2.2	<i>Statistical analysis</i> .....	75
7.3	RESULTS.....	75
7.3.1	<i>Intracellular labeling with neurobiotin and dendritic reconstruction</i> .....	75
7.3.2	<i>Effects of stress and tianeptine on body and organ weights</i> .....	76
7.3.3	<i>Effects of stress and tianeptine on the morphology of pyramidal neurons</i> .....	78
7.4	DISCUSSION.....	84
<b>8</b>	<b>APPENDIX</b> .....	<b>87</b>
8.1	EFFECT OF INTRAPERITONEAL INJECTION.....	88
	<i>Summary</i> .....	88
8.1.1	<i>Rationale</i> .....	89
8.1.2	<i>Design</i> .....	89
8.1.3	<i>Results</i> .....	90
8.1.3.1	<i>Effects of intraperitoneal injection on the morphology of pyramidal neurons in the infralimbic and prelimbic areas</i> .....	90
8.1.4	<i>Discussion</i> .....	92
<b>9</b>	<b>GENERAL DISCUSSION</b> .....	<b>94</b>
9.1	PREFRONTAL CORTEX AND STRESS RESPONSES.....	95
9.2	WHAT ARE THE CAUSES AND/OR FUNCTIONAL CONSEQUENCES OF THIS DENDRITIC REMODELING? 95	
9.3	SITE-SPECIFIC DENDRITIC REMODELING CAUSED BY STRESS.....	97
9.4	LATERALIZATION AND BRAIN FUNCTION.....	97
9.5	REGIONAL EFFECTS OF TIANEPTINE IN STRESS-INDUCED NEURAL PLASTICITY.....	98
<b>10</b>	<b>GENERAL SUMMARY</b> .....	<b>100</b>
<b>11</b>	<b>ACKNOWLEDGMENTS</b> .....	<b>101</b>
<b>12</b>	<b>REFERENCE LIST</b> .....	<b>103</b>
<b>13</b>	<b>CURRICULUM VITAE</b> .....	<b>118</b>

## List of Figures

---

Figure 1. Topographic map of the main efferent projections of the prefrontal cortex.....	7
Figure 2. Selection of prefrontal cortex areas in the adult rat brain. ....	14
Figure 3. Boundary delineation in the rat prefrontal cortex.....	16
Figure 4. Restraint stress procedure and intracellular labeling with neurobiotin.....	21
Figure 5. Sholl analyses of pyramidal neurons.....	24
Figure 6. Photomicrograph of an intracellular neurobiotin labeled pyramidal neuron in the prelimbic area .....	27
Figure 7. Sholl analyses of dendrites of pyramidal neurons in control and stress rats.....	29
Figure 8. Sholl analysis of pyramidal neurons in the right hemisphere of control and stressed rats .....	34
Figure 9. Drawings of representative neurons from the prefrontal cortex.....	36
Figure 10. Photomicrograph of a Golgi-stained neuron in layer III of the prelimbic area of a control rat..	46
Figure 11. Sholl analyses of basal dendrites and quantification of spines.....	47
Figure 12. Effects of seven days of restraint stress on body and adrenal glands' weight.....	49
Figure 13. Basal dendritic length and spine density in pyramidal neurons in the prelimbic area.....	51
Figure 14. Number of intersections of basal dendrites in rats stressed during the light-phase and controls .....	52
Figure 15. Length of basal dendrites of distinct branch orders in the prelimbic area in control and stressed rats.....	53
Figure 16. Number of intersections of basal dendrites in rats stressed during the dark-phase and controls .....	56
Figure 17. Simplified drawing illustrating the morphological remodeling of basal dendrites on pyramidal neurons caused by chronic stress .....	60
Figure 18. Impact of the diurnal cycle on dendritic length and spine density in control rats.....	64
Figure 19. Diurnal variations in the total number of intersections in basal dendrites of control rats.....	65
Figure 20. Impact of the diurnal cycle on dendritic length and spine density in stressed rats.....	66
Figure 21 Diurnal variations in the total number of intersections basal dendrites of stressed rats .....	67
Figure 22. Effects of tianeptine on body, adrenal and thymus weight in stressed and control rats .....	77
Figure 23. Effects of stress and tianeptine on the total dendritic length of basal and apical dendrites of the prelimbic area .....	80
Figure 24. Effects of stress and tianeptine on the dendritic distribution of pyramidal neurons in the prelimbic area .....	81
Figure 25 Length of dendrites of distinct branch orders in basal and apical dendrites of pyramidal neurons in the prelimbic cortex.....	82
Figure 26. Effect of daily handling or intraperitoneal injections on the dendritic length of infralimbic and prelimbic areas.....	91

## List of Tables

---

Table 1. Morphometric data of control and stressed rats .....	30
Table 2 Number of branching points and branches in control and stressed rats .....	31
Table 3. Morphometric data of pyramidal neurons in the prelimbic area of control and stressed rats treated with tianeptine (10 mg/kg/ml) or vehicle. ....	83

# **1 General introduction**



## 1.1 Stress changes the brain

Challenging or stressful situations require immediate individual physiological and behavioral responses in order to handle or even to survive threatening events. The resulting stress response requires the activation of several organs in order to alert the body for flight or fight (Selye, 1973). Even though these immediate responses are conducted to survive, repetitive stressful experiences might have harmful effects on the body, on the brain and as a consequence, on the behavior. Glucocorticoids and catecholamines are the key mediators of the stress response and released upon stimulation of the hypothalamus-pituitary-adrenal (HPA) axis and the sympathetic nervous system (Koolhaas et al., 1997). These neuroendocrine substances can activate different organs in order to respond to stressful events, but under chronic exposure they may have deleterious effects (Chrousos, 1998). For example, chronic stress exposure results in reduced neurogenesis in the dentate gyrus of the hippocampal formation (Gould and Tanapat, 1999; Gould et al., 1997; Czeh et al., 2000) retraction of dendrites in pyramidal neurons in the hippocampal cornu ammonis area CA3 and the prefrontal cortex (PFC) (Magarinos and McEwen, 1995a; Watanabe et al., 1992c; Radley et al., 2004, 2006; Cook and Wellman, 2004). The increased level of corticosterone and the structural reorganization of neurons in different brain areas produced by stress have been linked with impairments in memory and learning (Liston et al., 2006; Miracle et al., 2006 ; Radley and Morrison, 2005). Studies in humans revealed a strong correlation between the onset of major depression and previous stressful life experiences (Kessler, 1997). Moreover, in clinical studies, structural brain modifications in depressed patients are similar that those found in animal models of chronic stress (such as decreased volume or neuronal size in hippocampus and PFC) (Bremner et al., 2000; Rajkowska et al., 1999). Therefore, repeated or long-lasting stressors might cause physiological and functional impairments in the mammalian brain, resulting in mal-adaptive behaviors or even disease (i.e. depression or post-traumatic stress disorder, PTSD). Studying the consequences of stress on the brain's structure and function might help to understand the circuitry involved in the stress response and might help to create better psychological, social and medical strategies to avoid pathological conditions commonly triggered by chronic stress.

## 1.2 Plasticity of the brain: adaptive or mal-adaptive changes

As mentioned above, chronic restraint stress causes retraction of apical dendrites in the CA3 region of the hippocampus (Magarinos and McEwen, 1995a; Watanabe et al., 1992c) and in the PFC (Cook and Wellman, 2004; Radley et al., 2004). These structural modifications can be mimicked by chronic administration of the glucocorticoid hormone corticosterone (Watanabe et al., 1992b; Wellman, 2001). Corticosterone (rats) and cortisol (man) binds to two receptor types, the glucocorticoid (GR) and the mineralocorticoid receptor (MR). The MRs have restricted localization in limbic brain regions, such as the hippocampus, septal and amygdala nuclei but also in motor nuclei of the brainstem. By contrast, GRs are much widely distributed, and are found both in neurons and glial cells (see Joels, 2001). These two receptors do not only differ with respect to distribution pattern, but also in their binding properties. The MRs bind corticosterone *in vivo* with a 10-fold higher affinity than GRs, and consequently MRs are substantially occupied at basal levels of hormone, while the majority of GRs only become occupied at stress levels of circulating hormone (de Kloet et al., 1998). When activated, MR and GR are translocated to the nucleus. Depending on the amount of corticosteroid receptors that are activated by a stressful stimulus and its duration of its presence, different genes are regulated (see Meijer, 2006).

The mechanism of action of glucocorticoids to induce plastic changes in the brain has been linked to the excitatory actions of glutamate. To illustrate this theory, Stein-Behrens and colleagues have demonstrated that corticosterone administration causes an increase in extracellular levels of glutamate in the PFC and hippocampus (Stein-Behrens et al., 1994). Similar increases were found in rats exposed to stressful events (Moghaddam, 1993; Bagley and Moghaddam, 1997; Abraham et al., 1998). Furthermore, by blocking NMDA receptors the stress-induced dendritic remodeling in dendrites of CA3 pyramidal neurons can be abolished (Magarinos and McEwen, 1995b). Therefore, the structural remodeling observed in CA3 and PFC pyramidal neurons after chronic stress have been proposed to be an adaptive mechanism to avoid neuronal over-excitation by increased  $\text{Ca}^{2+}$  levels induced by glutamate increments after stressful experiences (Radley and Morrison, 2005).

There is an important difference between the hippocampal formation and the PFC regarding dendritic remodeling. Structural changes in hippocampal neurons can be detected only after three-weeks of daily stress, but not at earlier time points (Wood et al.,

2004; Magarinos and McEwen, 2000). In contrast, pyramidal cells of the PFC show structural remodeling even after a single stress episode (Izquierdo et al., 2006). Therefore, the PFC seems to react faster to stressful events, reflecting its important modulatory role to other cortical and subcortical brain areas (Vertes, 2004). On the other hand, this dendritic retraction in the hippocampus and in the PFC can be reversed after termination of stress (Conrad et al., 1999; Radley et al., 2005). Thus, plastic changes in these brain regions seem to be necessary in order to activate and terminate distinct responses to environmental challenges, as adaptive mechanism. When stressors are long-lasting or repeated consecutively, the potential cellular plasticity (and reversibility) might be disrupted leading to an impaired ability to cope with the stressors and producing irreversible damage to several brain circuitries or a loss of homeostasis. Hence, irreversible plastic changes induced by chronic stress can be regarded as maladaptive changes.

### **1.3 Prefrontal cortex of the rat: structure and functions**

The prefrontal cortex in the mammalian brain is defined as a cortical area that receives reciprocal projections from the mediodorsal thalamic nuclei (Uylings et al., 2003). The medial PFC of the rat is mainly subdivided into three cytoarchitectonic sub-areas: infralimbic (IL), prelimbic (PL) and anterior cingulate cortex (ACx) (Krettek and Price, 1977; Ray and Price, 1992). Each of these sub-areas has specific cortical and sub-cortical connections (Vertes, 2004) and distinct physiological functions (Heidbreder and Groenewegen, 2003). The dorsal PFC consisting of the ACx has been linked to motor behavior, while the ventral region (IL and PL) has been associated with diverse emotional, cognitive and mnemonic processes (Heidbreder and Groenewegen, 2003). It has been suggested that the ACx of the rat is homologous to the supplementary motor and premotor cortices of non-human primates (Neafsey et al., 1986; Reep et al., 1990; Conde et al., 1995). In contrast, more ventral regions of the PFC are linked to the limbic system (Heidbreder and Groenewegen, 2003). For example, lesions in the rat PL produce deficits in delayed response tasks (Dalley et al., 2004). Similar deficits are caused by lesioning the PL in non-human primates (Groenewegen and Uylings, 2000), associating the PL with cognitive processes. On the other hand, stimulation of the IL results in changes in respiration, gastrointestinal motility, heart rate and blood pressure (Terreberry and Neafsey, 1987). The IL is therefore regarded as a visceromotor center (Neafsey, 1990). Anatomical studies have confirmed and corroborated these functional

specializations of the different regions of the PFC, where the IL projects mainly to autonomic/visceral-related sites, PL projects primarily to limbic regions which are involved in cognition, and ACx projects to motor centers (Vertes, 2004 ;Gabbott et al., 2005) (see Fig 1).

#### **1.4 Different roles of the PFC in the stress response**

The PFC receives direct dopaminergic and noradrenergic projections from the ventral tegmental area and from the locus coeruleus, respectively (van Eden et al., 1987) (see Fig.1). These two systems are highly activated by stress (Jedema and Moghaddam, 1994; Kitayama et al., 1997) causing an immediate increase in the concentration of both dopamine and noradrenalin in the PFC (Sullivan and Gratton, 1998; Jedema and Moghaddam, 1994). On the other hand, the PFC is rich in corticosteroid receptors (Diorio et al., 1993) which become activated during stress (Figueiredo et al., 2003). Electrical stimulation of the PFC altered plasma levels of corticosterone (Feldman and Conforti, 1985) and lesioning the ACx increased plasma levels of corticosterone and ACTH in response to acute stress (Diorio et al., 1993). This suggests that the PFC plays an important role in the regulation of the HPA axis acting as a negative feedback element for the termination of stress responses (Diorio et al., 1993; Sullivan and Gratton, 1999).

As mentioned above, there are anatomical and functional differences between these three PFC sub-areas. These differences are also reflected in their specific roles in stress reactions. For example, lesion studies have shown that after acute stress, the ventral (Sullivan and Gratton, 1999) and the dorsal PFC (Diorio et al., 1993) regulate the release of corticosterone and ACTH in an opposite way (i.e. ACx lesions increased but IL lesions decreased corticosterone and ACTH levels). In addition, specific behavioral responses such as diminished fear reactivity (Lacroix et al., 2000) were observed after lesions in the IL (Fryszak and Neafsey, 1991), whereas increased fear reactivity is detected following lesions in the PL/ACx (Morgan and LeDoux, 1995). Furthermore, stimulation of the IL elicited sympathetic responses (Owens and Verberne, 2001), such as an increase in blood pressure (al Maskati and Zbrozyna, 1989) and elevation of corticosterone levels (Feldman and Conforti, 1985). In contrast, stimulation of PL/ACx resulted in parasympathetic responses and hypotension in rats (Powell et al., 1994). On the other hand, it has been proposed that short-term stress affects primarily ventral regions of the PFC (i.e. IL) (Izquierdo et al., 2006) while chronic stress leads to the

recruitment of more dorsal regions (i.e. PL and ACx) (Cook and Wellman, 2004;Radley et al., 2004;Radley et al., 2006). Therefore, analyzing the morphological consequences of stress in these three different areas of the PFC would help to understand the functional and anatomical differences between these brain regions.

### **1.5 Lateralized stress response in the prefrontal cortex**

Besides the anatomical and functional differences in the PFC, the frontal cortex has hemisphere-dependent functions. The idea that cortical areas are lateralized is well established, mainly for sensory and motor regions, but it is less accepted for other cortical locations (see Hutsler and Galuske, 2003). Broca pioneered this era with his first pronouncement of the frontal lobe specialization in language function specifically on the left hemisphere (see Berker et al., 1986). Since then, functional and anatomical studies on language and speech systems found evidence for a strong lateralization (see Davidson et al., 2000). Structural differences between hemispheres have also been described in language-associated cortical regions. Seldon reported quantitative differences in auditory regions, such as longer basal dendrites and increased branching in pyramidal cells from layer III on the left hemisphere (Seldon, 1981, 1982). In addition, hemispheric differences in size and number of neurons were described for the same area (Hutsler and Gazzaniga, 1996). Recently, Uylings et al. (2006) described an asymmetry in the volume and total number of neurons in Broca's area BA 44 with a left-over-right asymmetry in both male and female human brains (Uylings et al., 2006). However, up to now there are no studies comparing the morphology of pyramidal neurons in the left with those in the right hemispheres of the rat PFC.

Higher brain functions such as emotion (in part localized in the PFC) also have a strong asymmetric regulation. A wide range of human studies has suggested that the right hemisphere plays a prominent role in processes related to emotional states (Davidson et al., 2000). Patients with stroke in the left frontal lobe showed a disproportionate incidence of depression or catastrophic reactions, while comparable damages to the right frontal lobe produced indifference, or mania (Robinson et al., 1984). Furthermore, the right hemisphere is dominant in the sympathetic component of cardiovascular control (Yoon et al., 1997; Hilz et al., 2001), and right-biased asymmetries in frontal activity are associated with very high levels of plasma cortisol and fearful and defensive behavior (Kalin et al., 1998).

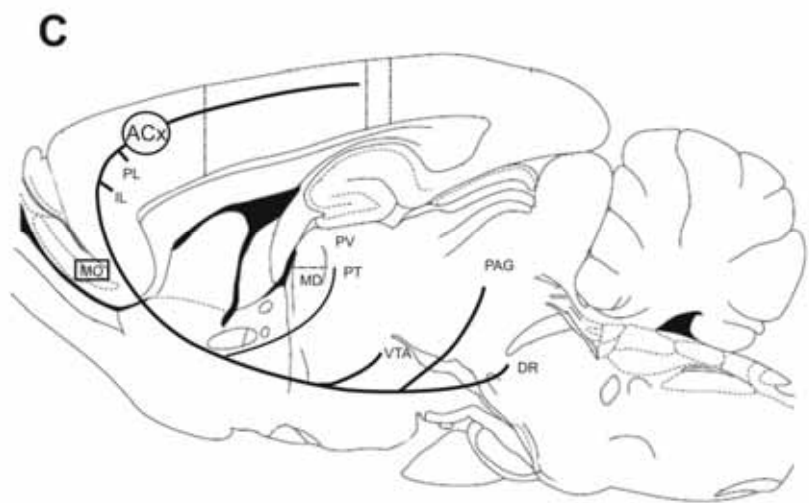
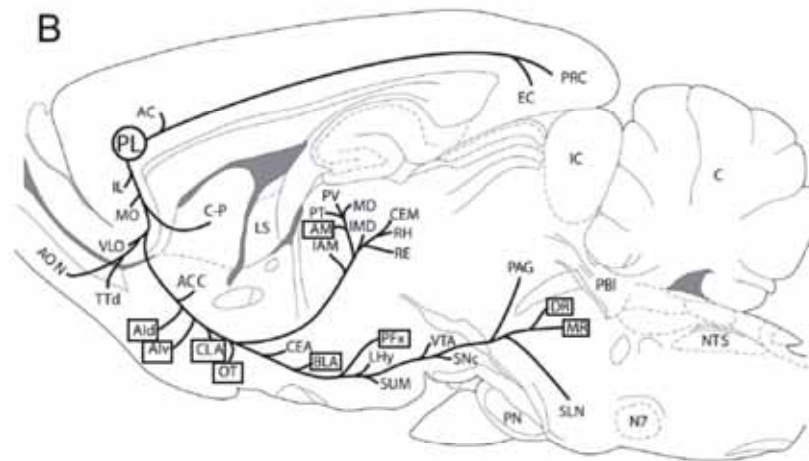
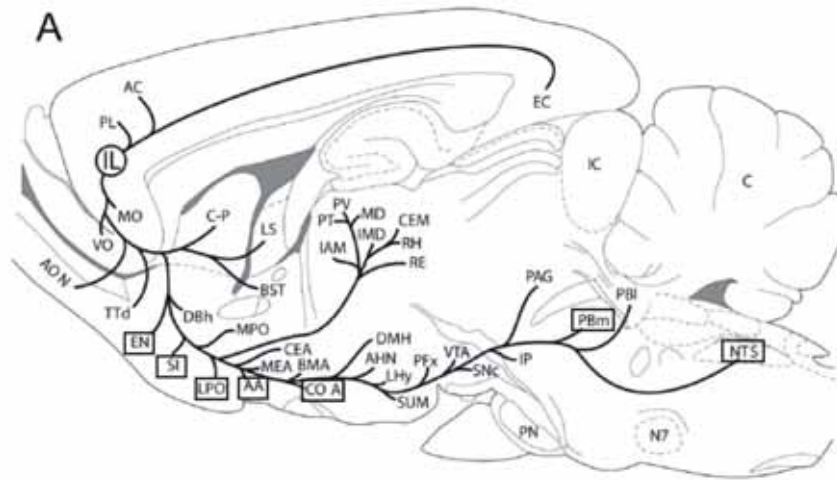


### Figure 1. Topographic map of the main efferent projections of the prefrontal cortex

Schematic sagittal sections summarizing the main efferent projection of the IL (A), PL (B) and ACx (C). Note that IL projections are much more widespread than PL projections, particularly to the basal forebrain, amygdala and hypothalamus. Abbreviations: AA, anterior area of amygdala; AHN, anterior nucleus of hypothalamus; AI,d,v, agranular insular cortex, dorsal, ventral divisions; AM, anteromedial nucleus of thalamus; AON, anterior olfactory nucleus; BMA, basomedial nucleus of amygdala; C, cerebellum; CEM, central medial nucleus of thalamus; CLA, claustrum; COA, cortical nucleus of amygdala; C-P, caudate/putamen; DBh, nucleus of the diagonal band, horizontal limb; DMH, dorsomedial nucleus of hypothalamus; DR, dorsal raphe nucleus; EN, endopiriform nucleus; IAM, interanteromedial nucleus of thalamus; IC, inferior colliculus; IMD, intermediodorsal nucleus of thalamus; IP, interpeduncular nucleus; LHy, lateral hypothalamic area; LPO, lateral preoptic area; LS, lateral septal nucleus; MEA, medial nucleus of amygdala; MO, medial orbital cortex; MPO, medial preoptic area; MR, median raphe nucleus; N7, facial nucleus; OT, olfactory tubercle; PBm,l, parabrachial nucleus, medial and lateral divisions; PFx, perifornical region of hypothalamus; PN, nucleus of pons; PRC, perirhinal cortex; RH, rhomboid nucleus of thalamus; SI, substantia innominata; SLN, suprallemniscal nucleus (B9); SUM, supramammillary nucleus; TTd, taenia tecta, dorsal part; VLO, ventral lateral orbital cortex; VO, ventral orbital cortex. Sub-area specific efferent projecting sties are highlighted with a rectangle. Adapted from Vertes (2004).

Animal studies have also found a strong correlation between right PFC activation and increased stress responses (see Sullivan, 2004). For example, uncontrollable foot shock (Carlson et al., 1993) or novelty stress (Berridge et al., 1999) resulted in a higher dopamine turnover in the right PFC, while anxiolytic responses were observed after lesioning the right IL (Sullivan and Gratton, 2002). In addition, right-side lesions reduced gastric ulcer formation induced by cold-restraint stress (Sullivan and Gratton, 1999). Therefore, taking into account previous studies on the important role of the right hemisphere in the stress response, the present morphological analysis coincides with the hypothesis of lateralized roles of the PFC in stress and possible in other neurological disorders.

## **2 Hypothesis**

On the basis of the findings on stress-induced morphological changes in the hippocampus, the hypothesis of the present work was that chronic restraint stress will induce morphological changes in pyramidal neurons of the rat prefrontal cortex in a hemispheric and region-specific manner.

## **3 Aim of the thesis and objectives**

The aim of the present thesis is to analyze whether the morphology of dendrites of pyramidal neurons in the rat prefrontal cortex is affected by stress in a hemisphere-specific manner.

In order to address this general objective the project consists of the following parts:

- I. Definition of the sub-areas of the rat prefrontal cortex by the use of different antibodies. The resulting map was later used to localize pyramidal neurons in specific regions and layers of the prefrontal cortex for the subsequent studies.
- II. The chronic restraint model, a validated stress paradigm to induce dendritic remodeling in the hippocampus, was used to induce morphological changes in the three sub-areas of the prefrontal cortex with a left and right discrimination.
- III. The short-term chronic restraint model, as a validated stress model to induce changes in the prefrontal cortex, was used to analyze changes in spine density as an indirect measurement of functional plasticity induced by stress applied during the light or the dark phase.
- IV. The use of an antidepressant in order to assess the beneficial effects of the drug on the morphological modifications induced by stress in pyramidal neurons of the prefrontal cortex.



## **4 Part I. Delineation of boundaries in sub-areas of the rat prefrontal cortex**

## Summary

The medial prefrontal cortex (PFC) of the rat has been subdivided into three areas based in anatomical and functional differences. In most studies, PFC area delineation is based on the use of Nissl staining; however, superficial layers in infralimbic and prelimbic area are not clearly discernible. The aim of the present study was to develop a reliable method to delineate cytoarchitectonically the boundaries between the infralimbic, prelimbic and anterior cingulated areas of the PFC by the use of antibodies against parvalbumin, SMI-32, and NeuN.

The marker for SMI-32 labeled almost exclusively neurofilaments in ACx, making it easy to recognize the border with PL. The antibody against parvalbumin, which labels a subpopulation of cortical interneurons was suitable for recognizing the boundaries between IL, PL and ACx. The NeuN antibody proved to be better than conventional stainings (i.e. Nissl staining) at defining cortical layers in IL and PL, but was not suitable to clearly distinguish layers in ACx. In this way, a PFC map was created which could be used for the exact localization of pyramidal neurons in subsequent experiments.

## 4.1 Rationale

The most common immunohistochemistry technique to define borders in the brain is the Nissl staining (Paxinos and Watson, 1997). Nissl dyes allow detecting the soma of neurons and glial cells, but not dendritic processes. The border delineation of different sub-areas of the prefrontal cortex (PFC) based in the use of Nissl staining does not show clear boundaries between IL and PL and no layers can be defined in these two ventral areas (Cerqueira et al., 2005b; Gabbott et al., 1997). In order to obtain an exact map of areas and layers of the PFC, different antibodies were used in order to stain the rat PFC. The pattern obtained (boundary map) will be used in the subsequent experiments to clearly localize labeled pyramidal cells in specific layers and areas of the PFC. It was hypothesized that based in the anatomical and functional differences between these PFC areas, neurons localized in PL may undergo different modifications compared to IL or ACx neurons, therefore it is important to discriminate between sub-areas cell localization in the following studies (see Part II, III and IV).

## 4.2 Methods

### 4.2.1 Animals

Adult male Sprague Dawley rats (Harlan-Winkelmann, Borchon, Germany) were housed in groups of three animals per cage with food and water *ad libitum*. Animals were maintained in temperature-controlled rooms ( $21 \pm 1$  °C.) with a light/dark cycle of 12 h on, 12 h off (lights on at 07:00 h). All animal experiments were performed in accordance with the European Communities Council Directive of November 24, 1986 (86/EEC), and were approved by the Government of Lower Saxony, Germany. The minimum number of animals required to obtain consistent data was used.

### 4.2.2 Perfusion and tissue preparation

Male rats ( $n = 5$ , weighing 220–250 g) were killed by intraperitoneal administration of an overdose of ketamine (50 mg/kg body weight; Ketavet<sup>®</sup>, Pharmacia & Upjohn, Erlangen, Germany), xylazine (10 mg/kg body weight; Rompun<sup>®</sup>, Bayer Leverkusen, Germany) and atropine (0.1 mg/kg body weight; WDT, Hannover, Germany). The descending aorta was clamped and the animals were transcardially perfused with cold 0.9% NaCl for five minutes, followed by cold 4% paraformaldehyde in

0.1 M phosphate buffer (PB) at pH 7.2 for 22 minutes. Development of postperfusion artifacts (Cammermeyer, 1978) was prevented by postfixing heads in fresh fixative at 4°C. The following day, the brains were gently removed and stored overnight in 0.1 M PB at 4°C. Brains were cryoprotected by immersion in 2% DMSO and 20% glycerol in 0.125 M phosphate-buffered saline (PBS) at 4°C.

The brains were then cut into blocks containing the entire PFC, frozen on dry ice and stored at -80°C before serial cryosectioning at a section thickness of 50 µm. A stereotaxic atlas of the rat brain (Paxinos and Watson, 1997) was used during the dissecting and cryosectioning procedures. A small hole in the left striatum was made with a thin needle to differentiate the left from the right hemispheres. Eight to ten complete coronal series were collected and stored in 0.1 M PBS until staining (see Fig. 2).

### **4.2.3 Immunocytochemistry**

Pilot experiments were performed to determine the optimal antibody concentration and incubation times for immunocytochemistry. Free-floating sections were washed in 0.1 M PBS and then treated with 0.5% H<sub>2</sub>O<sub>2</sub> for 30 min. After washing, nonspecific binding of antibodies was blocked by incubating the sections for one hour in 5% normal goat serum (NGS; DAKO, Glostrup, Denmark) in 0.1 M PBS containing 0.25% Triton X-100. The sections were subsequently incubated for 48 hours at 4°C with the primary antibodies, neurofilament SMI-32 (mouse-anti-SMI-32, Sigma Aldrich), parvalbumin (mouse-anti-PV; Sigma Aldrich) and neuronal-nuclei NeuN (mouse-anti-NeuN, Sigma Aldrich) at working dilutions of 1:1000, 1:2000, and 1:500, respectively, in PBS containing Triton X-100 (0.5% for SMI-32, 0.25% for parvalbumin and NeuN), sodium azide (0.1% for SMI-32, 0.05% for parvalbumin and NeuN), and NGS (3% for SMI-32 and NeuN, 1% for parvalbumin).

Following incubation, sections were thoroughly washed with 0.1 M PBS and incubated with biotinylated goat anti-mouse antibody (DAKO) diluted 1:200 in 0.1 M PBS with 3% NGS and 0.5% Triton X-100, for 1.5 hours, followed by washing in 0.1 M PBS. The sections were then incubated with 1:200 horseradish peroxidase-conjugated streptavidin (DAKO) in 0.1 M PBS with 3% NGS and 0.5% Triton X-100 for 1.5 hours. After washing, sections were stained with a DAB kit (Vector Laboratories, Burlingame, CA, USA), which uses 3,3'-diaminobenzidine (DAB) as chromogen. Staining time in DAB was 8–10 min for all sections; the reaction was stopped by washing the sections in 0.1 M

PBS. Sections were mounted on glass slides in 0.1% gelatin and dried overnight at 37°C, after which they were cleared in xylene for 30 min. and finally coverslipped with Eukitt (Kindler, Freiburg, Germany). A series of adjacent coronal sections was also mounted on glass slides, dried overnight at room temperature, and stained with cresyl violet to obtain a clear comparison with the immunocytochemical images.

#### **4.2.4 Analysis of immunocytochemically stained sections**

Areal and laminar staining patterns were examined microscopically. Coronal sections were analyzed and photographed using a Zeiss Axiophot II photomicroscope (Carl Zeiss, Germany) at magnifications of 2.5×, 10× and 20×. The prefrontal cortical areas were identified and their boundaries or transition zones were outlined on photomicrographs of the sections, and a contour pattern (delineating IL, PL and ACx sub-areas) was drawn and stored as a Corel Draw file. Localization of intracellularly filled cells (see below) was then corroborated by overlapping a picture of a filled cell with a picture of a boundary contour pattern closest to the same region (anterior or posterior PFC). SMI-32, parvalbumin and NeuN stained sections were compared to ensure that the defined areas coincided, and were treated identically for the methods and measurements described below. Layers I, II, III, V and VI in PFC subfields were identified using the description and terminology in Paxinos and Watson (1997) atlas of the rat brain and its companion text book (Zilles and Wree, 1995), and boundaries definition made by Gabbott et al. (1997).

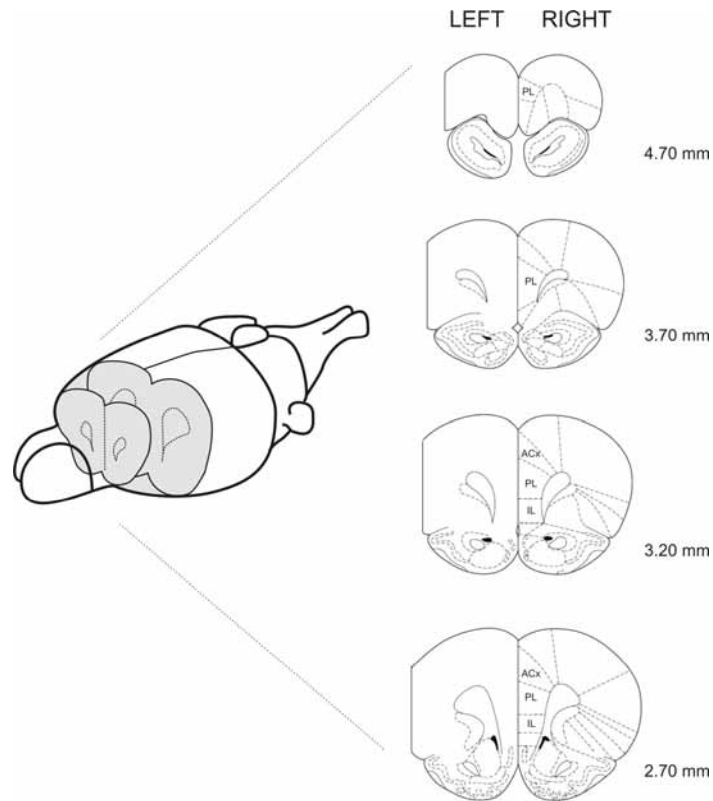


### Figure 2. Selection of prefrontal cortex areas in the adult rat brain

Coronal sections (50  $\mu\text{m}$ ) were obtained from the prefrontal cortex (PFC) by cryosectioning. A sagittal cut on the left side of the brain was made in order to further differentiate between hemispheres. Ventral (4.70 – 2.70 mm from Bregma) and dorsal (2.20 – 1.40 mm from Bregma) sections were stained by the use of different antibodies. A contour map was created in order to delineate borders between sub-areas of the PFC (IL: infralimbic; PL: prelimbic; ACx: anterior cingulate cortex) and layer definition using the description of PFC in Paxinos and Watson (1997)

## 4.3 Results

According to previous descriptions, the rat PFC can be divided into three sub-areas: IL, PL and ACx. As a basis for the reliable localization of neurobiotin labeled pyramidal neurons in the present thesis, the boundaries of these sub-areas were visualized by using specific antibodies. The three sub-areas that were reliably found at the same location in all investigated brains were defined as showing differential staining patterns with at least two staining methods.

Immunocytochemical staining with SMI-32 antibody gave a staining pattern that differentiates PL from ACx, and ACx from the premotor cortex (FR) in dorsal regions of the PFC (Figure 3A). In the PL, the SMI-32 antibody labeled layers III and V. This pattern became lighter and narrower in the ACx, where layer III was lightly stained whereas layer V was darker and broader. ACx could be distinguished from the premotor

cortex because in the later, the deep layers were intensely labeled by the SMI-32 antibody (Figure 3A, lower panel).

Parvalbumin proved to be a good marker to distinguish all PFC sub-areas and their respective layers. In IL, layer II was only lightly stained, layer III was slightly darker and layer V showed a pronounced staining. In the PL, layer II was distinctly stained by the PV antibody and layer III appeared wider than in the IL. The strong staining of layer V observed in the IL gradually disappeared in the PL. In the ACx, all layers had more parvalbumin-immunoreactive cells compared to PL. Layer II in ACx showed darker staining compared to the PL (Figure 3B).

Immunoreactivity for NeuN provided a boundary between IL and PL, and a clearly layered pattern in all PFC sub-areas with pronounced staining of layer II (Figure 3C). The IL was distinguished by a wide layer I and by densely packed cells in layers II. Compared to IL, the PL had a lighter layer III, and a broader layer V. In ACx, layer V was again broader than in the PL (Figure 3C). Using Nissl dyes, layer I can be clearly distinguished, however, it is difficult to distinguish the other cortical layers and to detect borders between PFC sub-areas (Figure 3D).

By comparing the location of each neurobiotin filled layer III neuron (see below) with the boundary patterns described above, it was possible to accurately localize the neurons in a defined sub-area-specific location.

#### **4.4 Conclusion**

In aim of this study was to identify the boundaries between the three PFC sub-areas. The border between PL and ACx could be visualized with the SMI-32 antibody which labels neurofilaments (Sternberger and Sternberger, 1983). The parvalbumin antibody, which stains a subpopulation of cortical interneurons (Gabbott and Bacon, 1996), strongly stained layer V and was suitable for recognizing the boundaries between IL and PL. The antibody against NeuN, a selective marker for neurons (Mullen et al., 1992), proved to be better than conventional Nissl staining at defining cortical layers II and III. Delineation of the sub-area boundaries and of cortical layers is a prerequisite for the exact localization of pyramidal neurons within the rat PFC. Exact localization of pyramidal neurons in specific layer and sub-areas of the PFC, was a prerequisite for subsequent experiments.

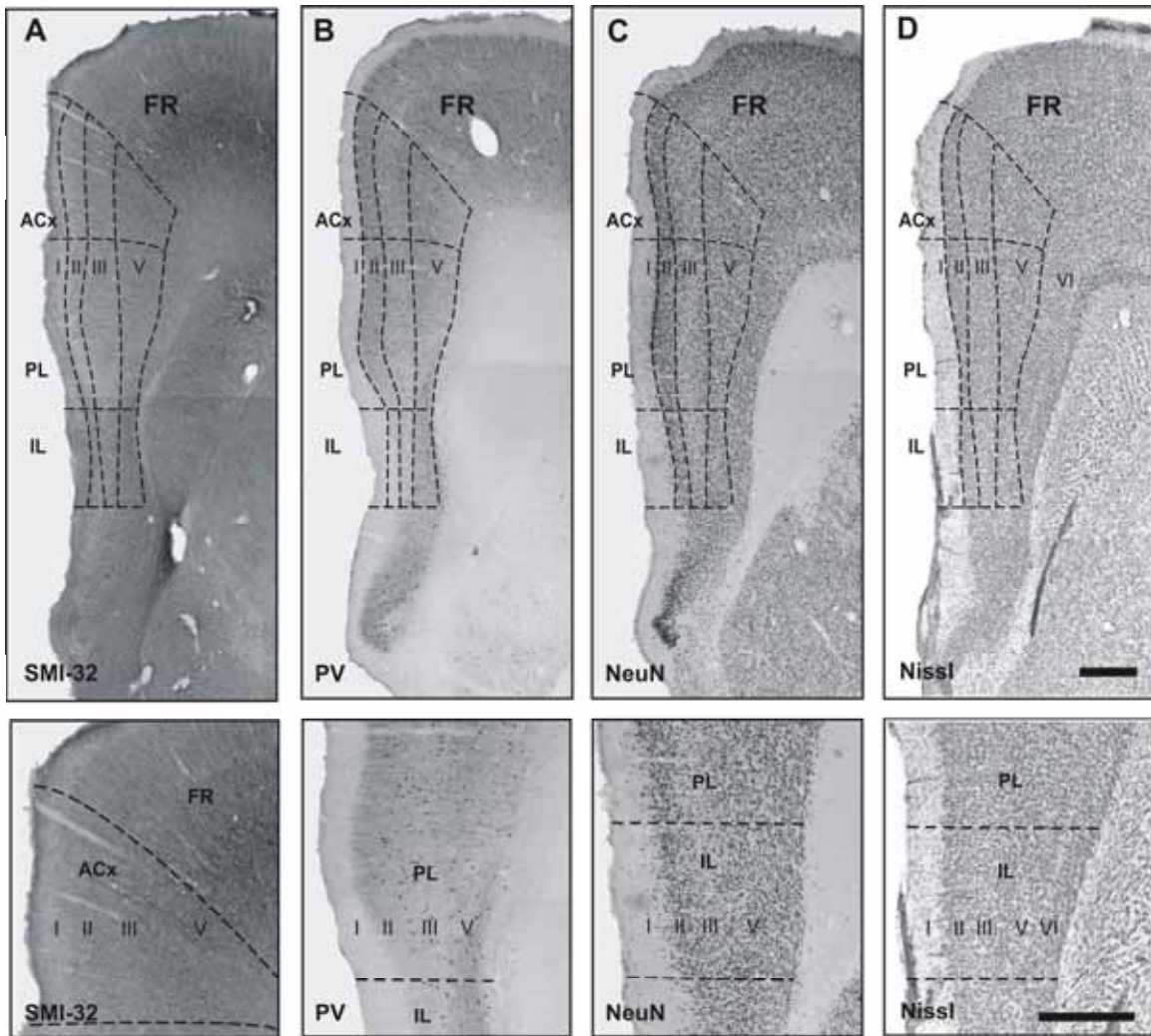


**Figure 3. Boundary delineation in the rat prefrontal cortex**

Boundaries of the PFC sub-areas in the rat visualized with antibodies. In the anterior PFC (3.70 -2.20 mm from Bregma), three sub-areas can be distinguished: IL, PL and ACx. Pictures in the lower panels show the same sections at higher magnification. **(A)** Staining with the SMI-32 antibody shows the border between PL and ACx, and between ACx and premotor cortex (FR). **(B)** Parvalbumin (PV) is a good marker to distinguish IL from PL. The PV antibody stains neurons in layer V and in the other cortical layers in all three sub-areas. **(C)** The NeuN antibody strongly labels layer II, and also layers I-V can be easily distinguished with this antibody. **(D)** With Nissl staining, it is possible to distinguish layer I but not the other cortical layers. Scale bars: 500  $\mu$ m.



**5 Part II. Dendritic morphology of  
pyramidal neurons in the rat prefrontal  
cortex: Lateralized dendritic remodeling by  
chronic restraint stress**

Perez-Cruz C, Muller-Keuker J, Heilbronner U, Fuchs E, Flugge G (2007)  
Neural Plasticity (*in press*)

## Summary

Previous studies demonstrated an important role of the rat prefrontal cortex (PFC) in the stress response that is abolished by lesioning the infralimbic and prelimbic cortices, but not the anterior cingulate cortex. This study investigated whether there might be morphological differences between pyramidal neurons in these PFC sub-areas and between the hemispheres, and whether chronic restraint stress changes pyramidal cell morphology. Using a whole-cell patch-clamp method with 400- $\mu\text{m}$  thick slices from the PFC 139 pyramidal neurons were filled in layer III of the infralimbic, the prelimbic and the anterior cingulate cortex with neurobiotin. Cells were three-dimensionally reconstructed and the length of their apical and basal dendrites, as well as the number of dendritic branches of distinct branch orders was determined.

In control rats, pyramidal neurons of infralimbic and prelimbic showed inter-hemispheric differences in the length of apical dendrites in middle and distal distances from the soma. No hemispheric differences were observed in anterior cingulate cortex. Stress abolished the intrinsic asymmetries by reducing the total length of apical dendrites selectively in the right hemisphere of the infralimbic and prelimbic sub-areas. In the anterior cingulate cortex, however, chronic stress reduced apical dendrites on the left-hemisphere. These chronic stress-induced region- and hemisphere-specific changes may be correlated with the specialized functions of PFC sub-areas in stress-related pathologies, and provide additional support for previous studies of stress-dependent activation of the right PFC.

## 5.1 Rationale

The prefrontal cortex (PFC) exhibits a hemispheric specialization with respect to its functional role in the integration of affective states suggesting that the right PFC is important in eliciting stress responses (see Sullivan, 2004). Uncontrollable foot shock (Carlson et al., 1993) or novelty stress (Berridge et al., 1999) resulted in a higher dopamine turnover selectively in the right PFC. The PFC has been subdivided into three main cytoarchitectonic sub-areas: Infralimbic (IL), prelimbic (PL) and anterior cingulate cortex (ACx) (Krettek and Price, 1977; Ray and Price, 1992). Each of these sub-areas has specific cortical and subcortical connections (Vertes, 2004) and distinct physiological functions. Lesion studies have shown that after acute stress, ventral (IL/PL) (Sullivan and Gratton, 1999) and dorsal PFC (PL/ACx) (Diorio et al., 1993) regulate the release of corticosterone and ACTH in an opposite way. Specific behavioral responses such as diminished fear reactivity (Lacroix et al., 2000) were observed after bilateral lesions in the IL (Fryszak and Neafsey, 1991), and increased fear reactivity was detected when the region PL/ACx was lesioned (Morgan and LeDoux, 1995). Anxiety-like responses were observed after lidocaine infusion into the IL (Wall et al., 2004) or lesioning the right IL (Sullivan and Gratton, 2002).

Recent studies in rats showed morphological changes in pyramidal neurons in the PFC following chronic restraint stress (Radley et al., 2004, 2006 ; Cook and Wellman, 2004) or after chronic corticosterone treatment (Wellman, 2001). Chronic exposure to corticosterone also reduced the volume of layer II in all PFC sub-areas (Cerqueira et al., 2005a). Chronic restraint stress for 21 days decreased the number and the length of apical dendrites in Cg1–Cg3 (corresponding to the region PL/ACx) (Cook and Wellman, 2004; Radley et al., 2004), an effect accompanied by reduced spine density in the proximal portions of the apical dendrites (Radley et al., 2006). However, these studies did not investigate regional or possible hemispheric differences.

The present study investigates whether pyramidal neurons in the three PFC sub-areas have a hemisphere-specific morphology, and whether their specific dendritic architecture would be remodeled in a lateralized manner in response to chronic stress. As reference for the exact localization of the neurons prior to their morphological reconstruction, the PFC sub-areas boundaries delineation described in Part I was used. To reconstruct the morphology of individual pyramidal neurons in layer III which is known to have reciprocal connections with the mediodorsal thalamic nucleus (Heidbreder and

Groenewegen, 2003) cells were filled with neurobiotin using a whole-cell patch-clamp technique. Intracellular neurobiotin staining is a highly sensitive method (Pyapali et al., 1998) for visualizing neuronal processes that are not obscured by more intensely stained portions of the neurons (Hill and Oliver, 1993; Oliver, 1994). The morphological characteristics of pyramidal cells in the three PFC sub-areas was investigated paying particular attention to hemispheric differences in dendritic morphology following three weeks of daily restraint stress.

## **5.2 Methods**

### **5.2.1 Animals**

Same as described in Part I (see Methods; Animals, section 4.2.1)

### **5.2.2 Chronic restraint stress**

Male Sprague Dawley rats initially weighing 150–170 g were housed in groups of three animals with *ad libitum* access to food and tap water. The first experimental phase (“Habituation”) lasted for 14 days, during which body weight was recorded daily. Animals were randomly assigned to the experimental (*Stress*, n= 16) and control (n = 16) groups. The second phase of the experiment (“Restraint stress”) lasted either for 21 days (in Part II and IV) or 7 days (in Part III), during which the animals of the *Stress* group were submitted to daily restraint stress for six hours per day (09:00–15:00 h). Restraint stress was carried out according to an established paradigm (Magarinos and McEwen, 1995a). During restraint, rats were placed in plastic tubes in their home cages and had no access to food or water. *Control* rats were not subjected to any type of stress except daily handling. At the end of the experiment, 24 h after the last stress exposure, animals were weighed, deeply anesthetized with a mixture of 50 mg/ml ketamine, 10 mg/ml xylazine, and 0.1 mg/ml atropine by intraperitoneal injection, and decapitated (see Fig 4).

Brains were rapidly removed and processed for slice preparation (see below). Increased adrenal and decreased thymus weights are indicators of sustained stress. These organs were therefore dissected immediately after decapitation and weighed. The data are expressed in milligrams per 100 grams body weight.

### 5.2.3 Prefrontal cortex slice preparation

After removal of the PFC from the brain, a sagittal cut was made in the left temporal cortex with a silver blade to further differentiate the hemispheres. The blocks containing the left and the right PFC were rapidly submerged in ice-cold oxygenated artificial cerebrospinal fluid (ACSF) of the following composition (in mM): NaCl 125.0; KCl 2.5; L-ascorbic acid 1.0; MgSO<sub>4</sub> 2.0; Na<sub>2</sub>HPO<sub>4</sub> 1.25; NaHCO<sub>3</sub> 26.0; D-Glucose 14.0; CaCl<sub>2</sub> 1.5 (all chemicals from Merck, Darmstadt, Germany). The PFC was glued to the stage of a vibratome (Vibracut 2, FTB, Bensheim, Germany) and cut in coronal, 400- $\mu$ m-thick PFC slices. The slices were allowed to recover for at least one hour in ACSF bubbled with 95% O<sub>2</sub>/5% CO<sub>2</sub> at a pH of 7.3 at 33°C, and then kept at room temperature for up to seven hours.

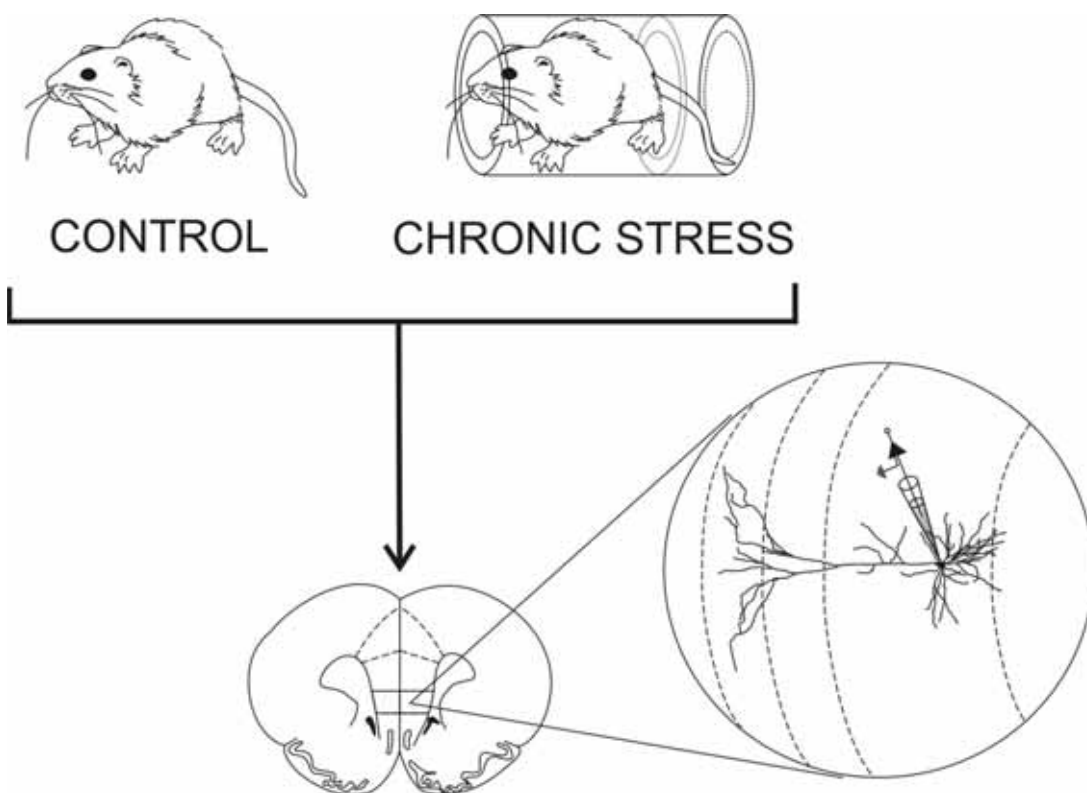


**Figure 4. Restraint stress procedure and intracellular labeling with neurobiotin**

For the restraint stress protocol, animals were placed in a plastic tube for 6 hours / per day during 21 days. The dimensions of the restraint tube were modified depending on the size of the animal to avoid any movement during the experimental sessions. Control animals were weighted everyday and returned to their home cages. Twenty-four hours after the last restraint session, animals were sacrificed and brains were dissected out. Coronal sections were prepared for the whole patch-clamp method and intracellular neurobiotin was injected into pyramidal neurons located in the selected regions of interest by a glass pipette during 20 minutes. Patch-pipettes were carefully withdrawn from the soma and slices were kept in paraformaldehyde for at least for 24 hours. Conventional immunocytochemical techniques were used for neurobiotin development.

### **5.2.4 Intracellular labeling and slice mounting**

The method for intracellular labeling previously described (Kole et al., 2004a) was used with some modifications. Neurobiotin was injected through borosilicate glass pipettes with 3–5 M $\Omega$  resistances, connected to an Axopatch 200B amplifier (Axon Instruments, Union City, CA, USA), using PULSE software (HEKA, Lambrecht, Germany). The standard pipette solution contained (in mM): K-MeSO<sub>4</sub> 120, KCl 20, HEPES 10, EGTA 0.2, ATP (magnesium salt) 2, phosphocreatine (disodium salt) 10, GTP (Tris-salt) 0.3, and 3 mg/ml neurobiotin (Vector Laboratories).

PFC slices were transferred to a submerged recording chamber, continuously oxygenated with ACSF (flow rate: 1–2 ml/min), and maintained at 33°C. Cell bodies were visualized by infrared–differential interference contrast (IR–DIC) video microscopy using an upright microscope (Axioskop 2 FS, Carl Zeiss, Germany) equipped with a 40 $\times$ /0.80 W objective (Zeiss IR-Acroplan). Negative pressure was used to obtain tight seals (2–10 G $\Omega$ ) onto identified pyramidal neurons. The membrane was disrupted with additional suction to form the whole-cell configuration. Pyramidal neurons with membrane potentials below –55 mV were excluded from the analysis. Cells were held at –70 mV for about 20 minutes.

Pyramidal cells are readily identified by their specific morphology, and only pyramidal-shaped somata located in layer III of the IL, PL and ACx sub-areas of the PFC (readily identified under IR-DIC video: Dodt and Zieglansberger, 1994) were used for neurobiotin filling. Layer III pyramidal somata, visible by transillumination, tend to be smaller than layer V somata. The border between layers II and III was difficult to identify; however, cells in layer III were mainly found at a depth of about 400  $\mu$ m from the pial surface (Gabbott and Bacon, 1996). *Post hoc* observation of labeled neurons with the depth from boundary definition (see Results) verified this location.

Neurobiotin injection lasted for about 20 minutes. Thereafter, patch pipettes were carefully withdrawn from the membrane and the slices were fixed in 0.1 M PB with 4% paraformaldehyde (pH 7.4) and stored at 4°C for at least 24 hours.

Whole slices were processed free-floating first washed 3 times in phosphate-buffered saline (PBS) for 10 min and incubated in a solution of 1% H<sub>2</sub>O<sub>2</sub> in 70% methanol for 30 min to suppress endogenous peroxidase activity. Thereafter, tissue was incubated in a solution containing 1% normal goat serum (Vector Labs) and 0.3% Triton X-100 in PBS to block non-specific protein binding and to permeabilize the cells.

Subsequently, the slices were incubated in avidin-biotin-complex (ABC) reaction solution (Vector Labs), at 4°C overnight. The following day, the slices were washed in PBS 3 x 5 min, 1 x 30 min, 1 x 60 min, and finally overnight. On the fourth day, the tissue was equilibrated by washing for 3 times in Tris-buffered saline (TBS, pH 7.6) and the histochemical reaction was completed by incubating the slices for 3-10 min in a solution containing 0.5 mg per ml 3,3'-diaminobenzidine (DAB) and 0.01% H<sub>2</sub>O<sub>2</sub> (Vector Labs) in TBS. The reaction was stopped after 3-15 min by rinsing the slices in TBS 3 x 10 min. The tissue was dehydrated in an ascending series of ethanol (30-100%) for 10 min at each concentration and cleared by 2 times incubation in xylene for 10 min. The slices were coverslipped using a xylene-based medium (Eukitt; Kindler, Freiburg, Germany). Slices from at least one stressed and one control animal were always processed simultaneously.

### **5.2.5 Neuronal reconstruction and morphometric analysis**

Labeled cells were examined by light microscopy to ensure that they fulfilled the following criteria: (1) a clear and completely stained apical dendritic tree; (2) at least three main basal branches, each branching at least to the third degree branch order; (3) soma location in layer III of an identified PFC sub-area; and (4) visibility of the most distal apical dendrites with clear, dense labeling of the processes (Kole et al., 2004a); (Radley et al., 2004). In a few cases, cell coupling was observed (<1%); such cells were omitted from the analysis, because the dendrites could not be assigned unequivocally to a single cell. Intracellularly labeled cells were located at 60–70 µm depth from the surface of the slice allowing reconstruction of almost all their main dendritic branches. Compromised cells that had truncated main apical or first order basal branches were omitted from the analysis.

Complete and optimally labeled pyramidal neurons meeting all criteria were reconstructed and quantified for dendritic morphometry using NeuroLucida software (MicroBrightField, Inc., Colchester, VT, USA) in combination with an automated stage and focus control connected to the microscope (Zeiss III RS). Data were collected as line drawings consisting of X, Y and Z coordinates. Dendritic length was measured by tracing dendrites using a 40× (N.A. 0.75) objective, giving a final magnification of 40,000× on the monitor. The step size of the circular cursor was 0.16 µm, sufficiently below the limits of light microscopy resolution (about 0.25 µm). Numerical analysis and graphical processing of the neurons were performed with NeuroExplorer

(MicroBrightField). Sholl plots (Sholl, 1953) were constructed by plotting the dendritic length as a function of distance from the soma center, which was set at zero. The length of the dendrites within each subsequent radial bin at 10  $\mu\text{m}$  increments was summed (Fig 5).

Ethanol dehydration and xylene clearance is known to cause tissue shrinkage (Pyapali et al., 1998). However, previous analyses from our laboratory suggested that the linear shrinkage correction has no direct effect on data used for morphological comparative analysis (Kole et al., 2004a). Therefore, any correction factor was applied.

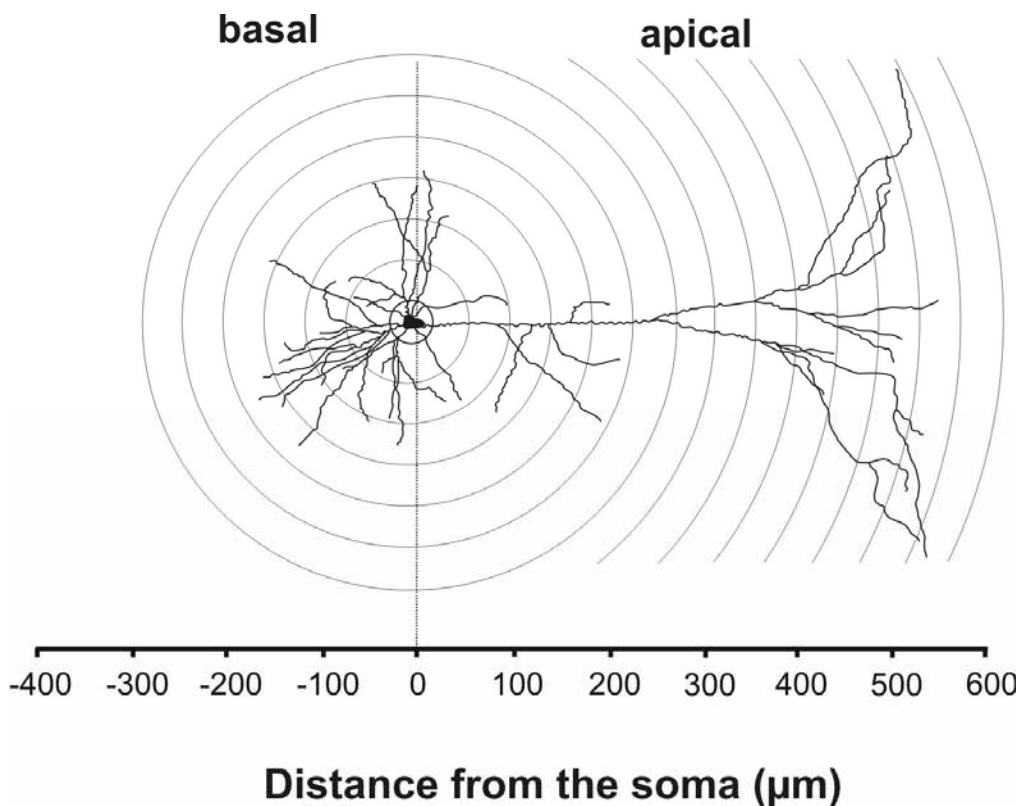


**Figure 5. Sholl analyses of pyramidal neurons**

Pyramidal neurons of the prefrontal cortex presented a typical pyramidal shape with a long apical dendrite projecting in most cases to the pia surface, and with several basal dendrites around the soma. Analyses of the dendritic morphology were performed by Sholl analysis (Sholl, 1953). A series of virtual circles are drawn around the soma (middle of the soma set at zero) with a fixed starting radius that is incremented by a constant amount as the starting radius. These radii are can be defined by the experimenter (i.e. 10  $\mu\text{m}$ , 20  $\mu\text{m}$ ...). The total numbers of intersections of dendrites that crossed these circles and the summed dendritic length within two circles can be determined by the Neuroexplorer software (MicroBrightField) for reconstruction of Sholl plots (see Result section).



### 5.2.6 Statistical analysis

Body weight (BW) and relative organ weight (in milligrams per 100 grams of BW) of control and stress animals at the end of the experiment were compared using the unpaired *t*-test.

The total number of labeled neurons that fulfilled the above criteria to be analyzed was 69 in the control and 70 in the stress group. Since these labeled cells were not evenly distributed among the animals, the means of the morphometric data were calculated for each hemisphere/animal. These mean data served as analysis unit for the statistical evaluation and are indicated as “n” in the tables. Data for the total length of dendrites, the total number of branching points and the total number of branches were evaluated by two-way ANOVA (factors: hemisphere x group) (Statistica software package, Release 6.0 StatSoft Inc., Tulsa, OK, USA). Numbers of branches per branch order were evaluated using three-way ANOVA (factors: branch order × hemisphere × group). Sholl analysis data were evaluated with three-way repeated measures ANOVA (factors: hemisphere x group × radius) (SPSS version 12.0, SPSS Inc., Chicago IL, USA). Bonferroni's *post hoc* test was used in all cases. Because the morphology of the pyramidal cells shows complex differences along the dendritic trees our *post hoc* analyses were restricted to distinct radii (10 μm, 20 μm, 30 μm, etc.) and single branch orders (1<sup>st</sup>, 2<sup>nd</sup>, 3<sup>rd</sup> order, etc.). Data are presented as mean±SEM (standard error of the mean). Differences were considered statistically significant at  $P<0.05$ .

## 5.3 Results

### 5.3.1 Effects of chronic restraint stress on body and organ weights

To assess the physiological effects of the chronic restraint stress, body weight and the weights of thymus and adrenal glands were measured. In rats subjected to the restraint stress for 21 days, a significant reduction in the final body weight (BW) was observed (*Control*:  $328.9 \pm 8.8$  g; *Stress*:  $292.3 \pm 7.0$  g;  $t=3.205$ ,  $P<0.05$ ). Adrenal weight was significantly increased in stressed animals (*Controls*:  $13.66 \pm 0.36$  mg/100 g BW; *Stress*:  $16.01 \pm 0.86$  mg/100 g BW;  $t=2.452$ ,  $P<0.05$ ) whereas thymus weight was significantly reduced (*Controls*:  $120.10 \pm 5.84$  mg/100 g BW; *Stress*  $100.40 \pm 4.27$  mg/100 g BW;  $t=2.755$ ,  $P<0.05$ ). These results agree with previous reports on

physiological changes induced by chronic restraint stress (Magarinos and McEwen, 1995a); (Watanabe et al., 1992c); (Wellman, 2001).

### **5.3.2 Intracellular labeling with neurobiotin and dendritic reconstruction**

Intracellular labeling provides a reliable and sensitive method for the study of dendritic morphology (Pyapali et al., 1998). In all experimental groups, there was complete staining of the main dendritic branches of each neuron with distal dendrites (high order branches) being reliably visualized (Fig. 6). The use of relatively thick slices (400- $\mu\text{m}$ ) increased the probability of obtaining complete dendritic arbors without compromised branches. In both groups together, *Control* and *Stress*, 384 cells were filled of which 36% (139 cells) fulfilled the criteria for complete staining suitable for a quantitative analysis of essential aspects of their dendritic morphology. Since these labeled cells were not evenly distributed among the animals and to avoid any bias the means/hemisphere/animal were calculated. These means served as analysis units for the statistical evaluation (see below).

### **5.3.3 Intrinsic morphological asymmetries**

For a close inspection of the dendritic trees in the left and the right hemisphere of control rats, Sholl analyses were performed (Fig. 7, left panel). For the length of basal dendrites in the IL, two-way ANOVA revealed significant effects of hemisphere and radius ( $F_{(1,450)}=11.80$  and  $F_{(29,450)}=32.53$ , respectively,  $p < 0.001$ ) and Bonferroni's *post hoc* test indicated a significant inter-hemispheric difference in proximal parts of the basal tree (10  $\mu\text{m}$ ;  $df=31$ ,  $p < 0.01$ ) (Fig 7A left). For apical dendrites in the IL, ANOVA revealed significant effects of hemisphere and radius ( $F_{(1,900)}=8.05$  and  $F_{(59,900)}=8.06$ , respectively,  $p < 0.01$ ), and Bonferroni's *post hoc* test showed longer apical dendrites in the right hemisphere at 10, 20 and 60  $\mu\text{m}$  ( $df=30$ ,  $p < 0.05$  in all cases) (Fig 7A left panel).

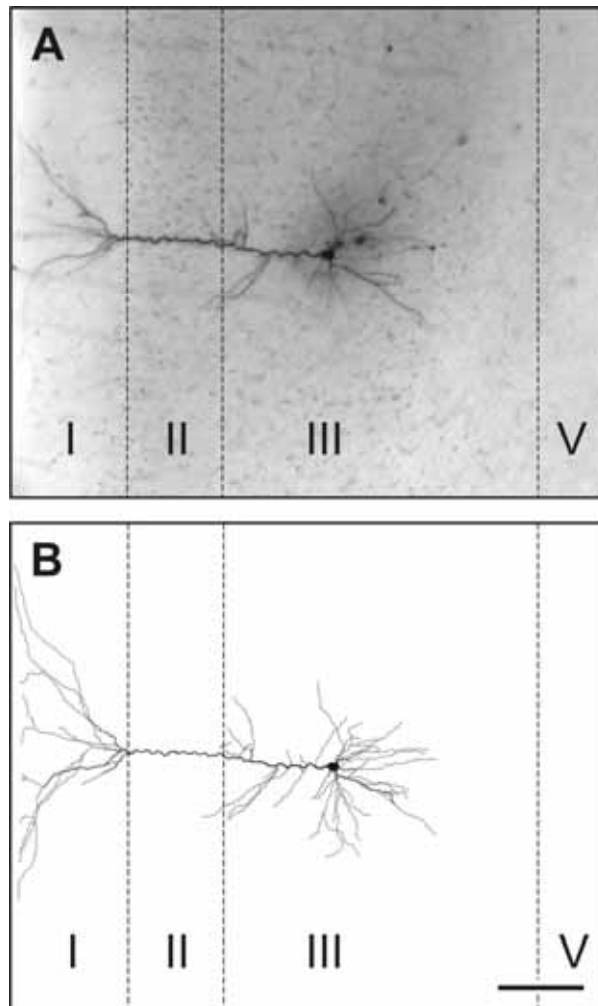


**Figure 6. Photomicrograph of an intracellular neurobiotin labeled pyramidal neuron in the prelimbic area**

Example of an intracellularly labeled and reconstructed pyramidal cell in the PFC of a control rat. **(A)** Photomicrograph of an intracellularly labeled pyramidal neuron in layer III of the prelimbic sub-area (left hemisphere). **(B)** Line-drawing of the neuron shown in **A** (reconstruction with NeuroLucida). The relative position of the pyramidal cell is shown by lines indicating the cortical layers (I–V). Scale bar: 100  $\mu\text{m}$ .

In the PL, Sholl analysis of the basal dendrites displayed significant effects of hemisphere and radius ( $F_{(1,240)}=10.5$  and  $F_{(29,240)}=9.7$ , respectively,  $p < 0.001$ ). However, the *post hoc* test depicted no reliable difference between basilar dendrites in the left and the right hemisphere of controls (Fig 3B). Apical dendrites in the PL showed a positive effect of hemisphere ( $F_{(1,480)}=24.33$ ,  $p < 0.001$ ) and a weak effect of radius ( $F_{(59,480)}=1.37$ ,  $p < 0.05$ ). Bonferroni's *post hoc* test revealed significant hemispheric differences in apical dendritic trees with longer dendrites in the right pyramidal neurons in middle portions of the soma (at 180 and 420  $\mu\text{m}$  from soma,  $df=25$ ,  $p < 0.01$ ; at 160, 170 and 190,  $df=25$ ,  $p < 0.01$ ) (Fig 7B left panel).

For the basilar dendrites in the ACx, three-way ANOVA indicated no reliable inter-hemispheric difference but only an effect of radius ( $F_{(29,399)}=15.55$ ;  $p < 0.001$ ). For the apical dendrites in ACx, ANOVA revealed a positive effect of the hemisphere ( $F_{(1,841)}=7.81$ ,  $p < 0.01$ ) and an effect of radius ( $F_{(51,841)}=3.11$ ,  $p < 0.001$ ). However, the *post hoc* test showed no inter-hemispheric difference with respect to apical dendrites in the ACx of controls (Fig. 7C left panel).

These data demonstrate a lateralized morphology of apical dendrites on pyramidal neurons in IL and PL but not in the ACx of control rats.

The total length of basilar and apical dendrites in control rats showed no significant inter-hemispheric differences although apical dendrites in the right tended to be longer than in the left hemisphere (Table 1).

To assess the complexity of the apical and basal dendritic trees, analyses of the branching pattern between the two hemispheres were made (Table 2). For basilar dendrites, two-way ANOVA indicated no reliable inter-hemispheric differences for the total number of branching points and branches in any of the sub-areas (Table 2). Numbers of branches of distinct branch orders were evaluated by three-way ANOVA (factors: hemisphere x group x branch order).

For basilar dendrites in the IL, an effect of the hemisphere ( $F_{(1, 182)}= 10.48$ ;  $p < 0.05$ ) and of the branch order ( $F_{(6, 182)}= 60.82$ ;  $p < 0.001$ ) was found (details not shown). For IL apical dendrites, numbers of branches of distinct branch orders revealed an effect of hemisphere ( $F_{(1, 288)}= 4.73$ ;  $p < 0.05$ ) and of branch order ( $F_{(11, 288)}= 13.74$ ;  $p < 0.001$ ) (Table 2). Bonferroni's *post hoc* test showed reliable inter-hemispheric differences for the number of branches of the orders 4, 6 and 11 ( $df=24$ ,  $p < 0.05$  in all cases) and of branch order 12 ( $df=24$ ,  $p < 0.01$ ). In the left IL, dendritic branches of the orders 11 and 12 could not be observed, but were only present in the right IL (Table 2).

For basilar dendrites in the PL, three-way ANOVA depicted no effect of the hemisphere but only an effect of the branch order ( $F_{(6, 168)}= 68.23$ ;  $p < 0.001$ ). Also for apical dendrites in the PL there was no effect of the hemisphere but only an effect of the branch order ( $F_{(10, 253)}= 9.86$ ;  $p < 0.001$ ). The *post hoc* test showed no significant inter-hemispheric difference for any branch order in the PL (Table 2).

In the ACx of control rats, there were no significant inter-hemispheric differences with respect to the total number of apical and basilar branches and branching points. Three-way ANOVA depicted only effects of the branch order (basal:  $F_{(5, 118)}= 36.11$ ;  $p < 0.001$ ; apical:  $F_{(10, 220)}= 9.92$ ;  $p < 0.001$ ) (Table 2).

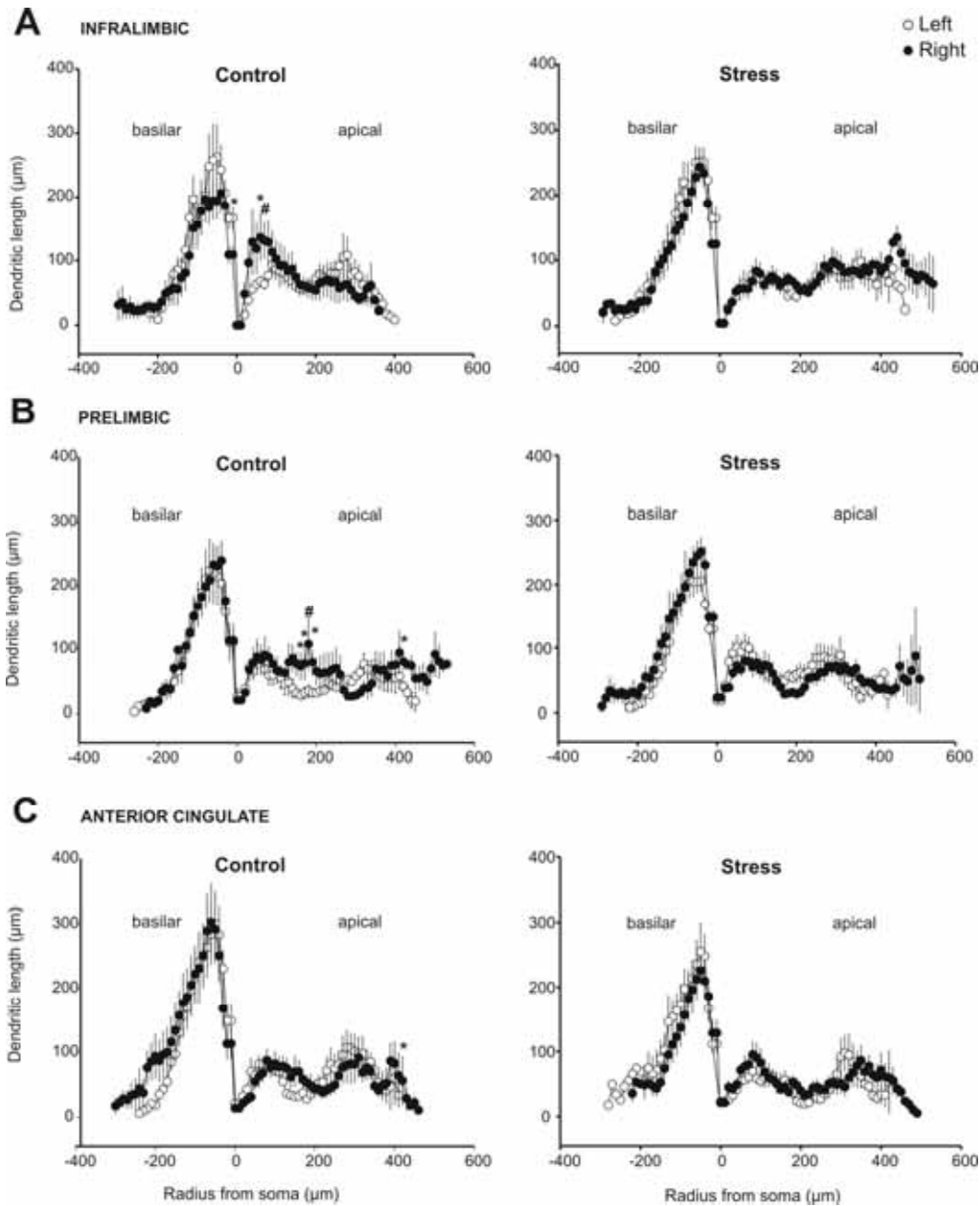


**Figure 7. Sholl analyses of dendrites of pyramidal neurons in control and stress rats**

Sholl analysis of dendrites on pyramidal cells in the left (open circles) and the right hemisphere (closed circles) of controls (left panel) and stressed rats (right panel). Basilar dendrites are plotted to the left and apical dendrites to the right as a function of the distance from the soma center (0). **(A)** In the infralimbic area of control rats (left panel), basilar dendrites close to the soma (at 10  $\mu\text{m}$ ) were longer in the left than in the right hemisphere. Apical dendrites showed hemispheric differences at several sites displaying longer dendrites in the right hemisphere. In the stressed rats (right panel), no hemispheric differences were found in basilar or apical dendrites. **(B)** In the prelimbic area of control rats, the apical dendrites in the right hemisphere showed more dendritic material at medium and far distances from the soma. In the stressed rats, no hemispheric differences were found in basilar or apical dendrites. **(C)** In the anterior cingulate cortex of control rats, neither apical nor basal dendrites displayed significant left-right differences in controls and stressed rats. Data points represent the sum of all dendrites detected at the respective distance (radius) from the soma center set as zero (mean  $\pm$  SEM). Symbols indicate significant differences within each 10  $\mu\text{m}$  ring determined by ANOVA with Bonferroni's *post hoc* test (\* $p < 0.05$ , # $p < 0.01$ ).

Table 1. Morphometric data of control and stressed rats

**Morphometric data in control and stressed rats (left vs right)**

Total length (sum of all dendrites,  $\mu\text{m}$ ) of basilar and apical dendrites on pyramidal neurons in the three PFC sub-areas of control and stressed rats. Hemispheric asymmetry refers to the dendritic length in the right compared to the left hemisphere (expressed as percentage). In the PL, chronic restraint stress reduced apical dendritic length exclusively in the right hemisphere (mean  $\pm$  SEM; n=number of animals).

		Control			Stress		
		Total dendritic length ( $\mu\text{m}$ )		Hemispheric asymmetry	Total dendritic length ( $\mu\text{m}$ )		Hemispheric asymmetry
		L	R	R as % of L	L	R	R as % of L
Basilar dendrites	IL	2928 $\pm$ 433 n=9	2471 $\pm$ 400 n=7	84%	2671 $\pm$ 441 n=9	2530 $\pm$ 463 n=9	95 %
	PL	2779 $\pm$ 135 n=5	2402 $\pm$ 333 n=5	86%	2742 $\pm$ 416 n=11	2257 $\pm$ 217 n=12	82 %
	ACx	3364 $\pm$ 406 n=9	3220 $\pm$ 564 n=9	96%	2811 $\pm$ 442 n=7	2265 $\pm$ 281 n=7	81 %
Apical dendrites	IL	2261 $\pm$ 295 n=9	2514 $\pm$ 383 n=7	111 %	2204 $\pm$ 301 n=9	2880 $\pm$ 412 n=9	131 %
	PL	2066 $\pm$ 186 n=5	3289 $\pm$ 625 n=5	159 %	2397 $\pm$ 444 n=11	1957 $\pm$ 170 * n=12	82 %
	ACx	2339 $\pm$ 212 n=9	2618 $\pm$ 283 n=9	112 %	1956 $\pm$ 416 n=7	2269 $\pm$ 408 n=7	116 %

Table 2. Number of branching points and branches in control and stressed rats

Number of branching points and of branches in basilar and apical dendrites on pyramidal neurons in PFC sub-areas.  
 \*  $P < 0.05$ , \*\*  $P < 0.01$  significant differences between right (R) and left (L); #  $P < 0.05$ , ##  $P < 0.01$  significant difference to *Control* as determined by ANOVA with Bonferroni's *post hoc* test. Numbers in parentheses indicate number of animals from which data (means $\pm$ SEM) were derived (n). Abbreviations: IL, infralimbic cortex; PL, prelimbic cortex; ACx, anterior cingulate cortex.

			Control			Stress		
			IL	PL	ACx	IL	PL	ACx
Basilar dendrites	Total number of branching points	L	17.3 $\pm$ 2.7 (9)	13.8 $\pm$ 0.7 (5)	18.8 $\pm$ 2.9 (9)	13.3 $\pm$ 1.7 (9)	13.4 $\pm$ 1.5 (11)	15.3 $\pm$ 2.1 (7)
		R	11.5 $\pm$ 1.3 (7)	13.1 $\pm$ 1.2 (5)	16.7 $\pm$ 2.0 (9)	11.7 $\pm$ 1.7 (9)	12.5 $\pm$ 1.0 (12)	13.3 $\pm$ 2.3 (7)
	Total number of branches	L	40.6 $\pm$ 5.6 (9)	35.3 $\pm$ 1.7 (5)	44.6 $\pm$ 6.2 (9)	32.2 $\pm$ 4.1 (9)	30.3 $\pm$ 3.7 (11)	37.7 $\pm$ 4.1 (7)
		R	30.5 $\pm$ 2.6 (7)	32.8 $\pm$ 2.7 (5)	41.3 $\pm$ 4.2 (9)	30.4 $\pm$ 3.9 (9)	31.9 $\pm$ 2.2 (12)	32.9 $\pm$ 4.9 (7)
Apical dendrites	Total number of branching points	L	12.4 $\pm$ 1.5 (9)	11.7 $\pm$ 0.8 (5)	13.0 $\pm$ 1.5 (9)	11.0 $\pm$ 2.3 (9)	11.6 $\pm$ 2.0 (11)	11.0 $\pm$ 2.3 (7)
		R	15.1 $\pm$ 2.4 (7)	17.3 $\pm$ 2.9 (5)	14.7 $\pm$ 1.6 (9)	13.6 $\pm$ 2.9 (9)	<b>10.5 <math>\pm</math> 0.8 # (12)</b>	13.6 $\pm$ 2.9 (7)
	Total number of branches	L	25.1 $\pm$ 2.7 (9)	24.5 $\pm$ 1.8 (5)	27.0 $\pm$ 2.9 (9)	23.3 $\pm$ 4.8 (9)	25.1 $\pm$ 4.1 (11)	23.3 $\pm$ 4.8 (7)
		R	31.4 $\pm$ 4.9 (7)	36.1 $\pm$ 5.9 (5)	30.8 $\pm$ 3.2 (9)	28.4 $\pm$ 5.8 (9)	22.8 $\pm$ 1.7 (12)	28.4 $\pm$ 5.8 (7)
	Number of branches (order 3)	L	2.9 $\pm$ 0.3 (9)	2.9 $\pm$ 0.4 (5)	3.1 $\pm$ 0.4 (6)	2.8 $\pm$ 0.4 (7)	3.3 $\pm$ 0.3 (9)	2.3 $\pm$ 0.3 (6)
		R	2.8 $\pm$ 0.4 (6)	4.0 $\pm$ 0.2 (5)	2.4 $\pm$ 0.2 (5)	2.5 $\pm$ 0.3 (7)	<b>2.9 <math>\pm</math> 0.3# (8)</b>	<b>4.1 <math>\pm</math> 0.7*# (6)</b>
	Number of branches (order 4)	L	2.9 $\pm$ 0.3 (9)	2.7 $\pm$ 0.3 (5)	3.1 $\pm$ 0.4 (6)	2.9 $\pm$ 0.4 (7)	3.7 $\pm$ 0.6 (9)	2.7 $\pm$ 0.4 (6)
		R	<b>4.3 <math>\pm</math> 0.8* (6)</b>	3.1 $\pm$ 0.4 (5)	4.0 $\pm$ 0.5 (5)	3.5 $\pm$ 0.3 (7)	3.3 $\pm$ 0.4 (8)	3.7 $\pm$ 0.8 (7)
	Number of branches (order 5)	L	3.8 $\pm$ 0.3 (9)	2.5 $\pm$ 0.4 (5)	3.3 $\pm$ 0.3 (6)	3.7 $\pm$ 0.6 (7)	4.1 $\pm$ 0.8 (8)	3.2 $\pm$ 0.7 (5)
		R	3.1 $\pm$ 0.4 (6)	3.6 $\pm$ 0.2 (5)	3.8 $\pm$ 0.5 (5)	3.6 $\pm$ 0.5 (7)	3.1 $\pm$ 0.3 (8)	3.0 $\pm$ 0.4 (7)
	Number of branches (order 6)	L	4.2 $\pm$ 0.6 (9)	2.8 $\pm$ 0.3 (5)	3.8 $\pm$ 0.8 (6)	4.0 $\pm$ 0.6 (7)	5.6 $\pm$ 1.0 (8)	2.5 $\pm$ 0.5 (5)
		R	<b>2.3 <math>\pm</math> 0.3* (6)</b>	4.6 $\pm$ 1.2 (5)	4.2 $\pm$ 1.2 (5)	3.6 $\pm$ 0.3 (7)	3.0 $\pm$ 0.3 (8)	3.7 $\pm$ 1.0 (7)
	Number of branches (order 11)	L	0 $\pm$ 0 (0)	2.2 $\pm$ 0.9 (3)	0 $\pm$ 0 (0)	0 $\pm$ 0 (0)	3.1 $\pm$ 0.7 (3)	3.3 $\pm$ 0.7 (3)
		R	<b>6.0 <math>\pm</math> 0.0* (3)</b>	2.5 $\pm$ 0.8 (3)	2.0 $\pm$ 1.1 (3)	3.3 $\pm$ 0.8 (3)	3.0 $\pm$ 1.0 (3)	<b>0 <math>\pm</math> 0 # (0)</b>
	Number of branches (order 12)	L	0 $\pm$ 0 (0)	0 $\pm$ 0 (0)	0 $\pm$ 0 (0)	0 $\pm$ 0 (0)	0 $\pm$ 0 (0)	0 $\pm$ 0 (0)
		R	<b>2.7 <math>\pm</math> 0.6 ** (3)</b>	0 $\pm$ 0 (0)	0 $\pm$ 0 (0)	<b>0 <math>\pm</math> 0 ## (0)</b>	0 $\pm$ 0 (0)	0 $\pm$ 0 (0)

### 5.3.4 Stress effects on dendritic morphology

Stress reduced the total length of apical dendrites on pyramidal neurons in the PL selectively in the right hemisphere (Table 1). No other stress effect on the total length of dendrites was observed.

Dendrites of pyramidal neurons in stressed rats are shown in Figure 7 (right panel) and in Figure 8. For basilar dendrites in the IL, three-way ANOVA depicted no reliable effect of stress. These dendrites also displayed no significant left-right difference in stressed animals (Figure 7A, right panel).

For apical dendrites in the IL, three-way ANOVA revealed an interaction hemisphere  $\times$  group ( $F_{(1, 1086)}=5.43$ ,  $p < 0.05$ ), but the *post hoc* test depicted no significant left-right difference for apical dendrites at defined distances from the soma (Figure 7A, right panel). However, in the right IL of stressed animals, the length of proximal dendrites at several sites was significantly shorter than in controls (at 10, 20, 30, 40 and 70  $\mu\text{m}$ ,  $df=30$ ,  $p < 0.05$ ; at 50 and 60  $\mu\text{m}$ ,  $df=30$ ,  $p < 0.01$ ) (Figure 8A).

In the PL of stressed rats, no reliable inter-hemispheric differences with respect to apical dendrites on pyramidal neurons were observed (Figure 7B, right panel). Three-way ANOVA for apical branches in the PL, performed with data from all groups, showed an interaction hemisphere  $\times$  group ( $F_{(1, 1018)}=17.40$ ,  $p < 0.001$ ). The *post hoc* test indicated that in the right PL, stress reduced the length of apical dendrites at 160, 170, 190, 420  $\mu\text{m}$  ( $df=25$ ;  $p < 0.05$ ) and at 180  $\mu\text{m}$  ( $df=25$ ,  $p < 0.01$ ) (Figure 8B).

For basilar dendrites in the ACx, three-way ANOVA depicted an effect of group ( $F_{(1, 399)}=9.23$ ,  $p < 0.01$ ) and an interaction hemisphere  $\times$  group ( $F_{(1, 399)}=6.40$ ,  $p < 0.05$ ). Also for the apical dendrites, three-way ANOVA showed an effect of group ( $F_{(1, 841)}=9.34$ ,  $p < 0.01$ ) but no interaction. In the left hemisphere of the ACx, stress reduced the length of apical dendrites at certain distances from soma (210, 220, 240 and 250  $\mu\text{m}$ ;  $df=21$ ,  $p < 0.05$  in all cases) (Figure 8C). Also for the right ACx, the *post hoc* test depicted a significant stress effect (at 20  $\mu\text{m}$  from soma;  $df=21$ ,  $p < 0.05$ ).

The effect of stress on the total number of branching points and the total number of dendritic branches was also analyzed (Table 2).

For apical dendrites in the IL, both basilar and apical dendrites showed no effect of group and no interaction. However, the *post hoc* test depicted a significant stress effect on numbers of branches of the order 12 in the right IL ( $df=24$ ,  $p < 0.01$ ). These dendritic branches could not be observed in stressed animals (Table 2).



In the PL, the branching pattern of basilar dendrites was apparently not affected by stress. For the total number of apical branching points, two-way ANOVA revealed an interaction group x hemisphere ( $F_{(1,31)}=3.28$ ,  $p < 0.05$ ) represented by a reliable stress induced decrease in the total number of branching points in the right hemisphere ( $df=29$ ,  $p < 0.05$ ). Stress also reduced the number of branches of the order 3 selectively in the right hemisphere of the PL (interaction: group x hemisphere;  $F_{(1,253)}=7.61$ ,  $p < 0.01$ ; *post hoc* test:  $df=23$ ,  $p < 0.05$ ) (Table 2).

For basilar dendrites in the ACx, three-way ANOVA showed an interaction hemisphere x group ( $F_{(1, 118)}=5.32$ ,  $p < 0.05$ ). For apical dendrites, there was a reliable effect of group ( $F_{(1, 220)}=5.46$ ,  $p < 0.05$ ) represented by a stress induced increase in the number of branches of the order 3 in the right hemisphere ( $df=20$ ;  $p < 0.05$ ). Moreover, there was a significant left-right difference with respect to order 3 branches in the ACx; no dendritic branches of this order could be observed in stressed rats ( $df=20$ ,  $p < 0.05$ ) (Table 2).

These data show that chronic restraints stress affects dendrites in the right hemisphere of IL and PL. In contrast in the ACx, it is the left hemisphere that is affected by stress.

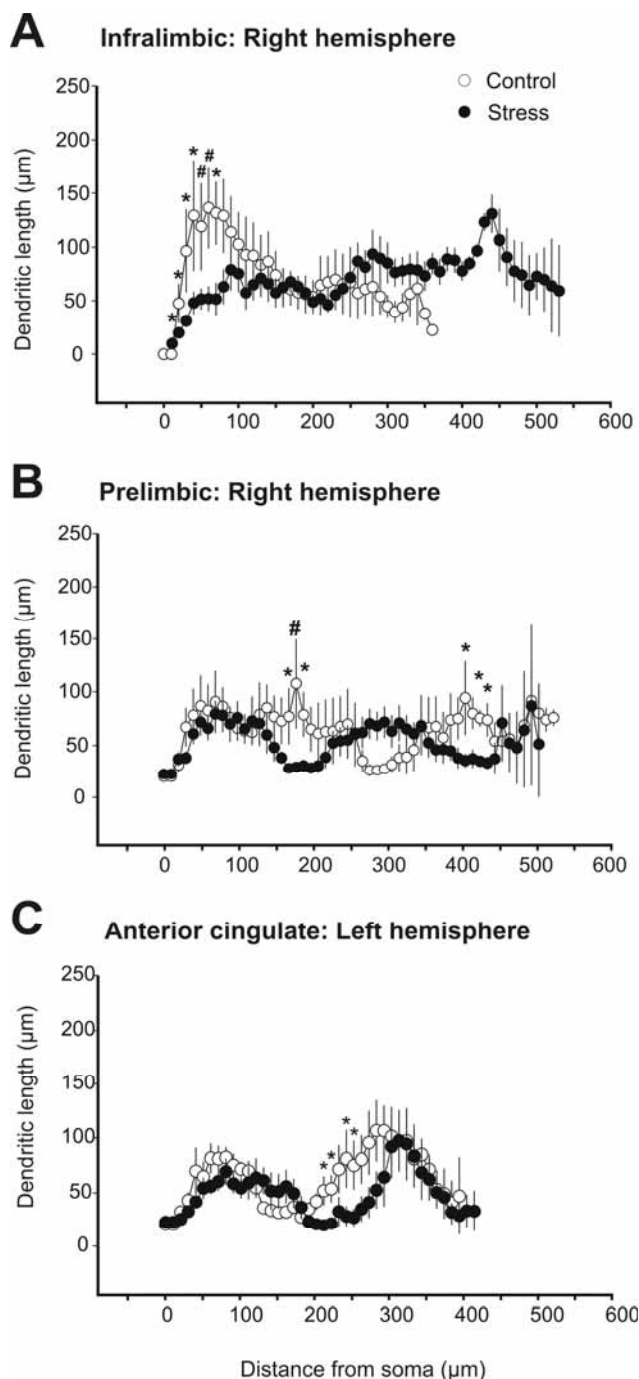


**Figure 8. Sholl analysis of pyramidal neurons in the right hemisphere of control and stressed rats**

Comparisons of apical dendrites in the *right* hemisphere of IL and PL, and in the *left* ACx of stressed (closed circles) and control rats (open circles). Apical dendrites were plotted as a function of distance from the soma center (0). **(A)** Right IL: In stressed rats, there was less dendritic material proximal to the soma compared to controls. **(B)** Right PL: In stressed rats, there was less dendritic material at several sites. **(C)** Left ACx: In stressed rats, there was less dendritic material at about 250  $\mu\text{m}$  from the soma. Data points represent the sum of all dendrites detected at the respective distance (radius) from the soma (mean $\pm$ SEM). Symbols indicate significant differences detected within each 10  $\mu\text{m}$  ring as determined by three-way repeated measures ANOVA (\* $p < 0.05$ , #  $p < 0.01$ ).

## 5.4 Discussion

The mammalian PFC is defined as brain region that possess reciprocal projections from the mediodorsal thalamic nucleus (Uylings et al., 2003). These projections principally target layer III and V of the PFC (Uylings et al., 2003; Gabbott et al., 2005; Krettek and Price, 1977), therefore, this study focused in the analysis of pyramidal cells exclusively in layer III. The neurons that were investigated showed apical dendrites extending to the brain surface, and the distance of their somata was up to 550  $\mu\text{m}$  from the pia mater. Their location agreed with a previous description of the PFC layers (Gabbott and Bacon, 1996). In contrast, Brown et al (2005) reported that the somata of the pyramidal neurons they examined were located closer to the cortical surface (distance of 250-280  $\mu\text{m}$ ), probably in layer II. It is important to mention that intracellular neurobiotin labeling allows a better staining of distal dendritic branches compared to conventional methods such as Golgi staining (Pyapali et al., 1998).

This study demonstrated intrinsic morphological asymmetries in the prefronto-cortical pyramidal cells of control animals. In PL and IL, there were inter-hemispheric differences in the length of apical dendrites at certain distances from the soma. These are new findings, because previous studies addressing the morphology of pyramidal neurons in the PFC did not discriminate between the hemispheres (Wellman, 2001; Cook and Wellman, 2004; Radley et al., 2004). Intrinsic asymmetries have been observed before in several regions of the human cerebral cortex, e.g. in entorhinal, auditory and language-associated cortices (Hayes and Lewis, 1993; Hutsler, 2003). Simic and co-workers found larger pyramidal neurons in the human left entorhinal cortex compared to the right, and hypothesized that this asymmetry reflects a more extended dendritic arborization and enlarged neuropil volume in the left hemisphere (Simic et al., 2005). The present data show that in PFC sub-areas PL and IL of the rat, the length of apical dendrites at certain distances from soma differs between the hemispheres.

When rats were chronically stressed, these inter-hemispheric differences found in the IL and PL were abolished. In the right PL, stress reduced dramatically the total length of the apical dendrites. The stress-induced factors that lead to these changes are not yet known, however, one may speculate that dopamine which is known to decrease excitability of PFC pyramidal neurons plays a role (Jedema and Moghaddam, 1994; Gullledge and Jaffe, 1998). Electrophysiological recordings have shown that dopamine enhances the spatiotemporal spread of activity in the rat PFC, at least in part via layer III

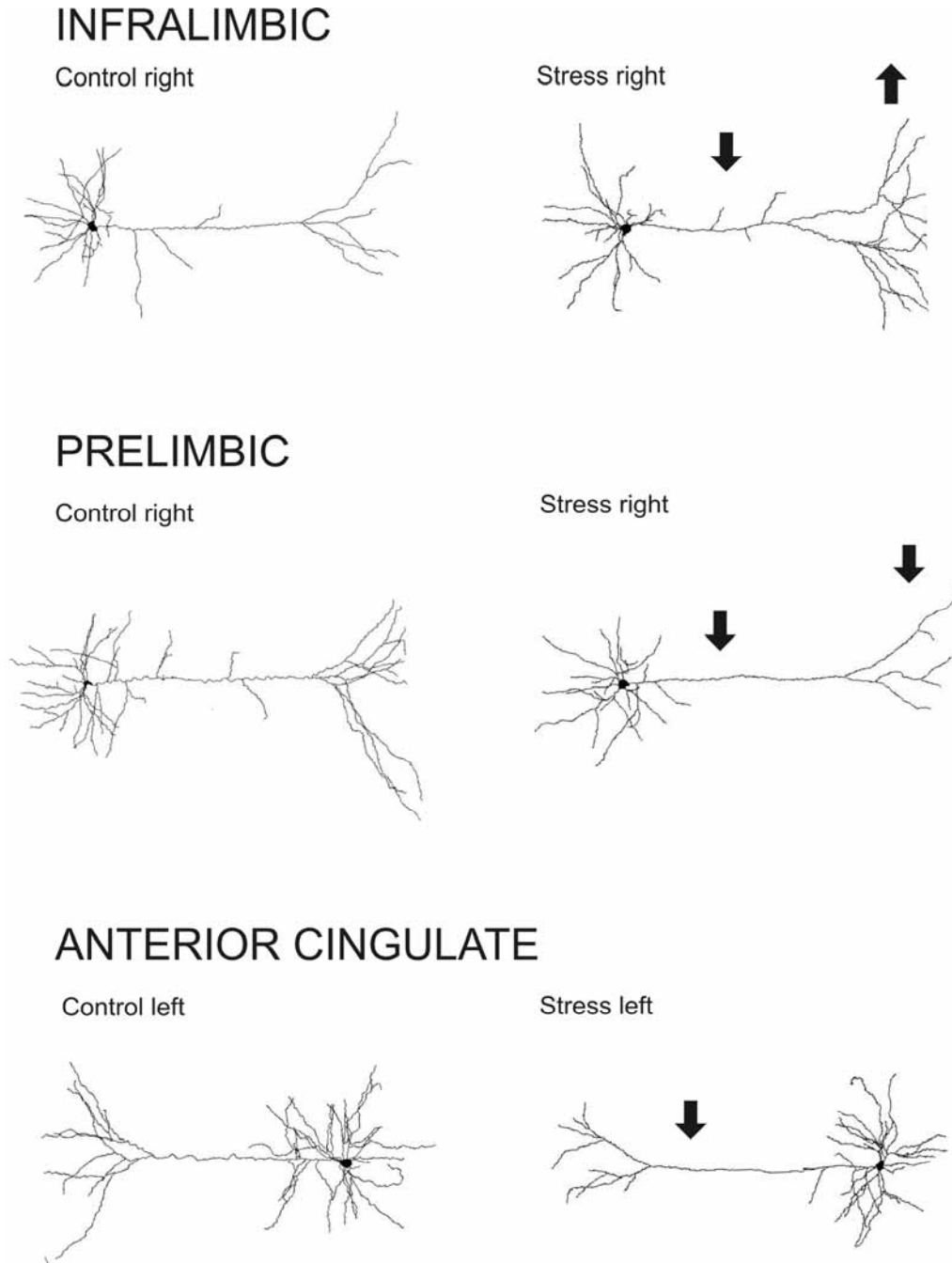


**Figure 9. Drawings of representative neurons from the prefrontal cortex**

Representative neurons after reconstruction by NeuroLucida Software. Labeled neurons from control (left panel) and stressed (right panel) rats were compared in the infralimbic, prelimbic and anterior cingulated cortex. Significant changes induced by chronic stress are symbolized by an arrow, indicating increases (arrow up) or decreases (arrow down) in the total dendritic length at specific distances from the soma. Stress induced significant modifications in the morphology of pyramidal neurons located in the right hemisphere of the Infralimbic and prelimbic areas whereas, in the anterior cingulated cortex, stress affected only left side pyramidal neurons.

pyramidal neurons (Bandyopadhyay et al., 2005). As mentioned above, stress can increase dopamine turnover in the right PFC (Carlson et al., 1993; Berridge et al., 1999; Slopsema et al., 1982) and chronic stress reduces the spontaneous activity of dopaminergic neurons in the ventral tegmental area (VTA) which project to the PFC (Moore et al., 2001; Benes et al., 1993). In coincidence with this it was found that repeated stress reduces dopamine (Mizoguchi et al., 2000), noradrenalin (Kitayama et al., 1997) and serotonin in the PFC (Mangiavacchi et al., 2001). Although it is not known whether in the present study, the chronic restraint stress induced a deficit in dopamine and/or other monoamines it may be hypothesized that the changes in dendrites observed here are related to adaptive neurochemical processes. In contrast to PL and IL, pyramidal neuron dendrites in the ACx of control rats showed no inter-hemispheric differences, but the stress induced a left-right difference. Previous reports described a stress induced decrease in apical dendritic length using a similar (Cook and Wellman, 2004; Brown et al., 2005) or the same stress protocol (Radley et al., 2004). While in this analysis only layer III pyramidal neurons were investigated the former studies focused on cells more widely distributed over layers II–III (Cook and Wellman 2004; Radley et al., 2004). Dendritic architecture is crucial for connectivity within neuronal networks. Sensory input or environmental enrichment has been shown to promote the formation of spines on proximal dendrites (Turner and Lewis, 2003). In hippocampal pyramidal neurons, extensive dendritic sprouting and enhanced spine density were observed when axonal afferents were increased (Kossel et al., 1997) whereas the loss of afferents can lead to dendritic atrophy (Valverde, 1968; Benes et al., 1977; Deitch and Rubel, 1984). One may speculate that the stress induced dendritic changes observed in the present study are related to alteration in axonal input. The observation that the dendritic alterations emerged at certain distances from soma may be related to the fact that axonal input to the PFC is site-specific and depends on the cortical layer. Furthermore, stress-induced reduction in the total length of dendrites in the right PL is in line with previous findings showing lateralization of the PFC mediated stress response. Right side lesions of the IL/PL reduced the peak stress-induced corticosterone response (Sullivan and Gratton, 1999) and decreased anxiety (Sullivan and Gratton, 2002), suggesting that a compromised right PFC activity results in a lack of control over the physiological and behavioral responses to stress. Especially the PL and the ACx are important to react to environmental stimuli (Cardinal et al., 2002). Therefore, one may assume that alterations in the morphology of PFC pyramidal neurons have an impact on the stress response.

Similar stress-related processes as in the PFC have been observed in the amygdala. Chronic restraint stress *increased* the length of apical dendrites of pyramidal cells in the basolateral amygdala (Vyas et al., 2002) which sends projections to and receives input from PL and ACx (Vertes, 2004). Like in the PFC, the activity of the basolateral amygdala appears to be lateralized under stress conditions (Adamec et al., 1999). Under normal conditions, the PFC inhibits the basolateral amygdala (Rosenkranz and Grace, 2002) but under stress, this inhibition might be impaired thus contributing to an over-reactivity of this nucleus. It is possible that the morphological remodeling of the pyramidal neurons in the rat PFC that is described in the present study is related to a presumptive stress-induced change in information transfer between PFC and amygdala.

Lateralization appears to be characteristic for normal PFC functioning. Studies in humans indicated that reduced lateralization correlates with pathological conditions or with aging processes as fronto-cortical activity during cognitive performance tends to be less lateralized in old compared to young adults (Dolcos et al., 2002). A recent investigation on the human dorsolateral PFC demonstrated a hemispheric asymmetry in pyramidal cell density in normal subjects (higher density left compared to right), which was reversed in schizophrenic patients (Cullen et al., 2006). Rotenberg suggested that in depressed patients, the right PFC hemisphere is over-activated (Rotenberg, 2004), and subjects with major depression displayed a reduced size of neurons in layer III of the right orbitofrontal cortex (Cotter et al., 2005). However, studies in depressed patients that did not focus on hemispheric differences reported on decreased activity in the PFC area ventral to the genu of the corpus callosum (Drevets et al., 1997), and on reduced cortical thickness, glial size and glial densities in supragranular layers of the orbitofrontal cortex (Rajkowska et al., 1999). The present study in rats shows that chronic restraint stress has a strong effect on the morphology of pyramidal neurons in the right hemisphere, at least in PL and IL.

The neurophysiological consequences of the dendritic alterations are not yet known. A shortening of even a few dendrites on CA1 hippocampal pyramidal neurons enhanced the back-propagation of action potentials (Golding et al., 2001; Schaefer et al., 2003). Moreover, experiments in our laboratory revealed that a stress-induced decrease in the length of apical dendrites of CA3 pyramidal neurons in the rat hippocampus correlates with reduced onset latency of excitatory postsynaptic potentials (Kole et al., 2004b). However, functional studies are required to assess the physiological implications of such morphological remodeling in the rat PFC.

## 5.5 Conclusions

This is the first study showing intrinsic hemispheric differences in the dendritic morphology of pyramidal neurons in sub-areas of the rat PFC. In PL and IL of control rats, inter-hemispheric differences in the length of apical dendrites at certain distances from the soma were observed. Chronic stress abolished these right-left differences and reduced the total length of apical dendrites in the right PL. In contrast in the ACx, there was no hemispheric difference in controls but stress induced a left-right difference. These chronic stress-induced regional changes may be correlated with the specialized functions of PFC sub-areas in stress-related pathologies, and provide additional support for previous studies of stress-dependent activation of the right PFC.

**6 Part III. The impact of the diurnal light cycle on the morphology of pyramidal neurons of the prelimbic area**



## 6.1 Effects of stress applied during the light-phase or during the dark-phase

### Summary

In this study the effects of a short-term stress exposure performed either during the light- or during the dark-phase of the diurnal cycle were investigated. The effects of the stress on the physiology of adult rats and on the morphology of pyramidal neurons in the prelimbic area (PL) were analyzed. It was found that stress applied during the dark-phase (representing the activity period) resulted in a more pronounced decrease in body weight gain compared to stress applied during the light-phase (representing the resting period). In addition, increased weights of adrenal glands (as indicator of sustained stress) was observed only in rats being stressed during the dark-phase.

Morphological analysis of pyramidal cells in the PL indicated that stress caused a retraction of basal dendrites exclusively on the *right* hemisphere under both light conditions. This dendritic retraction was accompanied by decreases in spine density on dendrites proximal to soma, but not on distal dendrites. In the PL, stress effects on the morphology of pyramidal neurons differed between phases. Stress applied during the light-phase caused reduction in proximal basal dendrites, while stress applied during the dark-phase resulted in dendritic reduction in medium distances from the soma. In addition, a circadian rhythmicity in the morphology of basal dendrites was observed in control rats. During the dark-phase, control rats had shorter dendrites than during the light-phase. These results extend previous findings regarding the important role of the right hemisphere in the PFC in stress-related pathologies, and highlight the impact of the light cycle on the morphology of pyramidal neurons in the PL.

### **6.1.1 Rationale and hypothesis**

Clinical and experimental studies have shown that biological rhythm disturbances are often linked to stress-induced disorders. Stressful events involve – among others – the activation of the hypothalamus-pituitary-adrenal (HPA) axis resulting in increased plasma levels of corticosterone and ACTH (Retana-Marquez et al., 2003).

Rats are nocturnal animals and present maximal plasma levels of ACTH and corticosterone at the beginning of the active period (dark-phase) and minimum levels at the beginning of the resting period (light-phase) (Rybkin et al., 1997). Several reports have demonstrated that neuroendocrine responses to acute stress in rats shown circadian variations: Maximal increases in ACTH and corticosterone in response to a single stressful situation are observed at the beginning of the resting period (light-phase), and minimal stress responses are observed at the beginning of the active period (dark-phase) (Bradbury et al., 1991; Dunn et al., 1972; Torrellas et al., 1981). Similar neuroendocrine alterations were observed after chronic stress, when plasma corticosterone increased significantly only when immobilization stress was applied during the light-phase, but not during the dark-phase (Ushijima et al., 2006). In spite of the activation of the HPA-axis, a stress-induced dissociation between diurnal cycle and bodily changes has been proposed by several authors. Rats submitted to chronic restraint stress during the dark-phase but not during the light-phase presented significant body weight reductions compared to controls (Harris et al., 2002; D'Aquila et al., 1997). In addition, stress caused a decrease in sucrose intake in rats immobilized during the dark-phase but not during the light phase (D'Aquila et al., 1997). Therefore, the diurnal cycle seems to modulate the neuroendocrine and physiological responses to stressful events.

On the other hand, previous studies have demonstrated that corticosterone administration causes dendritic retraction in apical dendrites of pyramidal neurons located in the prefrontal cortex (PFC) (Wellman, 2001). Similar reductions in apical dendrites were found when rats are submitted to chronic restraint stress (Radley et al., 2004, 2006; Cook and Wellman, 2004; Perez-Cruz et al., 2007). It has been hypothesized that stress-induced dendritic remodeling in the PFC is partly caused by increases in corticosterone release (Wellman, 2001). Based on the circadian rhythmicity of corticosterone and the corticosterone-induced morphological changes in pyramidal neurons in the PFC, it was hypothesized that effects of stress in the morphology of

pyramidal neurons of the PFC would be different when stress is applied during the light-phase compared to the dark-phase. Before the present study, there were no reports regarding the impact of stress applied at different time points of the diurnal cycle on the morphology of pyramidal neurons in the PFC.

Different methods exist to analyze neuronal morphology; the intracellular injection of neurobiotin produces high quality results compared to other intracellular labeling techniques in terms of dendritic quantification, due to the visibility of more distal branches (Pyapali et al., 1998). Dendritic protrusions (i.e. spines) are difficult to visualize in neurobiotin injected neurons due to the thickness of the sections (400  $\mu\text{m}$  thickness). Structural plasticity can be studied by analyzing, the morphology of the dendrites (as described in Part II) and the density of dendritic spines (Gibb and Kolb, 1998). The vast majority of synaptic inputs onto neurons are on dendritic spines and about 90 % of excitatory synapses are made on these dendritic protrusions. Furthermore, in adult rats nearly all spines in the cortex have a synaptic contact (Gray, 1959; Wilson et al., 1983). Therefore, counting the number of spines allows an estimate of the number of synapses (Harris and Kater, 1994) and might give an estimate of the synaptic input a cell is receiving. In order to further explore the stress-induced morphological and functional changes (i.e. spine density) in pyramidal neurons of the prefrontal cortex, the Golgi-Cox technique was used in the present study to quantify spine density on basal dendrites in the PL.

Several morphological studies have found that most of the learning or drug-induced modifications in pyramidal neurons of the PFC, occur in basal dendrites of pyramidal cells located in layer III and V, but not in layer II (Kolb et al., 1998). Therefore, it was hypothesized that major morphological modifications induced by stress can be detected on basal dendrites of pyramidal neurons located in layer III of the PL.

A short-term stress protocol was applied during the light-phase and during the dark-phase, and the Golgi-Cox technique was used to quantify dendritic morphology and spine density in the prelimbic area with a left – right discrimination.

## **6.1.2 Design and methods**

### **6.1.2.1 Short-term restraint stress**

Animals were obtained as described in Part I (Methods, section 4.2.1). Male Sprague-Dawley rats weighing 150–170 g at the beginning of the experiments were

housed in groups of three animals per cage with *ad libitum* access to food and tap water. The first experimental phase (“Habituation”) lasted for 14 days, during which body weight was recorded daily. For the second phase of the experiment a modification of short-term stress was used as described previously (Brown et al., 2005). Briefly, animals were randomly assigned to the experimental groups (Stress, Control). The *Stress* (n= 12) and the *Control* (n= 12) group were further subdivided in two groups, one kept on a normal light cycle (07.00 lights on, 19.00 lights off), and the other group kept on an inverse light cycle (19.00 lights on, 07.00 lights off). Short-term restraint stress consisted of daily restraint stress during six hours a day (0900–1500 h) for a period of 7 days. During restraint, rats were placed in plastic tubes in their home cages and during this time they had no access to food or water. Control rats were not subjected to any type of stress, except daily handling. On day 8, between 9.00 and 10.00 hr, animals were weighed, deeply anaesthetized with a mixture of 50 mg/ml ketamine, 10 mg/ml xylazine, and 0.1 mg/ml atropine by i.p. injection and perfused intracardially with 0.9% saline.

Increased adrenal weight is an indicator of sustained stress. Therefore, the adrenals were removed from the animals immediately before perfusion and weighed. Data are expressed in milligrams per 100 g body weight.

The brains were removed and processed for a modified Golgi–Cox staining as described by Gibb and Kolb (1998). The Golgi-Cox solution was prepared by mixing 5 vol. parts of solution A (5 % potassium dichromate, Sigma-Aldrich), and 5 vol. parts of solution B (5 % mercuric chloride, Sigma-Aldrich). Four vol. parts of solution C (5 % potassium cromate, Sigma-Aldrich) were diluted in 10 vol. parts of distilled water. Solutions A and B were slowly mixed and poured into solution C under continuous stirring. This Golgi-Cox solution was kept in the darkness for at least five days before use. Brains were placed in brown glass bottles filled with 20 ml of the Golgi-Cox solution and stored in darkness for 14 days. On day 15, brains were transferred to a solution containing 30% sucrose (dissolved in distilled water) and stored for a minimum of 3 days before sectioning. A vibratome (Vibracut 2, FTB, Bensheim, Germany) was used to obtain coronal sections of 250  $\mu$ m thickness. The vibratome reservoir was filled with 6 % sucrose solution (dissolved in distilled water) to a level that covered the sectioning blade. PFC sections were collected on cleaned, gelatin-coated microscopic slides (four to six sections / slide) and the stain was developed with 100 % ammonium hydroxide (Sigma-Aldrich) for 30 min. Slides were immersed in Kodak Film Fixer for another 30 min, and then washed with distilled water, dehydrated in a series of alcohols (75 %

alcohol, 5 min; 95 % alcohol, 10 min; 100 % alcohol, 15 min) and cleared for 15 minutes in a solution containing 1 vol. part chloroform, 1 vol. part xylene, and 1 vol. part 100 % alcohol. Finally, sections were mounted using Eukitt (Kindler, Freiburg, Germany), coverslipped and stored in the darkness while drying for at least one month before analyses.

Pyramidal neurons impregnated with the Golgi–Cox solution were readily identified by their characteristic triangular soma shape, apical dendrites extending toward the pial surface, and numerous dendritic spines (Robinson and Kolb, 1997) (see Fig. 10). Pyramidal cells located in layer III of the PL, were identified by comparing the location of a selected neuron with the boundary patterns described before in Part I (section 4.3). The criteria for dendritic reconstruction and respective procedures are described in Part II (section 5.2.5). Four neurons of each hemisphere per animal were three dimensionally reconstructed and morphometric parameters were quantified. Statistical analyses of basal dendrites were performed with the final average of the total number of neurons / rat / hemisphere (n =6).

Spine quantification was performed under a 100× (N.A. 0.75) objective, giving a final magnification of 100,000× on the monitor. The step size of the circular cursor was 0.16  $\mu\text{m}$ , sufficiently below the limits of light microscopy resolution (about 0.25  $\mu\text{m}$ ). Spines were counted in dendrites longer than 10  $\mu\text{m}$  in at least six proximal (at a distance between 0 - 30  $\mu\text{m}$  from soma) and six distal (at a distance between 30 - 120  $\mu\text{m}$  from soma, being most of the times the terminal tips) branch segments, per neuron (see Fig 11). For spine counting, straight branches were preferred in order to have a good spine resolution. Spine densities were calculated as the number of spines /  $\mu\text{m}$  / neuron and at least 4 neurons per animal were analyzed. Statistical analyses of the spine density were performed with the final average of the total number of spines /  $\mu\text{m}$  / neuron / rat / hemisphere (n = 6). Spines located in proximal dendrites and spines located in distal dendrites were analyzed separately.

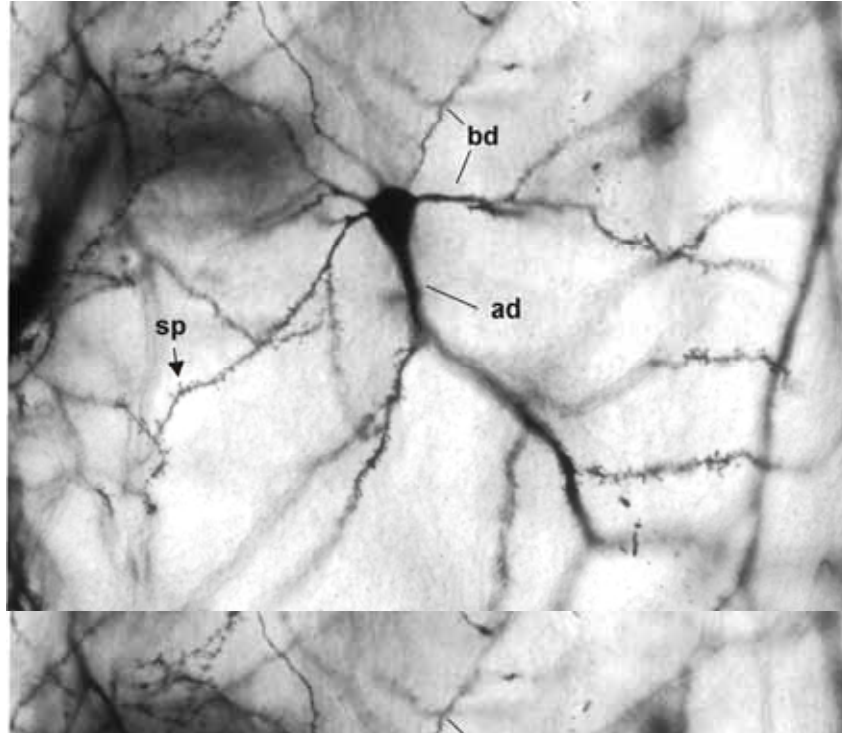


**Figure 10. Photomicrograph of a Golgi-stained neuron in layer III of the prelimbic area of a control rat**

Representative photomicrograph of a pyramidal neuron stained by the Golgi-Cox technique. Several basal dendrites (bd) and one single apical dendrite (ad) can be observed. Note spines (sp) as small protrusions present in both basal and apical dendrites. Scale bar = 100  $\mu\text{m}$ .

Numerical analysis and graphical processing of the neurons were performed with NeuroExplorer (MicroBrightField). In order to evaluate the distribution of dendritic arborizations in detail, the dendrites were subjected to Sholl analysis (Sholl, 1953). The virtual Sholl circles (see Fig 5) were set to 10  $\mu\text{m}$  constant increments between each radial bin. The number of times the basal dendrites cross a defined Sholl circle, is defined as the total number of intersections. Sholl plots were constructed by plotting the number of intersections as a function of distance from the soma center, which was set at zero.

### **6.1.3 Statistical analysis**

Body weight was measured on day 8 and compared to day 0. Changes in final body weight were compared among groups by two-way ANOVA (SPSS Inc., Chicago IL, v. 12.0), with group and phase as independent factors ( $P < 0.05$  was as considered significant). Relative adrenal glands weights (in milligrams per 100 g of BW) were also compared among groups with two-way ANOVA followed by a Bonferroni's *post-hoc* test.

To statistically evaluate the total dendritic length and the spine density in

proximal and distal basal dendrites, the mean differences were compared by two-way ANOVA (factors: group x hemisphere) followed by a Bonferroni's or Fisher *post-hoc* test when appropriate. For a closer inspection of the distribution of the dendritic material, the data from the Sholl analyses (number of intersections) as well as the length of all dendrites of a specific branch order (i.e. 1<sup>st</sup>, 2<sup>nd</sup>, 3<sup>rd</sup>....) were compared with three-way repeated measures ANOVA (factors: group x hemisphere x radius or branch order, respectively). Because the morphology of the pyramidal cells shows complex differences along the dendritic trees the *post-hoc* analyses were restricted to distinct radii (10  $\mu\text{m}$ , 20  $\mu\text{m}$ , 30  $\mu\text{m}$ , etc.) and single branch orders (1<sup>st</sup>, 2<sup>nd</sup>, 3<sup>rd</sup> order etc.; Statistica software package, Release 6.0 StatSoft Inc., Tulsa, OK, USA). Data are presented as the mean  $\pm$  SEM. Differences were considered significant at  $P < 0.05$ .

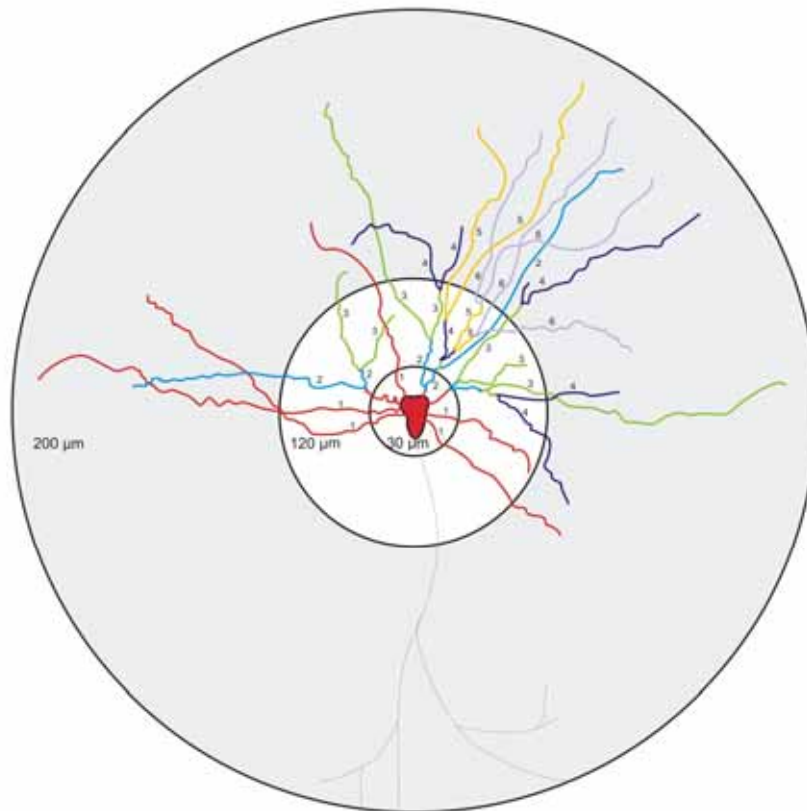


**Figure 11. Sholl analysis of basal dendrites and quantification of spines**

Basal dendrites were reconstructed by NeuroLucida Software, and analyzed by NeuroExplorer. The number of intersections in each Sholl ring, as well as length of all dendrites of specific branch orders (represented as line colors for each branch order, i.e. 1<sup>st</sup>, 2<sup>nd</sup>, 3<sup>rd</sup>...) were analyzed and compared between control and stressed rats. For spine quantification, the total number of spines on dendrites longer than 10  $\mu\text{m}$  were counted in at least six dendrites proximal to soma (proximal: 0 -30  $\mu\text{m}$ ) and six dendrites distal to soma (distal: 120 - 200  $\mu\text{m}$ ). Three concentric rings were drawn around the soma to delineate proximal and distal segments of basal dendrites.

## 6.1.4 Results

### 6.1.4.1 Effects of stress on body weight and adrenal glands

To assess the overall physiological effects of seven days of restraint stress, the final body weight was measured and compared between groups. Statistical analyzes by two-way ANOVA (factors: group x phase) showed a positive effect of phase on the final body weight ( $F_{(1,20)}=8.87$ ,  $p < 0.01$ ). *Post-hoc* test showed significant weight reductions in rats stressed during the dark-phase ( $268.0 \pm 2.6$  g) compared to control rats under both light phases (control light-phase:  $305.0 \pm 10.4$  g, and control dark-phase:  $296.3 \pm 6.4$  g,  $p < 0.05$  and  $p < 0.01$ , respectively) (Fig. 12A). This effect was corroborated by comparing body weight increases measured on day 8, expressed as percentage of body weight on day 0. Two-way ANOVA indicated effect of phase ( $F_{(1,20)}=10.7$ ,  $p < 0.01$ ) and group ( $F_{(1,20)}=10.07$ ,  $p < 0.01$ ) on final weight gain. *Post-hoc* test indicated that rats stressed during the dark-phase had significantly less weight gain ( $31.9 \pm 1.3$  %) compared to the other three groups (control light-phase:  $43.0 \pm 1.7$  %,  $p < 0.001$ ; stress light-phase:  $39.4 \pm 1.8$  %; and control dark-phase:  $39.6 \pm 1.9$  %,  $p < 0.01$ ) (Fig 12B). The relative weight of the adrenal glands (mg / 100 g body weight) showed a positive interaction between factors ( $F_{(1,17)}=4.49$ ,  $p < 0.05$ ). Rats stressed during the dark-phase presented enlarged adrenal glands ( $1.47 \pm 0.05$  mg / 100 g BW) compared to controls (control dark-phase:  $1.29 \pm 0.05$  mg / 100 g BW;  $p < 0.05$ ) (Fig 12C).



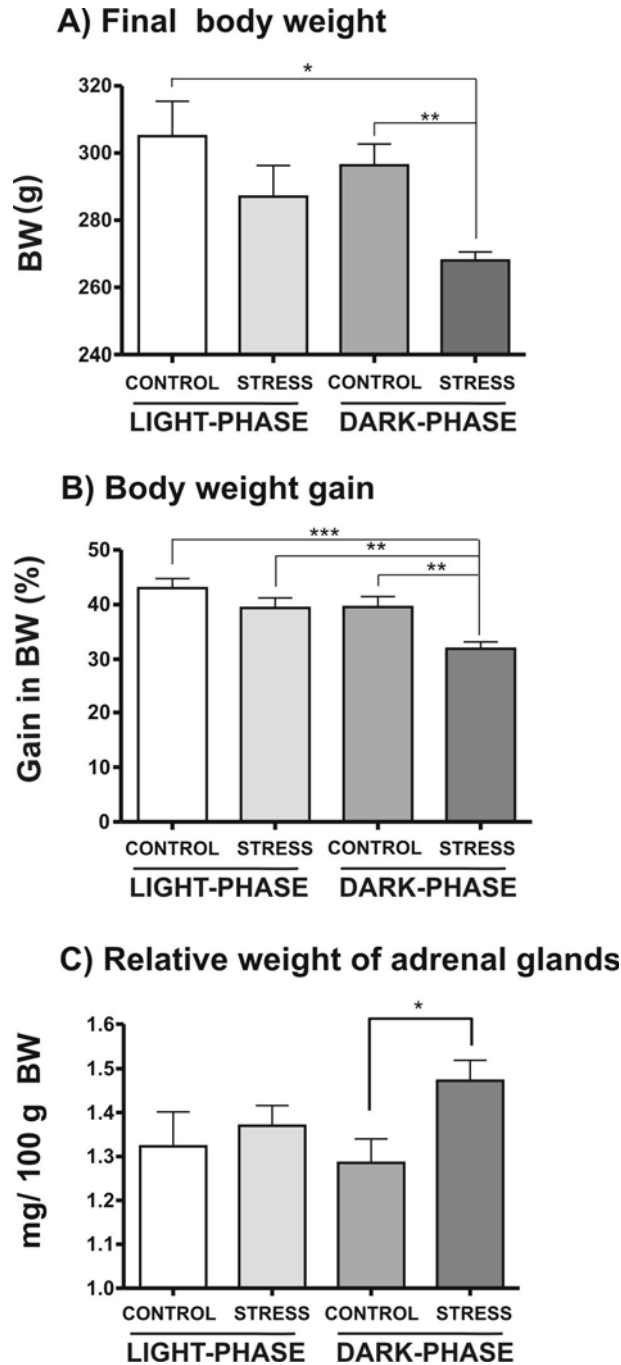


**Figure 12. Effects of seven days of restraint stress on body and adrenal glands' weight**

**A**, Stress caused a significant reduction in the final body weight only when rats were stressed during the dark-phase ( $p < 0.01$ ). **B**, Body weight gain as percentage of increased body weight from day 0 to day 8 was significantly lower in rats being stressed during the dark-phase compared to controls in the dark-phase ( $p < 0.01$ ) and controls and stressed rats in the light-phase ( $p < 0.001$  and  $p < 0.01$ , respectively). **C**, In the same order, adrenal glands were enlarged only in rats stressed during the dark-phase ( $p < 0.05$ ) but not during the light-phase. Data presented as mean  $\pm$  SEM. \* $P < 0.05$ , \*\*  $P < 0.01$ , \*\*\*  $P < 0.001$  significant differences determined by two-way ANOVA followed by Bonferroni's *post hoc* test.

### **6.1.4.2 Effects of stress on the morphology of basal dendrites of pyramidal neurons in the prelimbic area**

#### **6.1.4.2.1 Stress during the light phase**

To assess the impact of stress applied during the light-phase on the dendritic remodeling, pyramidal neurons of PL were analyzed in both hemispheres. Two-way ANOVA (hemisphere x group) indicated an effect of hemisphere ( $F_{(1,14)}=6.35$ ,  $p < 0.05$ ) on the total dendritic length. Bonferroni's *post-hoc* test showed significant dendritic retractions in the right hemisphere of stressed rats compared to the other three groups (control-left vs. stress-right by 23%,  $p < 0.01$ ; control-right vs. stress right by 25%; stress-left vs. stress-right by 27 %; all  $p < 0.05$ ) (Fig 13A left panel).

In order to determine where these differences might be located, Sholl data was statically analyzed by a three-way ANOVA with repeated measures. The number of intersections as a function of the distance from the soma was positively affected by radius ( $F_{(24,408)}=69.49$ ,  $p < 0.001$ ) and there was a weak interaction radius x group x hemisphere ( $F_{(24,480)}=1.69$ ,  $p < 0.05$ ). Fisher's *post-doc* test indicated significant reductions exclusively in the right hemisphere of stressed rats compared to control rats in segments proximal to soma (40  $\mu\text{m}$ , 60  $\mu\text{m}$  - 80  $\mu\text{m}$  and 100  $\mu\text{m}$ ,  $p < 0.05$ ; 50 $\mu\text{m}$ ,  $p < 0.001$ )(Fig. 14A). To assess how stress affects the complexity of the basal dendritic trees, the length of dendrites of different branch orders were compared between controls and stressed rats. Three-way ANOVA with repeated measures showed a positive effect of branch order ( $F_{(5,80)}= 10.37$ ,  $p < 0.0001$ ) and hemisphere ( $F_{(1,80)}=5.03$ ,  $p < 0.05$ ). Fisher's *post-hoc* test indicated significant reductions in dendrites of the branch order 2 in the left hemisphere of stress rats compared to controls ( $p < 0.05$ ) (Fig. 15A). In addition, pyramidal neurons in the right hemisphere of control rats presented higher branch order (i.e. branch order 9) compared to the other groups (Fig 15A). Hemispheric differences in control and stressed rats were also observed. In controls, the right hemisphere presented branch orders 9 whereas the left hemisphere reached only branch order 7. In the stress group, it was the left hemisphere that presented higher branch orders (order 8) compared to the right (order 6) ( $p < 0.05$ ) (Fig 15A).

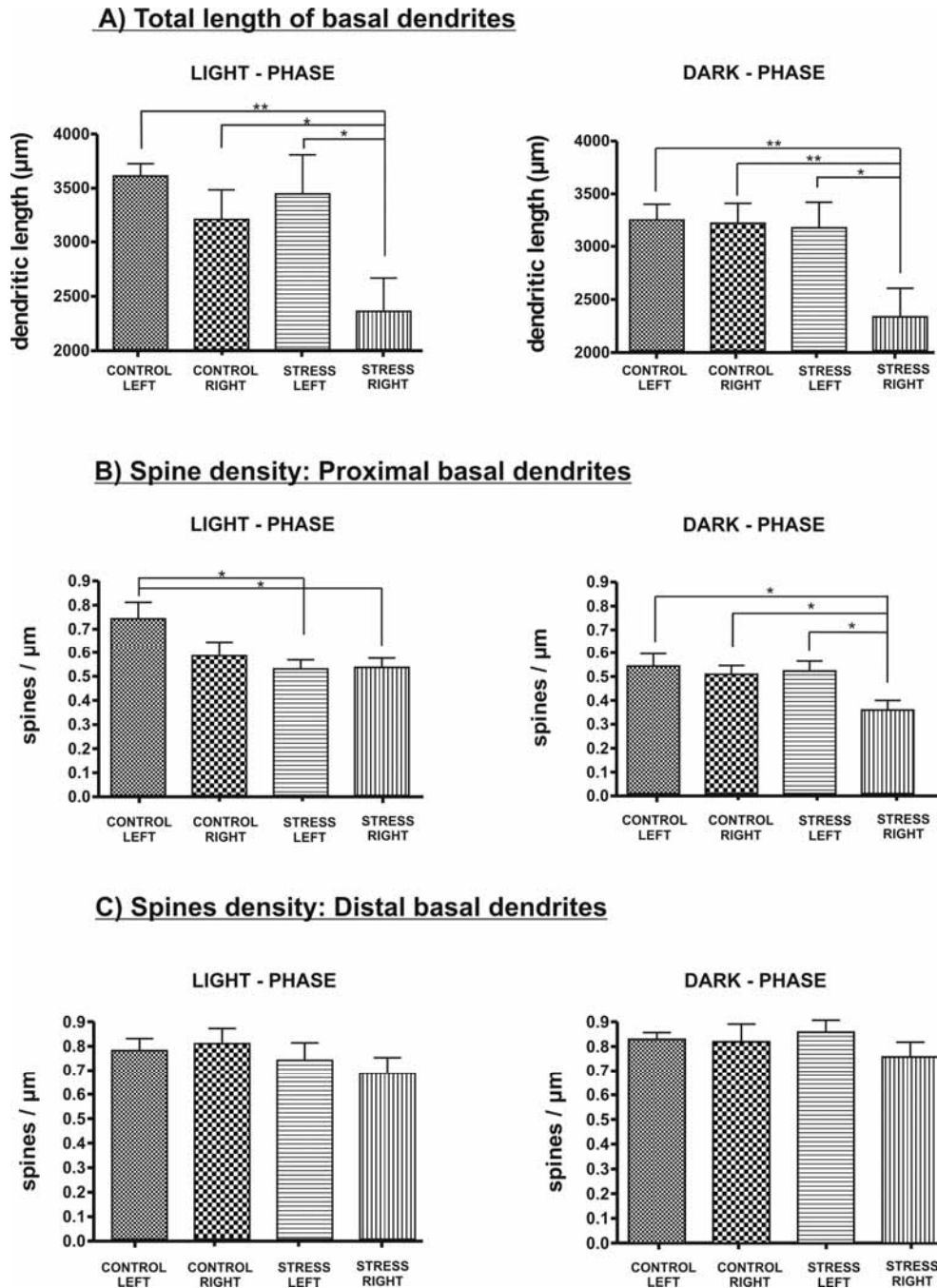
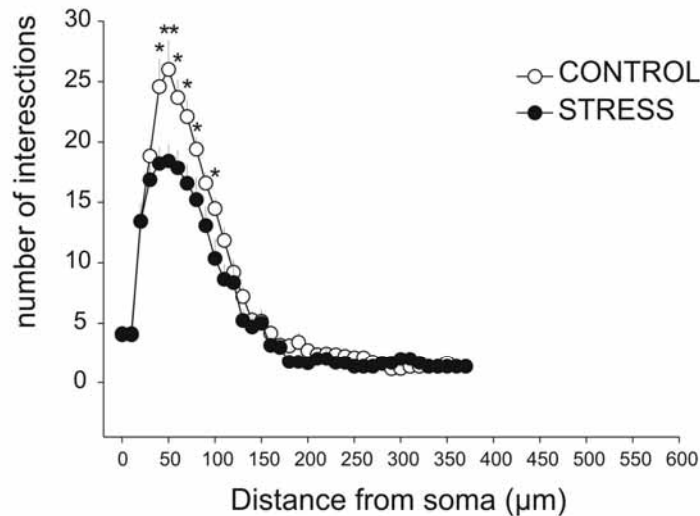


**Figure 13. Basal dendritic length and spine density in pyramidal neurons in the prelimbic area**

**A**, Light phase (left panel): Stress caused a significant reduction in the total basal dendritic length in pyramidal neurons of the right hemisphere compared to the three other groups. Dark-phase (right panel): Stress caused a reduction in the total basal dendritic length in the right hemisphere similarly to the effects of stress applied during the light-phase (**A**). **B**, Light-phase (left panel): Spine density on proximal dendrites was lower in the left and right hemispheres compared to control-left (both,  $p < 0.05$ ). Dark-phase (left panel): A strong reduction in spine density was detected in the right hemisphere of stressed rats compared to the other three groups (all  $p < 0.05$ ). **C**, Stress had no significant effects on the spine density on distal dendrites either during light-phase or dark-phase conditions. Data are mean  $\pm$  SEM. \*  $P < 0.05$ , \*\*  $P < 0.01$  significant differences as determined by two-way ANOVA followed by Bonferroni's *post hoc* test.

## LIGHT-PHASE

### A) Number of intersections: RIGHT hemisphere



### B) Number of intersections: LEFT hemisphere

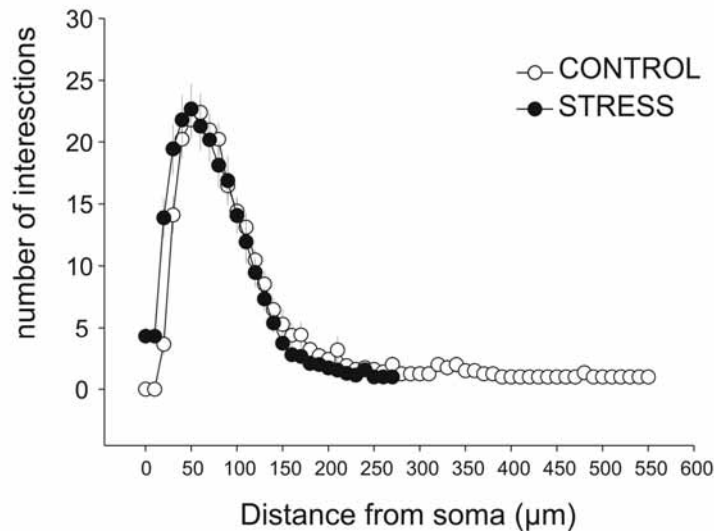


**Figure 14. Number of intersections of basal dendrites in rats stressed during the light-phase and controls**

The number of intersections is defined as the total number of intersecting points where basal dendrites cross a defined Sholl ring (see text for details). Rats were stressed during the light-phase and differences in the dendritic morphology were investigated with a hemispheric discrimination. **A**, Right hemisphere: Stress caused a drastic reduction of basal dendrites in segments proximal to soma (40 µm, 60 - 80 µm, 100 µm,  $p < .05$ ; and 50 µm,  $p < 0.01$ ). **B**, Left hemisphere: Note that pyramidal neurons of the left hemisphere in control rats presented more extended dendrites in distal segments of the basal trees compared to those of the right-hemisphere, but this difference was not significant. Data presented as mean  $\pm$  SEM. \*\* $P < 0.01$  and \*  $P < 0.05$ .

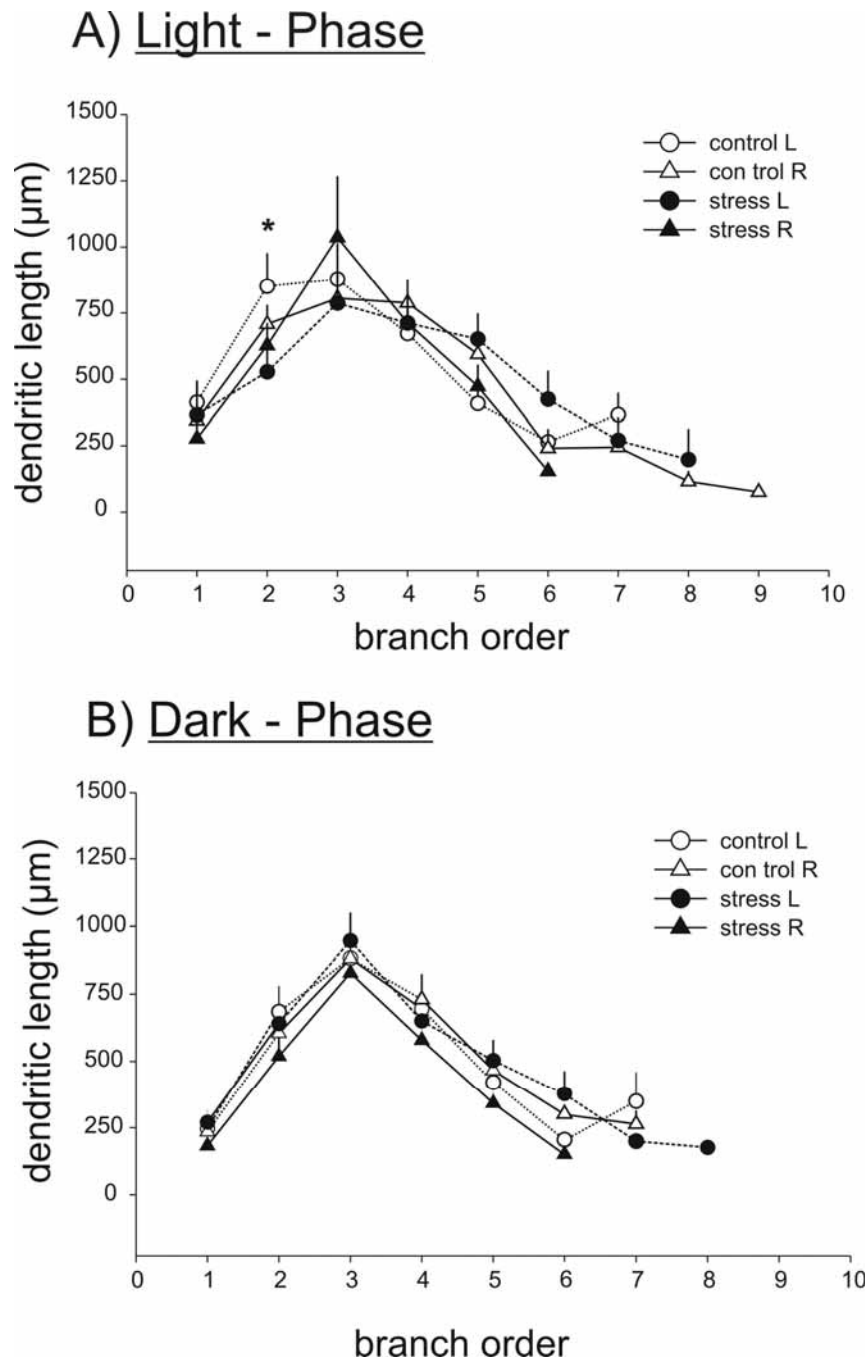


**Figure 15. Length of basal dendrites of distinct branch orders in the prelimbic area in control and stressed rats**

The length of dendrites of a specific branch order (i.e. 1<sup>st</sup>, 2<sup>nd</sup>, 3<sup>rd</sup>...) was compared between control and stressed rats under different light conditions with a hemispheric discrimination. **A**, Light-phase condition: Left hemisphere of stressed rats showed shorter branches order 2 compared to the left hemisphere of control rats ( $p < 0.05$ ). Hemispheric differences were found between groups: higher branching orders were observed in right hemisphere of controls (right: 9; left: 7), but in the left hemisphere of stressed rats (right: 6; left: 8). **B**, Dark-phase condition: No significant differences were found for any branch order. Note that hemispheric differences found in controls in the light-phase (A) disappeared under the dark-phase conditions (B). For stressed rats, same hemispheric differences were observed under both light conditions. Data presented are  $\pm$  SEM. \*  $P < 0.05$  significant differences.

The number of spines in basal dendrites at distances proximal or distal to soma was also analyzed. Dendrites proximal to soma presented a positive effect of group ( $F_{(1,14)}=5.24$ ,  $p > 0.05$ ) on the spine density. Stress caused significant reductions in spine densities in the left and right hemispheres of stressed rats compared to left hemisphere of controls (by 16.5 % and 15.7 %, respectively; both  $p < 0.05$ ) (Fig. 13B, left panel). Spine densities in dendrites distal to soma were not modified by stress (Fig. 13C, left panel)

#### **6.1.4.2.2 Stress during the dark-phase**

The impact of stress applied during the dark-phase was evaluated by determining the overall dendritic length of basal dendrites by two-way ANOVA. Results indicated that the total dendritic length was positively affected by group ( $F_{(1,19)}=6.25$ ,  $p < 0.05$ ) and group x hemisphere ( $F_{(1,19)}=4.61$ ,  $p < 0.05$ ). Bonferroni's *post-hoc* test demonstrated that stress caused significant dendritic reductions in the right hemisphere of stressed rats compared to the left (by 26 %,  $p < 0.05$ ), and compared to both hemispheres of control rats (right: by 28 %; left by 30 %; both  $p < 0.01$ ) (Fig 13A, right panel).

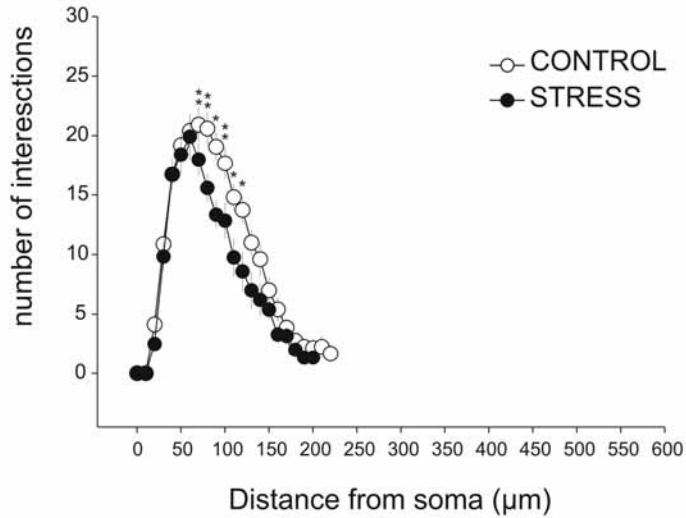
Sholl analyses were used to compare the total number of intersections across the dendritic tree. Three-way ANOVA indicated a positive effect of group x hemisphere ( $F_{(1,703)}=4.17$ ,  $p < 0.05$ ), radius ( $F_{(19,703)}=141.3$ ,  $p < 0.0001$ ), and an interaction radius x hemisphere x group ( $F_{(19,703)} = 2.84$ ,  $p < 0.001$ ). *Post-hoc* test indicated that stress causes a significant decrease in number of intersections in middle portions of basal dendrites in the right hemisphere (70  $\mu\text{m}$  - 80  $\mu\text{m}$ , and 100  $\mu\text{m}$ ,  $p < 0.01$ ; 90  $\mu\text{m}$  and 110  $\mu\text{m}$ ,  $p < 0.01$ ) (Fig. 16A). In the left hemisphere, no significant differences were found between stress and control rats (Fig. 16B). In addition, hemispheric differences were found in stressed rats, where right hemisphere presented shorter dendrites compared to the left in middle portions of the dendritic trees (80  $\mu\text{m}$ , 100 - 120  $\mu\text{m}$ ,  $p < 0.01$ ; data not shown). To assess the impact of stress on the complexity of the dendritic arbors, the length of dendrites of different branch orders were analyzed. Three-way ANOVA indicated a positive effect of branch order ( $F_{(5,135)}=17.8$ ,  $p < 0.001$ ), but no significant effect of stress on the length of dendrites of specific branch orders. Hemispheric differences were observed in stressed rats, presenting high branch orders in the right hemisphere (i.e. branch order 8) compared to the left (branch order 6). No hemispheric

differences were found in control rats (Fig. 15B).

The number of spines in proximal and distal dendrites was quantified and analyzed by two-way ANOVA. In dendrites proximal to soma there was a positive effect of hemisphere ( $F_{(1, 14)}=4.75$ ,  $p < 0.05$ ) on the spine density, with significant reductions in the right hemisphere of stressed rats compared to the other groups (control-left by 35 %; control-right by 31 %; stress-left by 32 %; all  $p < 0.05$ ) (Fig 13B, right panel). In more distal dendritic segments, spine density was affected neither by stress nor by hemisphere (Fig 13C, right panel).

## DARK-PHASE

### A) Number of intersections: RIGHT hemisphere



### B) Number of intersections: LEFT hemisphere

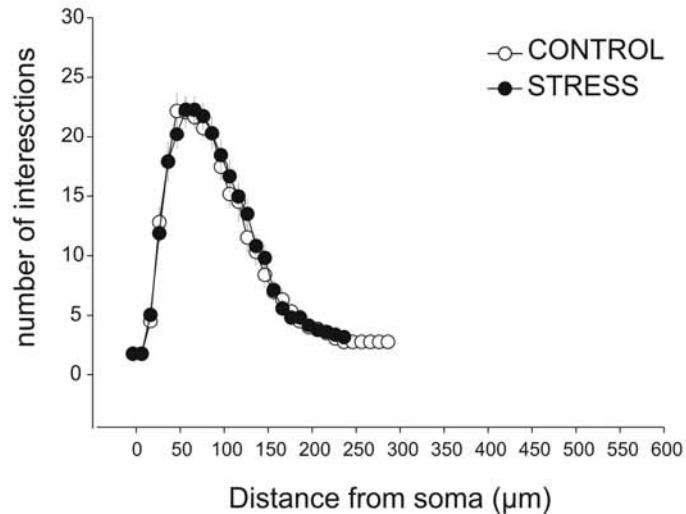


**Figure 16. Number of intersections of basal dendrites in rats stressed during the dark-phase and controls**

Rats were submitted to restrain stress during the dark-phase and number of intersections across basal dendrites was compared to controls. **A**, Right hemisphere: stress caused significant reductions in number of intersections in middle portions of the basal dendrites (70 – 80 µm and 100 µm,  $p < 0.01$ ; 90 µm, 110 -120 µm,  $p < 0.05$ ). Left hemisphere: stress did not affect the number of intersections in stressed rats compared to controls. Data are mean  $\pm$  SEM. \*\* $P < 0.01$  and \*  $P < 0.05$ .



### **6.1.5 Discussion**

This study demonstrates that stress applied during the dark-phase had a stronger impact on the physiology compared to stress applied during the light-phase, as reduced body weight gain and increased adrenal weights were significant only in rats being stressed during the dark-phase. These results agree with previous studies (Harris et al., 2002; D'Aquila et al., 1997) and coincide with the hypothesis that chronic restraint stress induces distinct disturbances in bodily stress-responses depending on the diurnal cycle.

Analysis of the dendritic morphology showed that control rats during the dark-phase, corresponding to the active-period, presented shorter dendrites compared to the light-phase. Stress-induced dendritic retractions, however, were similar under both light-conditions. These results could be related to a disruption of the diurnal rhythm in the HPA axis activity. The circadian rhythm of corticosterone (highest at the beginning of dark-phase and lowest at the beginning of the light-phase (Rybkin et al., 1997) is lost in chronically stress rats with maximal corticosterone responses to stress when it is applied during the light-phase and minimal response to stress during the dark-phase (Retana-Marquez et al., 2003). Structural modifications and neuronal plasticity induced by corticosterone have been reported previously for hippocampal (Watanabe et al., 1992a) and PFC (Wellman, 2001) pyramidal neurons. Based on these findings, it can be proposed that diurnal rhythms of corticosterone are partially linked to the intrinsic dendritic morphology observed in control rats, as longer dendrites are found at the lowest corticosterone levels (light-phase), and shorter dendrites are found when corticosterone is at the highest level (dark-phase). Other neurotransmitter systems might be implicated in such morphological modifications, as circadian rhythm patterns have been described for e.g. serotonin (Nakayama, 2002; Rueter and Jacobs, 1996), noradrenalin and adrenaline (de Boer and van der Gugten, 1987).

In this context it is interesting to note that the noradrenergic system is particularly active during times of vigilance, which is during the active period in rats (dark-phase) (Aston-Jones and Bloom, 1981). Furthermore, as mentioned in the introduction, corticosterone receptors (GRs and MRs) upon activation, translocate to the cell nucleus and bind specific response elements (GREs) in the promoter region of target genes (Kitchener et al., 2004). Diurnal patterns in GRs nuclear translocation have been described, and more GR nuclear translocation has been found during the dark-phase

compared to the light-phase (Kitchener et al., 2004). Thus, the circadian activity of several neurotransmitter and neuromodulator systems being highest during the dark-phase might play an important role in the structural remodeling of pyramidal neurons of the PFC. Further analysis under hypocortisolic (induced by adrenalectomy, ADX) and hypercortisolic (ADX with high-dose dexamethasone supplementation) rats would provide better understanding of the morphological changes in pyramidal neurons of the PFC induced by stress with a direct focus on the impact of corticosterone plasma levels.

On the other hand, the effects of stress on pyramidal neurons of the PL occurred exclusively in the right hemisphere (see Fig. 17). These are new finding, as previous studies (using light-phase conditions) failed to detect any changes in basal dendrites (Brown et al., 2005). Therefore, discrepancies between the previous and the present results might be explained by the use of a detailed analysis discriminating the left and the right hemispheres. The criterion for cell sampling is another possible explanation. Brown et al. sampled pyramidal cells located mainly in the border between layer II and III (150 - 250  $\mu\text{m}$  from pial surface) and irrespectively from different PFC areas (IL, PL and ACx) (Brown et al., 2005). In this study selected neurons were located in layer III (300 – 450  $\mu\text{m}$  from the pial surface) and restricted to the PL area (using the boundary definition developed in Part I).

Structural changes in neuronal connections are believed to be important components underlying brain plasticity. Synaptic input correlates with dendritic geometry (Purves and Lichtman, 1985) and the structure of the dendritic trees affects neuronal firing properties (Schaefer et al., 2003). In this study, the Golgi-cox technique was employed to analyze dendritic morphology, and to evaluate changes in dendritic spine (Gibb and Kolb, 1998). The vast majority of synaptic inputs onto neurons are on dendritic spines and about 90 % of excitatory synapses are made on these dendritic protrusions. Functional studies indicated that increased spine size and spine numbers are associated with long-term potentiation (LTP) (Nimchinsky et al., 2002) whereas a decrease in spine number and/or size is associated with long-term depression (LTD) (Zhou et al., 2004). The present results might have functional implications, as it was demonstrated that stress caused significant reductions in spine densities only in basal dendrites proximal to soma, but not in distal dendrites. Similarly to the dendritic changes induced by stress, spine reductions were found only in pyramidal neurons in the right hemisphere. This lateralized alteration in spine number after stress is a new finding as no previous studies have reported left – right differences in spine densities of pyramidal neurons of the rat

PFC. Lateralized specializations of the PFC, though, have been demonstrated in regards to stress responses (see Sullivan, 2004). Most of the neuroendocrine and hormonal systems activated by stress target principally the right hemisphere (Carlson et al., 1991; Carlson et al., 1993; Andersen and Teicher, 1999; Thiel and Schwarting, 2001; Slopsema et al., 1982; Berridge et al., 1999). Lesioning the right PFC reduced the neuroendocrine responses triggered by stress (Sullivan and Gratton, 1999). The present study offers further evidence of a lateralized stress response in the PFC, where the right hemisphere presented reduced dendritic lengths in basal dendrites proximal to soma with a simultaneous reduction in spine density in the same branches.

Some studies have tried to understand the impact of stress on PFC functioning. The PFC and respective sub-areas are well known for their cognitive and emotional functions, but they also have important visceromotor regulatory functions (Heidbreder and Groenewegen, 2003). Lesioning the ventral PFC (i.e. the infralimbic area) reduces the anticipatory increases in body temperature to the presentation of food, but prompted the anticipatory locomotor activity (Recabarren et al., 2005). On the other hand, the same PFC lesions impair fear conditioning, but fear extinction seems to be increased after PFC stimulation (Quirk et al., 2003). Moreover, Ushijima et al. (2006) reported that chronic restraint stress disrupted the rhythm pattern of rectal temperature, where ventral areas of the PFC are mainly implicated (Recabarren et al., 2005). Thus, ventral parts of the PFC (IL, PL) are intimately involved in stress responses and impaired functioning of these areas may lead to abnormal stress responses.

On the other hand, chronic stress impairs spatial memory (Conrad et al., 1996) and produces depressive-like symptoms such as anhedonia (Gronli et al., 2005). Chronic restraint stress also decreases sexual activity in male rats and increases activity in the open field test (Gronli et al., 2005). The sleep-pattern is also affected by chronic stress by increasing the number of REM episodes and arousals (Gronli et al., 2004). Mizoguchi et al. (2000) have related the impaired memory and learning caused by stress with dysfunctions of the dopamine system in the PFC (Mizoguchi et al., 2000). However, more functional studies are required in order to understand the impact of dendritic remodeling caused by stress in the right hemisphere of the PFC.

The results from the present study demonstrated that light-phase conditions have a differential impact on the physiological responses to stress. However, the morphology of basal dendrites of pyramidal neurons in the PL was similarly affected in under both light-conditions. The importance of hemispheric discrimination is highlighted as stress causes a reduction in basal dendritic length and in spine density exclusively on basal dendrites of the right PL.

## STRESS EFFECTS ON BASAL DENDRITES

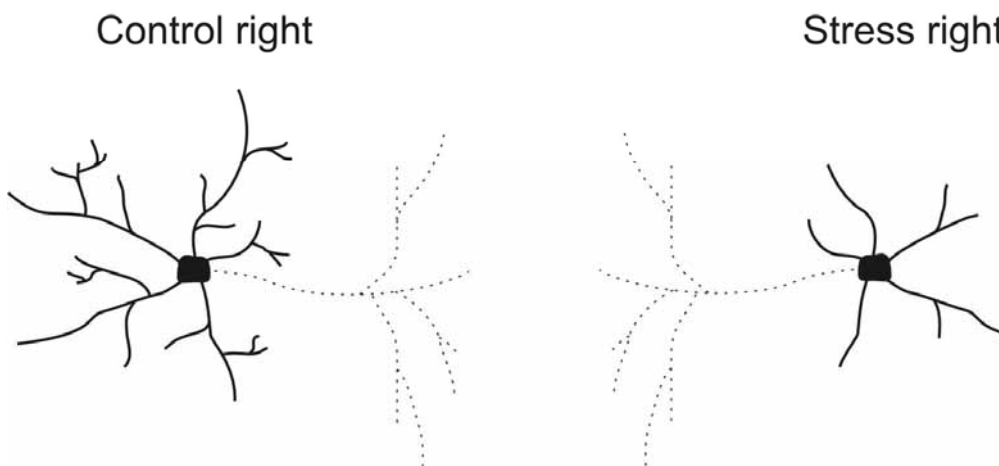


**Figure 17. Simplified drawing illustrating the morphological remodeling of basal dendrites on pyramidal neurons caused by chronic stress**

This scheme represents the dendritic remodeling resulting from 7 days immobilization stress. Stress caused a retraction in proximal basal dendrites in the right hemisphere with a concomitant reduced branching complexity. Because stress caused significant differences mainly in the right hemisphere, schematic neurons representing the left hemisphere are not shown (see Results for details).

## 6.2 Morphology of basal dendrites of pyramidal neurons in the prelimbic area in relation to the diurnal cycle

### Summary

Rats are nocturnal animals and hence, are active during the dark phase. Diurnal variations in behavioral activity are highly correlated with neuroendocrine circadian rhythms, such as the rhythm of the hypothalamus-pituitary-axis, noradrenalin and serotonin. On the other hand, corticosterone administration can induce plastic changes in apical dendrites of pyramidal neurons of the prefrontal cortex (PFC) and depletion of monoamine neurotransmitters after sleep deprivation increase spine density in motor cortex. Therefore, it can be hypothesized that neuroendocrine circadian variations will have an affect on the morphology of pyramidal cells of the PFC.

This study focused on the effects of the diurnal cycle (light- vs dark-phase) on the morphology of basal dendrites of pyramidal neurons in the rat prelimbic area. Data from section 6.1 was re-analyzed in order to compare diurnal variations in the morphology of pyramidal neurons of control and stressed rats. Results show that the total length of basal dendrites did not change across the diurnal cycle in control rats. A closer inspection of the dendritic arborization, however, demonstrated an effect of light-cycle on proximal basal dendrites in the right hemisphere, and on distal dendrites in the left-hemisphere. In contrast, animals experiencing stress at different time points of the diurnal cycle presented dramatic reductions in the total dendritic length in the right hemisphere compared to left in a parallel manner under both light-conditions.

Spine density in dendrites proximal to soma presented a circadian variation in the *left* hemisphere of controls, with more spine densities during the light-phase compared to the dark-phase. In stressed rats, spine density presented an opposite circadian variation, in that the *right* hemisphere showed more spines during the light-phase compared to the dark-phase. These results indicate that the number of spine found in basal dendrites depends on diurnal activity and stress affects this circadian variation.

It is concluded that hemisphere and light-phase discrimination are crucial parameters that determine the length of dendrites of pyramidal neurons and their number of spines.

### **6.2.1 Rationale**

Rats are nocturnal animals whose active period is during the dark-phase (lights-off) and their resting period during the light-phase (lights-on). Their circadian activity is accompanied by diurnal changes in the hypothalamus-pituitary-adrenal (HPA) axis activity and other neurotransmitter systems. For example, maximal levels of ACTH and corticosterone in rats are found at the beginning of the active period (dark-phase) and minimum levels are found at the beginning of the resting period (light-phase) (Retana-Marquez et al., 2003; Nicholson et al., 1985). Similar cyclic pattern (higher plasma levels during the active period or dark-phase) are described - among others - for serotonin (Nakayama, 2002), noradrenalin and adrenaline (de Boer and van der Gugten, 1987). The important role of noradrenalin in attention, arousal and vigilance (Aston-Jones and Bloom, 1981) is well established. Neurons in the locus coeruleus (LC) provide noradrenergic innervation to different areas of the brain such as the PFC. LC neuronal activity is directly correlated with the sleep-walking cycle, while during REM-sleep episodes they become virtually silent (Aston-Jones and Bloom, 1981). Ramesh et al. (1999) show that sleep deprivation resulted in reduced levels of different monoamine neurotransmitters (i.e. dopamine, serotonin, noradrenalin), but at the same time dendritic spine counts in motor cortex was increased. Thus, it can be suggested that low levels of monoamines (as during the light-phase of the rat) yield spine formation and dendritic growing. On the other hand, previous studies have demonstrated that corticosterone administration causes dendritic retraction in apical dendrites of pyramidal cells located in the PFC (Wellman, 2001). Based on the circadian cycle of corticosterone and other neurotransmitter systems, and the corticosterone-induced morphological changes in pyramidal cells of the PFC (Wellman, 2001) it was hypothesized that differences in the morphology of pyramidal neurons of the PFC can be detected in the light-phase compared to the dark-phase of the diurnal cycle.

The diurnal variations in dendritic morphology and in spine density in basal dendrites of pyramidal cells of the prelimbic area (PL) were analyzed in controls and in stress rats, separately.

### **6.2.2 Design and methods**

For this study the same data as in section 6.1 was used, but the focus of this analysis was to compare the circadian variation in the morphology of pyramidal cells in

control and stressed rats separately. The total dendritic length of basal dendrites and the spine densities in proximal and distal basal dendrites were compared by two-way ANOVA, with hemisphere and phase as independent factors (SPSS Inc., Chicago IL, v. 12.0). Sholl data was analyzed by three-way ANOVA, with hemisphere, phase and radius as independent factors. These analyzes were followed by Bonferroni's *post-hoc* test for statistical differences (Statistica software package, Release 6.0 StatSoft Inc., Tulsa, OK) ( $p < 0.05$ ).

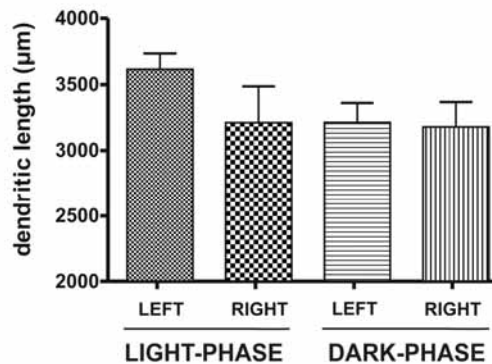
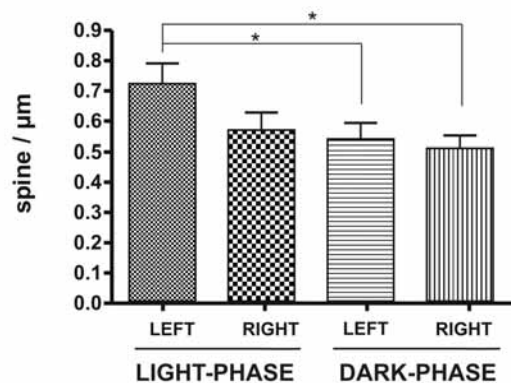
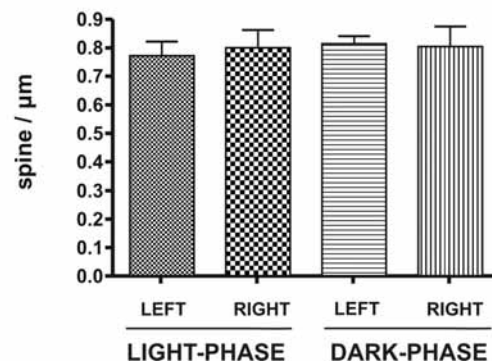
### **6.2.3 Results**

#### **6.2.3.1 Circadian variation in the morphology of pyramidal neurons in control rats**

The length of basal dendrites of pyramidal cells sampled either during the light-phase or during the dark-phase showed a positive interaction between factors ( $F_{(1,18)}=1181.9$ ,  $p < 0.0001$ ). There were slightly longer dendrites in the left hemisphere in the light-phase compared to the dark-phase, but this was not significant (Fig 18A).

A closer inspection of the dendritic arborization by Sholl analysis demonstrated an effect of radius ( $F_{(19,570)}=97.45$ ,  $p < 0.001$ ) and radius x phase ( $F_{(19,570)}=4.29$ ,  $p < 0.001$ ). Fischer *post-hoc* test indicated that pyramidal neurons in the right hemisphere presented higher numbers of intersections proximal to the soma during the light-phase compared to the dark-phase (right: 40 - 50  $\mu\text{m}$ ,  $p < 0.05$ ) (Fig 19A). Importantly, pyramidal neurons in the right hemisphere showed longer distal dendrites (> 350  $\mu\text{m}$ ) during the light-phase compared to the dark-phase (> 200  $\mu\text{m}$ ) but this was not significant (Fig 19A). In the left hemisphere, distal dendrites extended more during the light-phase (> 550  $\mu\text{m}$ ) compared to dark-phase (> 300  $\mu\text{m}$ ) but this was not significant (Fig. 19B).

Spine density analyses showed an effect of hemisphere ( $F_{(1,14)}=5.78$ ,  $p < 0.05$ ) in proximal dendrites. Lower spine densities were found during the dark-phase in both hemispheres compared to the left hemisphere during the light-phase ( $p < 0.05$ ) (Fig. 18B). Distal dendrites presented no differences either between hemispheres or phases (Fig 18C).

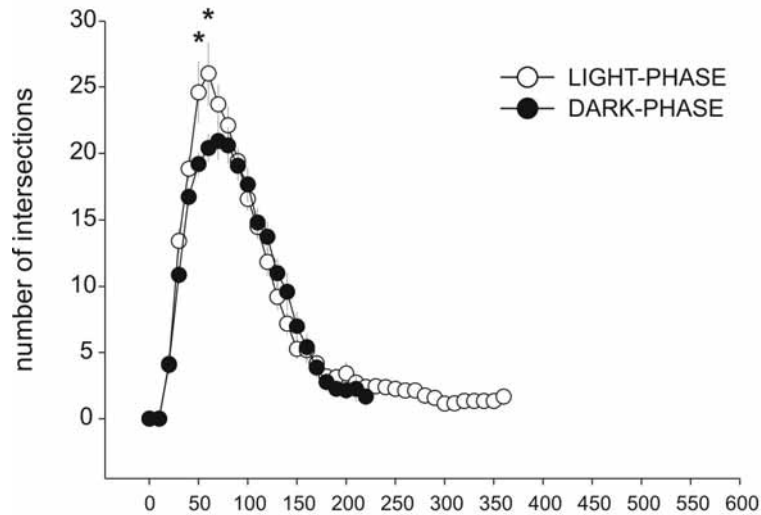
**A) Total length of basal dendrites in control rats****B) Spine density: Proximal dendrites in control rats****C) Spine density: Distal dendrites in control rats****Figure 18. Impact of the diurnal cycle on dendritic length and spine density in control rats**

The diurnal variations in the morphology of pyramidal neurons were analyzed between the light-phase and the dark-phase with left-right discrimination. **A**, No significant differences were observed for the total dendritic length in control rats tested during light- or dark-phase. **B**, Spine density on basal dendrites proximal to soma was higher in left hemisphere in the light-phase compared to both hemispheres in the dark-phase ( $p < 0.05$ ). **C**, No differences were observed in distal basal dendrites. Data presented as mean  $\pm$  SEM. \*  $P < 0.05$ .

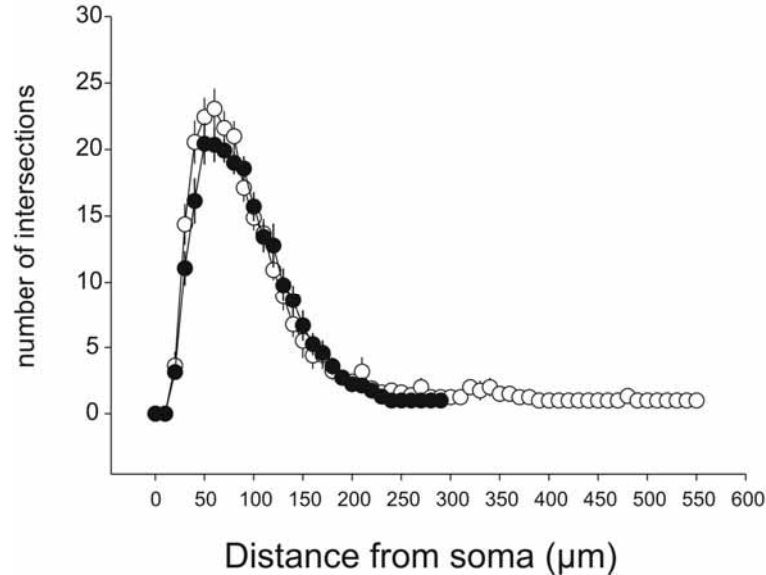


## CONTROL RATS

### A) Number of intersections: Right hemisphere

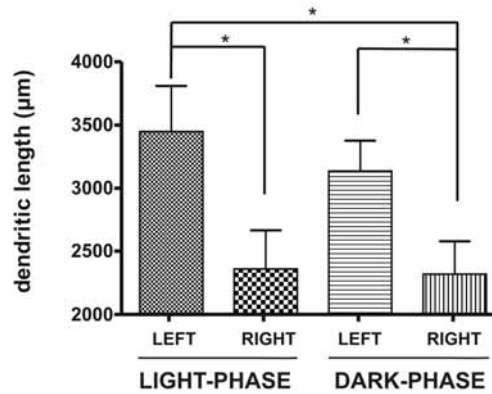
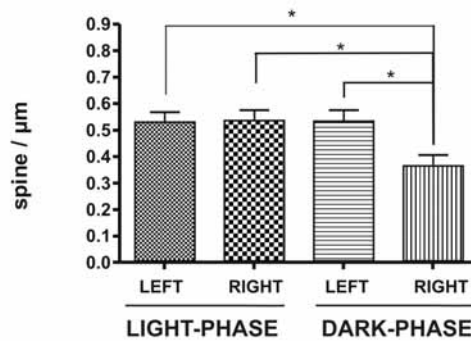
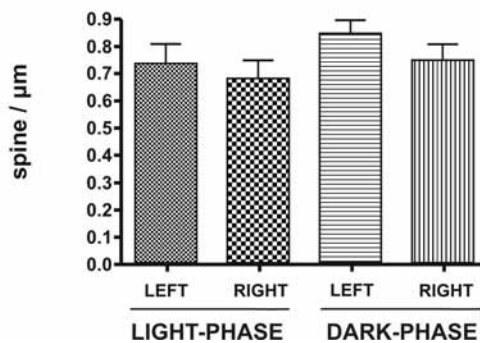


### B) Number of intersections: Left hemisphere



**Figure 19. Diurnal variations in the total number of intersections in basal dendrites of control rats**

This figure shows the effects of light schedule on the total number of intersections in control rats. **A**, Right hemisphere: the diurnal cycle affected the total number of intersections in basal dendrites as showed by a reduced number of intersections in proximal distances to soma (40 - 50 µm,  $p < 0.05$ ). **B**, Left hemisphere: Note that under both light conditions, pyramidal neurons extended longer in distal distances from the soma during the light-phase compared to the dark-phase, although this was not significant. Data are mean  $\pm$  SEM. \*  $P < 0.05$ .

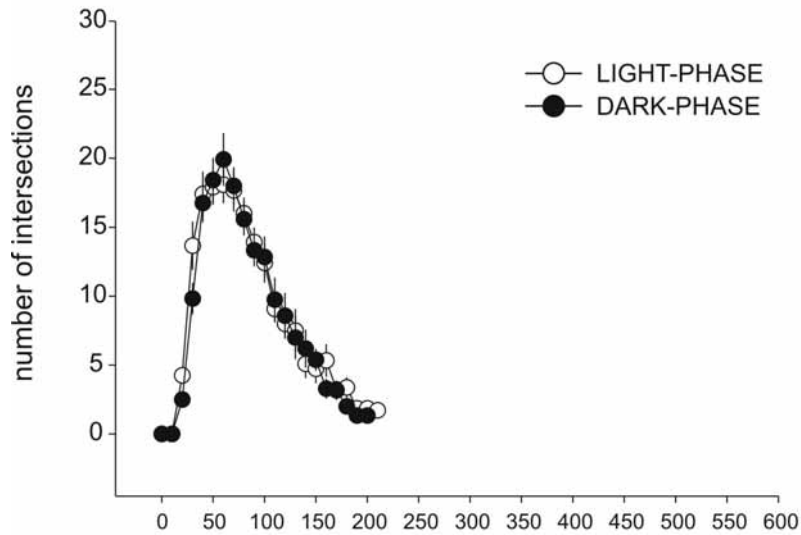
**A) Total length of basal dendrites in stressed rats****B) Spine density: Proximal dendrites in stressed rats****C) Spine density: Distal dendrites in stressed rats**

**Figure 20. Impact of the diurnal cycle on dendritic length and spine density in stressed rats**

The diurnal variations in the morphology of pyramidal neurons were analyzed in stressed rats. **A**, Stressed rats presented shorter dendrites in the right hemisphere compared to the left hemisphere during the light- and during the dark-phase conditions ( $p < 0.05$ ). **B**, Spine density in dendrites proximal to soma was lower in the right hemisphere compared to the left hemispheres during the light- and the dark-phase ( $p < 0.05$ ) and compared to the right hemisphere during the light-phase ( $p < 0.05$ ). **C**, No differences were observed in distal segments of basal dendrites. Data presented as mean  $\pm$  SEM. \*  $P < 0.05$ , \*\* $P < 0.01$

## STRESSED RATS

### A) Number of intersections: Right hemisphere



### B) Number of intersections: Left hemisphere

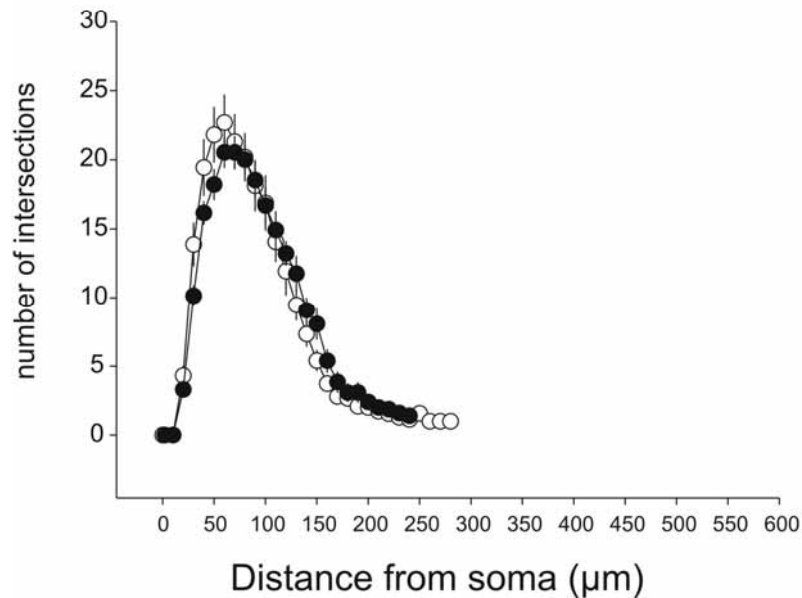


**Figure 21 Diurnal variations in the total number of intersections basal dendrites of stressed rats**

Effects of the light schedule on the total number of intersections in stressed rats were compared between hemispheres. **A**, Right hemisphere: The diurnal cycle did not affect the total number of intersections across the basal dendrites in stressed rats. **B**, Left hemisphere: No significant differences in the total number of intersections were found under different light-conditions. Data are mean  $\pm$  SEM.

### 6.2.3.2 Circadian variation in the morphology of pyramidal neurons in stressed rats

In stressed rats two-way ANOVA showed a positive effect of hemisphere ( $F_{(1,15)}=10.884$ ,  $p < 0.01$ ) on the total dendritic length of basal dendrites. *Post-hoc* analyses demonstrated a pronounced difference between right hemispheres compared to left hemispheres ( $p < 0.05$ ) (Fig.20A). Sholl analysis indicated a positive effect of radius ( $F_{(18,468)}=94.69$ ),  $p < 0.0001$ ) in the total number of intersections as function of distance from the soma (Fig. 21). No significant differences in the number of intersections were found between the two light-conditions in both hemispheres (Fig 21A and B).

Analyzes of spine densities showed an effect of hemisphere ( $F_{(1,13)}=4.36$ ,  $p < 0.5$ ) in dendrites proximal to soma, where the right hemisphere during the dark-phase had lower spine densities compared to left hemisphere ( $p < 0.01$ ) and compared to both hemispheres during the light-phase (right,  $p < 0.05$ ; left,  $p < 0.01$ ) (Fig 20B). No differences in spine densities were found in distal segments of basal dendrites (Fig 20C).

### 6.2.4 Discussion

This study describes circadian variations in the morphology of pyramidal cells located in the PL of the PFC. In control rats, the overall dendritic morphology was not modified during the diurnal cycle; however, a closer inspection of the dendritic trees indicated a positive effect of the light-cycle as the right hemisphere presented longer proximal dendrites during the light-phase compared to the dark-phase. It is interesting to note, that dendritic length was reduced during the activity period of the animals (the dark-phase). In stressed rats, besides the dramatic reduction in the total dendritic length produced by stress, there were no detectable effects of the light-phase or hemispheres.

Spine counting analysis showed that in controls, spine density also presented hemispheric-dependent circadian variations in that pyramidal cells located in the *left* hemisphere had higher spine densities during the light-phase compared to the dark-phase. In stressed rats, there was an opposite circadian variation in spine density where lower spine numbers were observed in the *right* hemisphere during the dark-phase compared to the light-phase.

The PFC has been implicated in a number of higher-brain functions, such as selective attention, behavioral flexibility, working memory and regulation of mood (Drevets et al., 1997; Heidbreder and Groenewegen, 2003). Many of these functions are

subjected to diurnal rhythmicity. The suprachiasmatic nucleus (SCN) is a probable source of these rhythms since it is the master circadian pacemaker in the brain (Reppert and Weaver, 2002). Recently, Sylvester et al. (2002) demonstrated by tracing studies that the SCN projects to the PFC (mainly the IL) via a relay in the paraventricular thalamic nucleus. The SCN influences HPA-axis activation by stress, in that ablation of the SCN abolished the diurnal rhythmicity of corticosterone and blunted the stress-induced increases of this hormone either during the light- or dark-phase (Sage et al., 2001). Therefore, diurnal rhythms of the SCN and/or other nuclei projecting to the PFC may have an impact on the morphology of pyramidal cells on this area, as it has been demonstrated by Wellman (2001) that increases in corticosterone induced-dendritic retractions in apical dendrites of pyramidal neurons in the PFC, whereas decreases in monoamines induced by sleep-deprivation might cause increases in spine densities (Ramesh et al., 1999). On the other hand, differences in spine morphology have been associated with differences in synaptic functions (McKinney, 2005). The smaller the head of the spine the smaller is the associated postsynaptic density. In contrast, larger mushroom-shaped spine allows larger postsynaptic densities. Rapid changes in spine density have been shown in pyramidal neurons of the somatosensory cortex, where growth and retraction were observed within a day (Holtmaat et al., 2005). Furthermore, it has been hypothesized that most of the new spines found in the adult cortex are filopodia, being in the process of spine formation or elimination (Holtmaat et al., 2005). Filopodia are long and thin protusions without a bulbous head, many of which do not form synaptic contact with presynaptic axons (Dailey and Smith, 1996; Yuste and Bonhoeffer, 2004). Zuo et al. (2005) suggested that filopodia are transient structures in the formation and elimination of spines (Zuo et al., 2005).

In this study, despite differences in shape and possible distinct functions, spine density was taken as the number of protrusions perpendicular to the dendrite and spines and filopodia-like spines were counted together (Seib and Wellman, 2003; Bock et al., 2005; Murmu et al., 2006). Further studies discriminating filopodia and the different spines types are necessary in order to address the question whether these changes in spine density represent spine loss or a decrease in the generation of new spines (i.e. filopodia) during the diurnal cycle. Such analyses would offer a better understanding about the functional implications of synaptic alterations caused by the diurnal light-cycle and the stress.

This study demonstrated a hemispheric-dependent circadian variation in spine density of basal dendrites of the PL in control and in stressed rats. In control rats, there was a circadian variation in *left* pyramidal neurons, but in stressed rats this circadian variation was shifted to the *right* hemisphere.

**7 Part IV. Effects of the antidepressant  
tianeptine on stress-induced  
morphological modifications in pyramidal  
cells of the prelimbic cortex**

## Summary

It has been shown that stress-induced dendritic remodeling in hippocampal neurons can be successfully blocked by tianeptine, but not by other conventional antidepressant compounds (Watanabe et al., 1992b);(Magarinos et al., 1999). Tianeptine is an antidepressant drug with proven clinical efficacy (Cassano et al., 1996). Based on experimental data from the hippocampal formation, it was hypothesized that stress-induced remodeling in pyramidal neurons of the PFC can be successfully blocked by tianeptine. Adult rats were chronically restrained for 21 days and received daily intraperitoneal injections of either vehicle or tianeptine. Acute slices (400  $\mu\text{m}$ ) were obtained from the PFC and a total of 187 neurons were filled with neurobiotin. Pyramidal neurons in the prelimbic area were three-dimensionally reconstructed and the dendritic length, the amount of apical and basal dendrites, and the maximum branch order were quantified.

Stress-induced decrease of body weight and increase of adrenal gland weight were successfully blocked by tianeptine. Morphological analysis of pyramidal neurons showed that stress abolished the hemispheric asymmetry found in control rats, whereas tianeptine in stressed rats caused further decreases in apical dendrites in the left hemisphere. These results suggest that the effects of tianeptine in stressed rats are not directly correlated with restoration of dendritic remodeling of pyramidal neurons in the prelimbic area, but perhaps further remodeling induced by the drug might be associated with the positive effects of the antidepressant.



## 7.1 Rationale

Part II of this thesis described an intrinsic hemispheric asymmetry in the morphology of pyramidal cells of the prefrontal cortex (PFC). The right hemisphere presented longer dendrites in proximal and middle segments of the apical trees in infralimbic (IL) and prelimbic (PL) areas of control rats. No hemispheric differences were found in pyramidal neurons in anterior cingulate cortex (ACx) of controls. Chronic restraint stress significantly reduced apical dendrites in the IL and PL, resulting in a loss of intrinsic lateralization. In addition, stress affected the *right* hemisphere in IL and PL, but the *left* hemisphere in ACx. As mentioned above (see Introduction), important functional differences exist between the sub-areas of the rat PFC. Dorsal regions (ACx) are mainly related to motor behaviors, and ventral regions (IL and PL) to emotional and cognitive processes (Heidbreder and Groenewegen, 2003). Moreover, these areas have different efferent projection targets (Vertes, 2004; Heidbreder and Groenewegen, 2003). On the other hand, several studies have reported a consistent structural remodeling induced by chronic stress in pyramidal neurons of CA3 hippocampal region in rats (Magarinos and McEwen, 1995a; Kole et al., 2004a) and tree shrews (Magarinos et al., 1996). This dendritic remodeling was selectively prevented by tianeptine (Watanabe et al., 1992b) but not by other antidepressants, such as fluoxetine or fluoxetine (Magarinos et al., 1999). Tianeptine is suggested to enhance the uptake of monoamines, such as serotonin (Mennini et al., 1987; Fattaccini et al., 1990), and prevents the  $K^+$  - induced increases in extracellular concentrations of serotonin in the ventral hippocampus of rats (Whitton et al., 1991).

Based on experimental data from the hippocampal formation, it is hypothesized that tianeptine will be able to abolish the structural modifications caused by stress in pyramidal neurons in the PFC. Since previous results presented in this thesis demonstrated important structural changes in the PL compared to IL and ACx, this study focused only on pyramidal neurons in the PL area. The effects of chronic stress and tianeptine treatment on the morphology of pyramidal neurons in the PL were investigated with left – right hemisphere discrimination. A validated chronic restraint stress paradigm and a tianeptine regime that has been proved to be highly efficient in blocking the stress-induced hippocampal remodeling (Watanabe et al., 1992b; Magarinos et al., 1999) were used for the present study. The whole-cell patch clamp technique combined with neurobiotin cell filling was used for morphological analysis.

## 7.2 Design and Methods

### 7.2.1 *Chronic restraint stress and antidepressant treatment*

Animals were obtained as described in Part I (Methods, section 4.2.1)). Male Sprague-Dawley rats weighing 150–170 g at the beginning of the experiments were housed in groups of three animals per cage with ad libitum access to food and tap water. The first experimental phase (“Habituation”) lasted for 14 days, during which bodyweight was recorded daily. For the second phase of the experiment a validated drug regime previously described by Magarinos and McEwen (1995) was strictly followed. This is a well established experimental design for the hippocampal region studies that has been shown to separate the effects of stress, drug administration and their interaction (Watanabe et al., 1992b; Magarinos et al., 1999; Kole et al., 2004a). Briefly, animals were randomly assigned to the experimental groups (Stress, Control). The Stress (n= 21) and the Control (n= 19) groups were further subdivided in two groups, one received daily intraperitoneal (i.p.) injections of vehicle (control-vehicle and stress-vehicle) and the other received daily i.p injections of tianeptine (control-tianeptine, stress-tianeptine) (10 mg/kg/ml) right before the daily stress sessions were started (approx. 09.00 h). Chronic restraint stress consisted of daily restraint during six hours a day (09.00–15.00 h) for a period of 21 days according to Magarinos and McEwen (1995) and Kole et al. (2004). During restraint sessions, rats were placed in plastic tubes in their home cages with no access to food or water. Control rats were not subjected to any type of stress, except daily i.p. injections of either vehicle or tianeptine on same time schedule as for the stress groups. After 21 days of stress or treatment, rats were allowed to recover for 24 hours. On day 23, animals were weighed, deeply anaesthetized by i.p. injection with a mixture of 50 mg/ml ketamine, 10 mg/ml xylazine, and 0.1 mg/ml atropine and decapitated. Brains were rapidly removed and processed for slice preparation as described in Part II (section 5.2.3). Increased adrenal and decreased thymus weights are indicators of sustained stress. Therefore, these organs were removed from the animals immediately after decapitation and weighed. Data are expressed in milligrams per 100 gram body weight.

Fresh solutions were prepared every third day and kept under 4°C light protected in brown glass bottles. Vehicle injections consisted of sterile 0.9 % NaCl dissolved in double distilled water. Tianeptine injections consisted of tianeptine (Stablon®, S01574-01, *N*-(8-chloro-10-dioxo-11-methyl-dibenzo(c,f)(1,2)-5-thiazepinyl) sodium heptanoate,

Servier, France) in a concentration of 10 mg /kg/ml dissolved in sterile 0.9 % NaCl. This dose was selected as it has been shown to be in the range to produce neuroendocrine and behavioral responses (Delbende et al., 1991, 1994; Broqua et al., 1992). Slice preparation, neuronal reconstruction and morphometric analyses were performed as previously mentioned in Part II (section 5.2.3 – 5.2.5).

### **7.2.2 Statistical analysis**

For statistical analysis, body weight (BW) is given as the change in body weight from starting day (day 0) until day 21. Final body weights of control and stress groups from the different treatments were compared by two-way ANOVA (factors: treatment x group) (SPSS Inc., Chicago IL, v. 12.0). Relative organ weights (in milligrams per 100 grams of BW) were also compared between groups by two-way ANOVA.

It was attempted to label the same number of cells in all animals but there was a high variability in numbers of neurons that could be reconstructed because not all cells fulfilled the criteria for being included in the analyses. Data from the cells in each hemisphere and sub-area were averaged per animal and these mean data served as analysis unit for all statistical procedures. Two-way ANOVA (factors: treatment x group) was used to statistically evaluate the effects of treatment and stress on the total dendritic length, the total number of branching points and the amount of basal and apical dendrites. For a closer inspection of the distribution of the dendritic material, Sholl data was compared by three-way ANOVA repeated measures (with factors: treatment x group x radius). The complexity of the dendritic material, expressed by the number of branches per branch order, was also tested with three-way ANOVA (factors: treatment x group x branch order). All analyses were followed by Bonferroni's *post hoc* test (Statistica software package, Release 6.0 StatSoft Inc., Tulsa, OK). Data are presented as the mean  $\pm$  SEM. Differences were considered statistically significant at  $P < 0.05$ .

## **7.3 Results**

### **7.3.1 Intracellular labeling with neurobiotin and dendritic reconstruction**

Intracellular labeling provides a reliable and sensitive method for the study of dendritic morphology (Pyapali et al., 1998). In all experimental groups, there was complete staining of the main dendritic branches of each neuron with distal dendrites being reliably visualized (see Fig 6). In both groups together, *Control* and *Stress*, a total

of 480 cells were filled of which 39% (187 cells) fulfilled the criteria for complete staining suitable for a quantitative analysis of essential aspects of their dendritic morphology. The final percentage of recovered cells was similar to previous studies with same method of intracellular labeling (Perez-Cruz et al., 2007). This indicates that the whole-cell patch clamp method is a highly reproducible technique for the morphological analyses of pyramidal cells of the PFC. Filled cells were localized in layer III of the PL, readily identified by comparing the location of a neurobiotin filled neuron with the boundary patterns previously described (see, Part I). Briefly, a contour map based on the immunocytochemistry staining pattern in parvalbumin- and NEU-N- coronal stained sections from adult rats was overlapped into the selected neurobiotin-filled cells slides and the specific cell location was determined. Reconstructed neurons were located at depths of 400-450  $\mu\text{m}$  from the brain surface.

### **7.3.2 Effects of stress and tianeptine on body and organ weights**

To assess the beneficial effects of tianeptine on the physiological changes induced by stress, body weight and the weights of thymus and adrenal glands were measured. Two-way ANOVA indicated a positive interaction between group and treatment ( $F_{(1,27)}=4.28$ ,  $p < 0.05$ ), and an effect of tianeptine ( $F_{(1,27)}=7.24$ ,  $p < 0.05$ ) on the final body weight. Bonferroni's *post-hoc* test revealed a significant difference in the final body weight between stress-vehicle vs. control-vehicle ( $t = 30.25$ ,  $p < 0.05$ ), stress-vehicle vs. control-tianeptine ( $t = 33.88$ ,  $p < 0.05$ ) and stress-vehicle vs. stress-tianeptine ( $t = 36.21$ ,  $p < 0.05$ ) (Fig. 22A). Restoration of body weight was found in stress-tianeptine group, as values were close to control values.

Relative adrenal and thymus gland weights (mg per 100 g body weight) were also compared between groups by two-way ANOVA. Relative adrenal weight showed a positive interaction between factors ( $F_{(1,30)}=1428.75$ ,  $p > 0.0001$ ) where adrenals were significantly enlarged in stress-vehicle vs. control-vehicle ( $t = 3.46$ ,  $p < 0.01$ ) and stress-vehicle vs control-tianeptine ( $t = 2.48$ ,  $p < 0.05$ ). Normalization in the adrenal glands weight in the stress group was found after tianeptine treatment, as values were close to control values (Fig 22B). On the other hand, thymus weight was not affected neither by stress nor by treatment (Fig 22C).

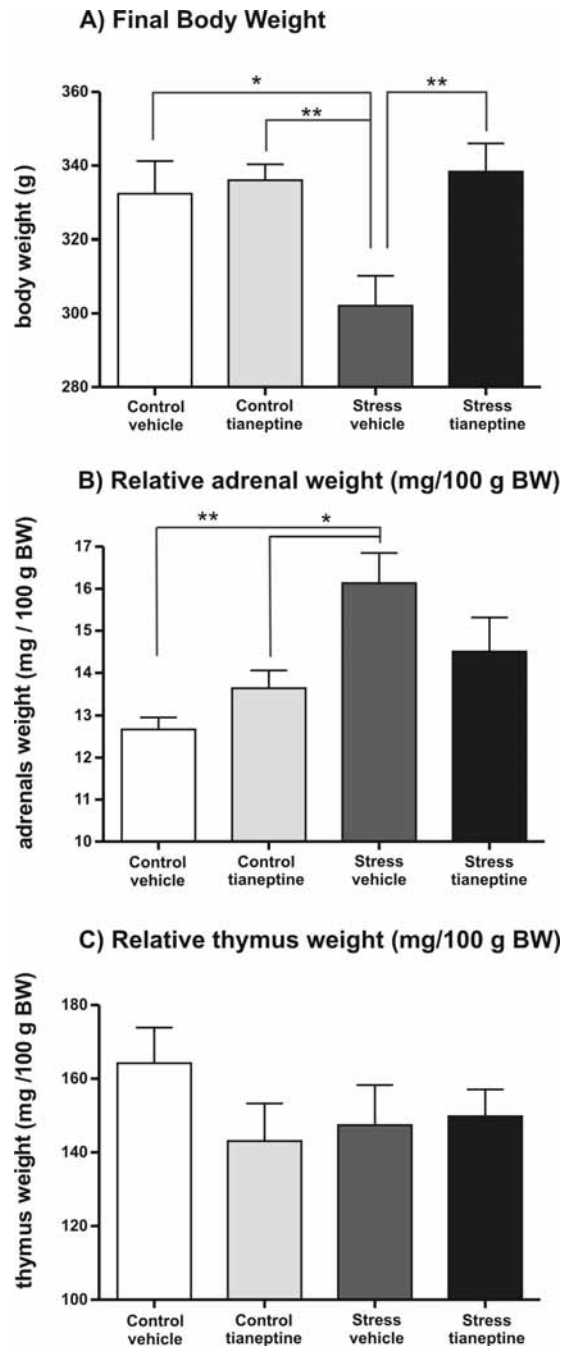


**Figure 22. Effects of tianeptine on body, adrenal and thymus weight in stressed and control rats**

**A**, Body weight increases were significantly reduced in stress-vehicle compared to control-vehicle ( $p < 0.05$ ) and to control-tianeptine ( $p < 0.01$ ). Tianeptine was able to block the decreases in body weight in stress-tianeptine rats ( $p < 0.01$ ). **B**, Relative adrenal glands weight (in mg per 100 g body weight) was increased in stress-vehicle compared to control-vehicle ( $p < 0.01$ ) and control-tianeptine ( $p < 0.05$ ). Normalization in adrenal gland weight was found in stress-tianeptine as values were close to control values. **C**, on the other hand, thymus weight was affected neither by stress nor by treatment. Data are mean  $\pm$  SEM. \*\*  $P < 0.01$ , \*  $P < 0.05$

### 7.3.3 Effects of stress and tianeptine on the morphology of pyramidal neurons

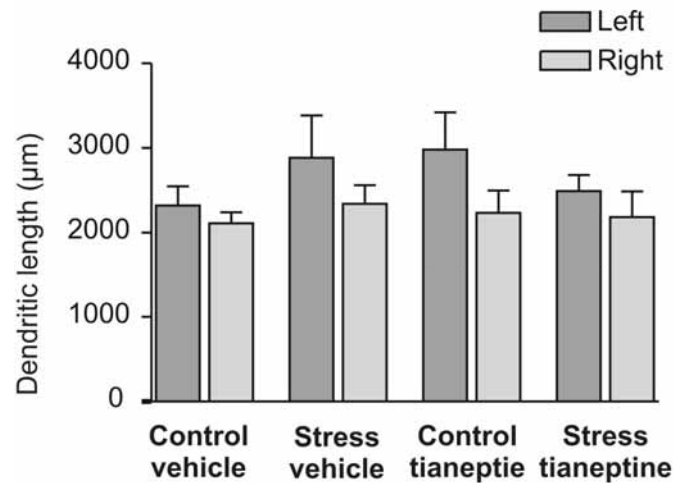
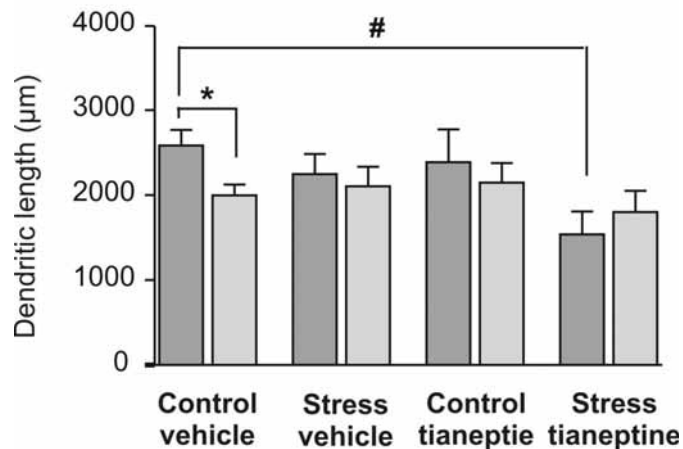
For a general evaluation of the structural changes induced by stress and tianeptine on pyramidal neurons of the PL, basal and apical dendritic lengths were compared between groups. Basal dendrites were not modified either by stress or by tianeptine (Fig 23A).

For apical dendrites, two-way ANOVA indicated a positive effect of treatment ( $F_{(3,46)}=2.71$ ,  $p < 0.05$ ) and *post-doc* test indicated significant reductions in the left hemisphere of control-vehicle compared to stress-tianeptine (by 41 %) ( $p < 0.05$ ) (Fig 23B). Based on the findings of Part II, left and right hemispheres were compared in each group. Only control-vehicle rats presented hemispheric asymmetries in that left hemisphere had longer dendrites compared to right ( $p < 0.05$ ) (Fig 23B).

Sholl analyses were performed to have a closer inspection of the dendritic reorganization induced by stress and tianeptine. For basal dendrites on the right hemisphere, three-way ANOVA indicated a positive effect of radius ( $F_{(8,248)}=100.18$ ,  $p < 0.0001$ ). *Post-hoc* test demonstrated longer basal dendrites in the control-tianeptine group at 20  $\mu\text{m}$  and 80  $\mu\text{m}$  compared to stress-vehicle and control-vehicle, respectively (both  $p < 0.05$ ). At distal distances from soma control-vehicle had shorter dendrites compared to stress-tianeptine (180  $\mu\text{m}$ , 200  $\mu\text{m}$ ,  $p < 0.05$ ) and stress-vehicle (200  $\mu\text{m}$ ,  $p < 0.5$ ). At 210  $\mu\text{m}$  distance from the soma control-tianeptine also had shorter dendrites compared to stress-vehicle ( $p < 0.05$ ) (Fig 24A). Apical dendrites of the right hemisphere had a rather homogenous dendritic distribution between groups, but three-way ANOVA indicated a positive effect of radius ( $F_{(15,480)}=4.11$ ,  $p < 0.001$ ) on the general dendritic organization. *Post-hoc* test indicated larger dendrites in the control-vehicle compared to stress-tianeptine at 20  $\mu\text{m}$  from soma ( $p < 0.05$ ) (Fig 24A).

In the left hemisphere, three-way ANOVA indicated a positive interaction between radius and treatment ( $F_{(8,144)}=2.49$ ,  $p < 0.05$ ) and a positive effect of radius ( $F_{(8,144)}=29.28$ ,  $p < 0.05$ ) in the distribution of basal dendrites. *Post-hoc* analyses showed that control-tianeptine had larger dendrites compared to control-vehicle, stress-vehicle and stress-tianeptine at 20  $\mu\text{m}$  ( $p < 0.05$ ; Fig 24B). In apical dendrites in the left hemisphere, three-way ANOVA an interaction between stress and radius ( $F_{(15,270)}=2.64$ ,  $p < 0.001$ ), and between radius x stress x treatment ( $F_{(15,270)}=2.27$ ,  $p < 0.05$ ), and a positive effect of radius ( $F_{(15,270)}=2.14$ ,  $p < 0.01$ ) on the dendritic architecture. *Post-hoc* test indicated that control-vehicle rats had longer dendrites in distal dendrites compared

to stress-tianeptine (260  $\mu\text{m}$ ,  $p < 0.01$ ; 280  $\mu\text{m}$ ,  $p < 0.001$ ; 300  $\mu\text{m}$  and 320  $\mu\text{m}$ , both  $p < 0.05$ ) and compared to the stress-vehicle (280  $\mu\text{m}$  and 320  $\mu\text{m}$ ,  $p < 0.001$ ; 300  $\mu\text{m}$ ,  $p < 0.05$ ) (Fig 24B). Detailed analyses of the dendritic complexity were done by comparing the amount of apical and basal dendrites, as well as the number of branching points between groups. In both hemispheres, apical and basal trees presented no significant differences in the amount of dendrites. Hemispheric differences, however, were found in stress-vehicle group in that left hemisphere presented more basal dendrites compared to right ( $t = 2.39$ ,  $p < 0.05$ ) (Table 3). For the total number of branching points, two-way ANOVA demonstrated a positive interaction between factors ( $F_{(1,25)} = 203.42$ ,  $p < 0.0001$ ) in basal dendrites in that more branching points were detected in the right hemisphere of stress-vehicle rats compared to control-vehicle rats (Table 3). The total number of branching points in apical dendrites also presented a positive interaction between factors ( $F_{(1,21)} = 208.33$ ,  $p < 0.0001$ ) and *post-hoc* analysis indicated significantly less branching points in the left hemisphere of stress-tianeptine rats compared to stress-vehicle ( $p < 0.05$ ), and control-tianeptine animals ( $p < 0.05$ ; Table 3). Because major changes were found between control-vehicle and stress-tianeptine groups (i.e. reduced total length of apical dendrites in the left hemisphere), it was of interest to analyze the complexity of the dendrites only between these two groups, with left - right discrimination. The length of dendrites of each branch order was compared by a three-way ANOVA (group x treatment x branch order). For the right hemisphere, basal dendrites showed a positive effect of treatment ( $F_{(1,40)} = 8.29$ ,  $p < 0.01$ ) and branch order ( $F_{(2,40)} = 34.49$ ,  $p < 0.001$ ). Although stressed rats treated with tianeptine presented higher branch order than controls (stress-tianeptine: 6; control-vehicle: 5) no significant differences were detected between groups (Fig 25A, left panel). Apical dendrites in the right hemisphere presented a positive interaction between factors ( $F_{(1,35)} = 481.11$ ,  $p < 0.001$ ) and *post-hoc* test demonstrated that control-vehicle rats presented longer dendrites order 9 compared to stress-tianeptine rats ( $p < 0.01$ ; Fig 25A, right panel). In the left hemisphere, basal dendrites presented a positive interaction between factors ( $F_{(1,18)} = 85.19$ ,  $p < 0.001$ ) and branch order ( $F_{(3,18)} = 7.95$ ,  $p < 0.01$ ) but no differences were found between groups (Fig. 25B, left panel). Apical dendrites in the left hemisphere had a positive effect of branch order ( $F_{(7,42)} = 2.71$ ,  $p < 0.05$ ) and a positive interaction between branch x group x treatment ( $F_{(7,42)} = 2.62$ ,  $p < 0.05$ ). Even though control rats receiving vehicle presented higher order branches compared to stress (control-vehicle: 8; stress-tianeptine: 7), no significant differences were detected between groups (Fig 25B, right panel).

**PRELIMBIC****A) Dendritic length of basal dendrites****B) Dendritic length of apical dendrites**

**Figure 23. Effects of stress and tianeptine on the total dendritic length of basal and apical dendrites of the prelimbic area**

**A**, Basal dendrites: no significant differences were found between stress and control rats receiving vehicle or tianeptine. Larger values are found in the left hemispheres of stress-vehicle and control-vehicle group, but this was not significant. **B**, Apical dendrites: Reduced total dendritic length was found in the left hemisphere of stress-tianeptine rats compared to control-vehicle. Hemispheric asymmetries were only found in control-vehicle with a left over right difference. \*,  $P < 0.05$  hemispheric differences as determined by unpaired  $t$ -test; #,  $P < 0.05$  significant differences between stress and control rats as determined by two-way ANOVA with Newman-Keuls *post hoc* test. Values are means  $\pm$  SEM.



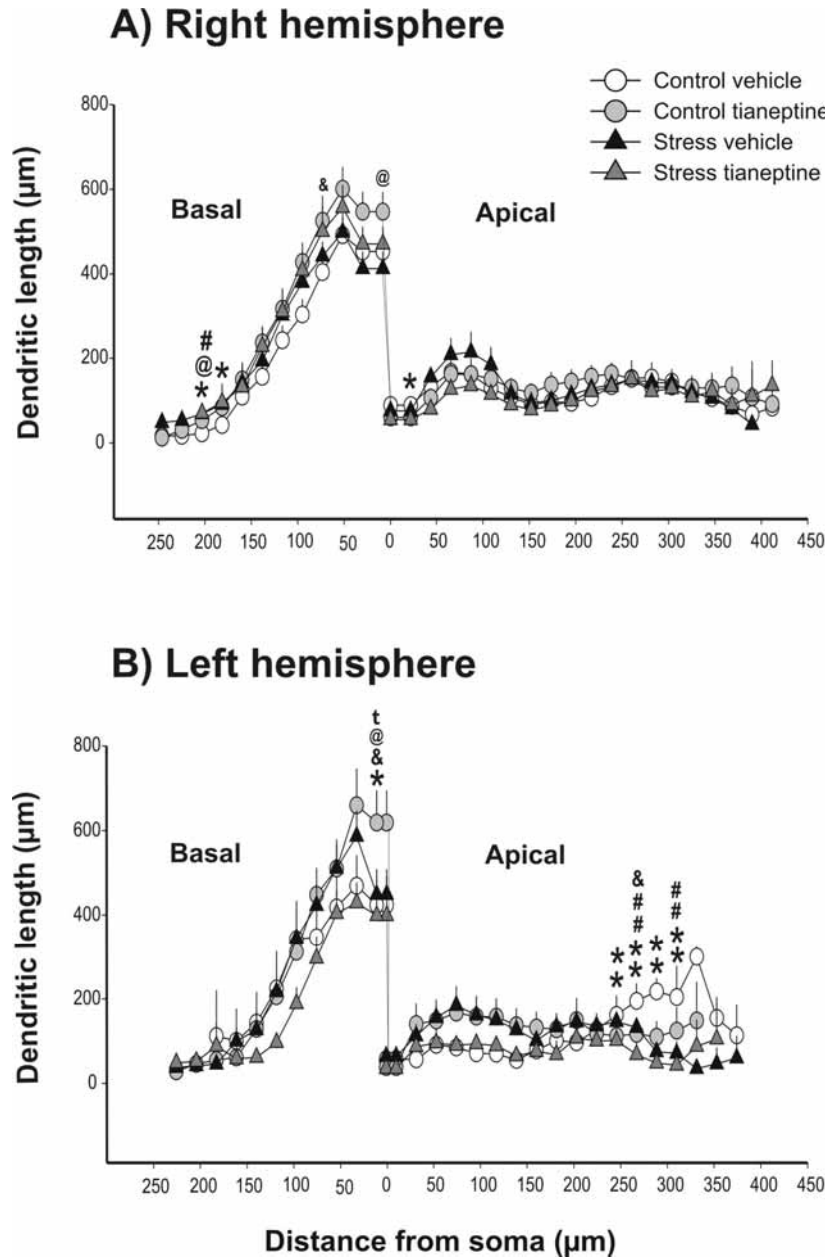


**Figure 24. Effects of stress and tianeptine on the dendritic distribution of pyramidal neurons in the prelimbic area**

**A**, Right hemisphere: basal dendrites presented significant differences between groups at 20  $\mu\text{m}$  where control-tianeptine had longer dendrites compared to stress-vehicle (@,  $p < 0.05$ ), and at 80  $\mu\text{m}$  control-tianeptine had also longer dendrites compared to control-vehicle (&,  $p < 0.05$ ). In middle portions of the basal trees, control-vehicle presented longer dendrites compared to stress-tianeptine (at 180 - 200  $\mu\text{m}$ , \*  $p < 0.05$ ) but compared to stress-vehicle only at 200  $\mu\text{m}$  (@,  $p < 0.05$ ). In addition, control-tianeptine presented longer dendrites compared to stress-vehicle at 200  $\mu\text{m}$  (#,  $p < 0.05$ ). Apical dendrites had a homogeneous distribution between groups and significant differences were only found only at 20  $\mu\text{m}$  between control-vehicle vs. stress-tianeptine (\*,  $p < 0.05$ ). **B**, Left hemisphere: basal dendrites of control-tianeptine were larger compared to stress-tianeptine (t,  $p > 0.05$ ), stress-vehicle (@,  $p < 0.05$ ) and control-vehicle (&,  $p < 0.05$ ) at 20  $\mu\text{m}$ . Apical dendrites were significant different between groups in middle portions of the tree, where control-vehicle presented larger dendrites compared to stress-tianeptine (at 260 - 320  $\mu\text{m}$ , \*\*,  $p < 0.01$ ), and compared to stress-vehicle (at 280 - 320  $\mu\text{m}$ , ###,  $p < 0.01$ ) and control-tianeptine (at 280  $\mu\text{m}$ , &,  $p < 0.05$ ). Symbols indicate significant differences within each 20  $\mu\text{m}$  ring. Data are mean  $\pm$  SEM.

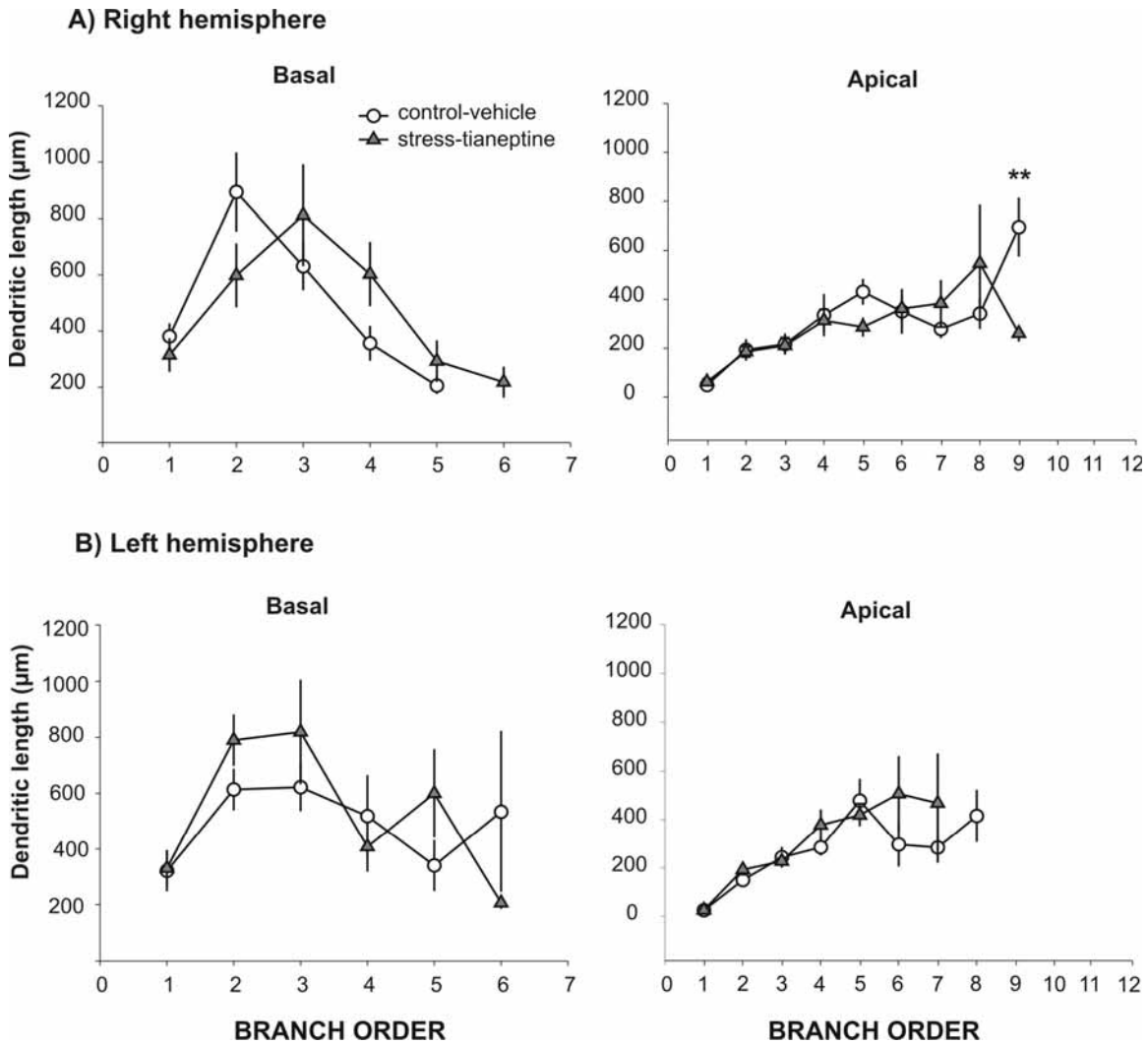


**Figure 25 Length of dendrites of distinct branch orders in basal and apical dendrites of pyramidal neurons in the prelimbic cortex**

The length of dendrites of different branch orders (i.e. 1<sup>st</sup>, 2<sup>nd</sup>, 3<sup>rd</sup>, etc.) were compared between control rats receiving vehicle (control-vehicle) and stress rats receiving tianeptine (stress-tianeptine). **A**, Right hemisphere: no significant differences were found in basal dendrites (left panel), but apical dendrites of control-vehicle presented longer dendrites order 10 compared to stress-tianeptine (right panel). **B**, Left hemisphere: no significant differences were found in basal dendrites (left panel), but control-vehicle rats had dendritic branches of the order 8 that did not exist in stress-tianeptine. Data presented are  $\pm$  SEM. \*\*  $P < 0.01$ , \*  $P < 0.05$  significant differences.

**Table 3. Morphometric data of pyramidal neurons in the prelimbic area of control and stressed rats treated with tianeptine (10 mg/kg/ml) or vehicle.**

		<b>Control-vehicle</b>	<b>Control-tianeptine</b>	<b>Stress-vehicle</b>	<b>Stress-tianeptine</b>
<b>Basal dendrites</b>					
Number of basal dendrites	RIGHT	6.2 ± 0.3	6.5 ± 0.6	<b>5.2 ± 0.6 *</b>	5.8 ± 0.5
	LEFT	5.6 ± 0.7	7.3 ± 0.7	7.0 ± 0.5	5.8 ± 0.7
Number of branching points	RIGHT	9.0 ± 0.7	12.5 ± 1.1	<b>14.3 ± 2.2 #</b>	13.2 ± 2.1
	LEFT	12.2 ± 4.5	13.5 ± 2.2	13.9 ± 5.0	11.5 ± 1.8
<b>Apical dendrites</b>					
Number of branching points	RIGHT	9.1 ± 1.0	10.3 ± 1.5	11.4 ± 1.7	8.2 ± 1.0
	LEFT	11.8 ± 0.8	12.0 ± 2.0	12.1 ± 1.2	<b>7.4 ± 1.7 &amp; @</b>

Morphometric data of basal and apical dendrites of pyramidal neurons in the prelimbic area of stress and control rats treated with vehicle or tianeptine. In basal dendrites, only stress-vehicle presented hemispheric differences in that left hemisphere had larger amount of basal dendrites compared to the right (\*,  $P < 0.05$ ). For the number of branching points, significant differences on the right hemisphere were found between stress-vehicle and control-vehicle (#,  $p < 0.05$ ). In apical dendrites, significant differences were found between stress-tianeptine and stress-vehicle (&,  $p > 0.05$ ), and stress-tianeptine control-tianeptine (@,  $p > 0.05$ ). Data are presented as mean ± SEM.

## 7.4 Discussion

The antidepressant and anxiolytic properties of tianeptine have put this drug at the top of the antidepressants with additional morphological protective effects in the hippocampal formation (see McEwen and Olie, 2005). Stress-induced hippocampal dendritic remodeling, and declines in spatial memory and anxiety are effectively blocked after chronic tianeptine administration (Watanabe et al., 1992b; Conrad et al., 1996; Delbende et al., 1994). Moreover, single injection of tianeptine suppressed stress-induced release of corticosterone, ACTH (Delbende et al., 1991), and noradrenalin (Sacchetti et al., 1993). Thus, tianeptine seems to suppress endocrine changes caused by stress. This may explain the present findings regarding successful body and adrenal weights restoration after tianeptine treatment in stressed rats. Previous studies, however, have failed to detect beneficial effects of the drug on physiological parameters (i.e. no changes in body weight) (Watanabe et al., 1992; Magarinos et al., 1999; Kole et al., 2004). Such contradictory results can be explained by differences in drug preparation (i.e. 50 % propylene glycol) or the route of administration (i.e. subcutaneous injection) (Watanabe et al., 1992). The pharmacological profile of tianeptine shows that chronic intraperitoneal administration (i.p.) results in plasma levels that peak very quickly (5-15 minutes post-injection), appearing in brain tissue almost immediately after administration (Couet et al., 1990). Therefore, the administration route chosen for this study (i.p.) allows an efficient plasma and brain concentration during the whole treatment. Moreover, previous reports addressing the impact of tianeptine in chronically stressed rats failed to detect changes in body or adrenal gland weights in the stressed rats (Magarinos and McEwen, 1995). In the present study, changes in body and adrenal weights (as important factors to assess the effectiveness of the stress protocol) were detected in stressed rats. Therefore, it is concluded that this antidepressant drug effectively abolished the bodily changes induced by chronic stress.

On the other hand, it is well known that stress-induced dendritic retraction in the CA3 hippocampal neurons (Conrad et al., 1999; Magarinos et al., 1999; Watanabe et al., 1992) as well as reduced neurogenesis in the dentate gyrus of three shrews (Czeh et al., 2001) are successfully blocked by tianeptine. Thus, tianeptine has important protective effects against stress-induced plastic changes in the hippocampus. Moreover, chronic restraint stress causes hypertrophy of pyramidal cells in the basolateral amygdala (Vyas et al., 2002), and this dendritic remodeling was also reversed by tianeptine (Pillai et al.,

2004). In the present study, no significant protection exerted by tianeptine against stress-induced remodeling in the PL could be detected. One explanation could be that the compound acts region-specific. This idea is supported by previous studies reporting regional effects of tianeptine after systemic administration. Louilot et al. (1990) reported increased DA metabolism in the PFC but not in the nucleus accumbens after tianeptine administration. Moreover, tianeptine facilitated serotonin uptake in the PFC but not in the hippocampus (Pineyro et al., 1995). Contrary, increases in serotonin levels were found in the CA3 hippocampal region, but not in the PFC after tianeptine administration (Frankfurt et al., 1995). Therefore, one can assume that differences in brain distribution and/or metabolism might be a causal factor for the differential actions of tianeptine between the hippocampus and the PFC. Interestingly, previous studies reported neuroendocrine modifications in control rats after tianeptine treatment (Louilot et al., 1990; Pineyro et al., 1995; Frankfurt et al., 1995). In the present study, tianeptine caused some morphological modifications in control animals as well. Therefore, morphological changes induced by tianeptine can be found in control and stressed animals in a region-dependent manner. Further experiments with a different route of administration, will address the questions as if injection procedure *per se* uncover potential beneficial effects of tianeptine in pyramidal neurons of the PFC.

Electrophysiological data from hippocampal neurons have shown that acute tianeptine increases the firing frequencies of CA1 pyramidal cells (Dresse and Scuvee-Moreau, 1988). Moreover, chronic restraint-stress reduced the EPSC amplitude of CA3 pyramidal neurons and EPSC amplitude was normalized after tianeptine treatment (Pineyro et al., 1995; Kole et al., 2004). In PFC neurons acute injection of tianeptine reversed the impairment in LTP caused by acute stress on an elevated platform (Rocher et al., 2004). Until now, however, there are no reports regarding the functional effects of chronic tianeptine treatment in PFC neurons. However, an opposite action of antidepressant in the electrical properties of hippocampal neurons compared to PFC neurons have been reported: fluoxetine induced an *increase* in field potentials in the dentate gyrus (Stewart and Reid, 2000) but same drug in the PFC *decreased* the number of spontaneously active cells (Ceci et al., 1994). As mentioned above, tianeptine abolished the dendritic remodeling induced by stress in the CA3 hippocampal pyramidal neurons (Magarinos and McEwen, 1995). In contrast, the present study found further reductions of apical dendrites in the left PL. A decrease in apical dendritic length, however, does not necessarily imply a loss of function. Shortening of even a few

dendrites can lead to enhanced back-propagation of action potentials (Golding et al., 2001; Schaefer et al., 2003). Moreover, previous experiments in our laboratory revealed that social defeat causes a decrease in the apical dendritic length of the CA3 pyramidal neurons in the rat hippocampus, an effect directly correlated with a shortening of the onset latency of EPSPs (excitatory postsynaptic potential) (Kole et al., 2004). Putting all this data together one can suggest that the dendritic remodeling found in PL pyramidal neurons in response to tianeptine treatment (dendritic retraction), might have beneficial effects in order to restore cortical functions, despite the negative connotation of the term “dendritic retraction” due to long established association with neurodegenerative processes. It is proposed that retractions in apical length induced by tianeptine may be part of a mechanism to counteract structural and functional imbalances induced by stress, and will help to restore PFC functioning. However, one cannot rule out the possibility that the protective effects of tianeptine against stress (i.e. physiological recovery, decreased anxiety, and improvement of spatial memory) might relay in other brain areas such as the hippocampus or the amygdala, but not in PFC. Functional studies are needed in order to understand the implications of dendritic retractions in pyramidal neurons of the left PL.

This study indicated that the beneficial effects of tianeptine on depressive symptoms are regional-dependent, in that the PFC dendritic remodeling caused by stress was not significantly prevented by this antidepressant.

## **8 APPENDIX**

## 8.1 Effect of intraperitoneal injection

### **Summary**

In Part IV of the present thesis, it was noted that chronic intraperitoneal (i.p.) injection *per se* caused alterations in the morphology of pyramidal cells in some areas of the prefrontal cortex (PFC). This mild stressful factor seems to have specific regional and hemispheric effects. Therefore, it was of interest to analyze the effects of i.p. injection on apical and basal dendrites in the infralimbic (IL) and prelimbic (PL) areas of the PFC. Results indicated that saline i.p. injections during 21 consecutive days produced a retraction in apical dendrites in the *right* PL. Apical dendrites in IL were not affected by i.p. injections, nor the basal dendrites from PL or IL areas. Previously, it was demonstrated that chronic stress (applied for 21 or 7 days, see Part II and Part III, respectively) reduces the apical dendrites exclusively in pyramidal cells located in *right* PL and IL. These results suggest that, mild stress (i.p. injection), short-chronic stress (7 days restraint) as well as long-chronic stress (21 days restraint) have a more pronounced effect on the morphology of pyramidal neurons in the right PL compared to other PFC sub-areas. Putting all this data together, it can be concluded that is the right PL the most sensible area of the PFC to external stimuli. These results also show that injection procedures as well as other stimuli have an effect on the dendritic morphology of PFC neurons. Therefore, it is strongly suggested the use of different drug administration route (i.e. per oral) in order to discriminate drug and treatment effects on stress induced morphological changes in the PFC.



### **8.1.1 Rationale**

The protective effects of tianeptine on stress-induced dendritic remodeling of pyramidal cells of the CA3 hippocampal region (Magarinos et al., 1999; Kole et al., 2004) formed the basis for hypothesize that tianeptine can counteract the morphological modifications of chronic stress also in the prefrontal cortex (PFC) (Part IV). Part II of this thesis described a lateralized morphology in pyramidal cells of different areas of the PFC, where chronic stress reduced dendrites exclusively in the right hemispheres of the IL and PL areas. Part IV of this thesis described an attempted to block this stress-induced dendritic remodeling by the use of chronic tianeptine treatment. When comparing the dendritic morphology of pyramidal neurons from the IL and PL between vehicle injected rats (Part IV) and handled controls (Part II) slight differences was observed for some regions of the PFC. Therefore, this study aimed to compare the effects of intraperitoneal injections *versus* handling in control rats. The data from Part II (control rats) and from Part IV (vehicle injected rats) was re-analyzed and compared to investigate the effects of injection procedure *per se* on the morphology of pyramidal neurons in the IL and PL sub-areas of the PFC.

The results indicate that injection *per se* causes a mild stress effect in some areas of the PFC. Retraction of apical dendrites was found in the right PL of chronically injected rats compared to handled controls. No differences were found in the left hemisphere of PL or in dendrites of the IL. The right PL seems to be highly sensitive to external stimuli, and structural modifications in this area can be observed after mild stress before other PFC sub-areas are modified.

### **8.1.2 Design**

For this study the data from control rats of Part II, and control rats receiving vehicle (control-vehicle) of Part IV were re-analyzed. New name codes were given to them, as “Handled” (control rats handled only for weight measurements during 21 consecutive days), and “Injected” (control rats receiving i.p. injections during 21 consecutive days). Comparisons between the total dendritic length were performed by the use of two-way ANOVA (factors: hemisphere x group) followed by Bonferroni’s *post-hoc* test for statistical differences ( $p < 0.05$ ).

### **8.1.3 Results**

#### **8.1.3.1 Effects of intraperitoneal injection on the morphology of pyramidal neurons in the infralimbic and prelimbic areas**

In order to assess the overall effects of i.p. injection on the dendritic architecture of neurons from IL and PL areas, basal and apical morphometric data was compared between “Handled” and “Injected” rats with a left-right discrimination.

In the prelimbic area, two-way ANOVA indicated a positive interaction between factors ( $F_{(1, 20)}=9.07$ ,  $p < 0.001$ ) in the total dendritic length. Bonferroni's *post-hoc* analysis demonstrated that in “Injected” rats, i.p. injections produced a dramatic reduction in apical dendrites of the PL only in the right hemisphere compared to “Handled” rats ( $p < 0.05$ ) (Fig 26A). No statistical differences were found for basal dendrites of PL.

In the IL, no significant differences were found for basal or apical dendrites between “Handled” and “Injected” rats (Fig 26B).

In addition, the asymmetrical morphology favoring the right apical dendrites of the PL in “Handled” rats was lost in pyramidal cells from “Injected” rats (Fig 26A). Therefore, the route of drug administration, i.p. can be considered as mild stress that produced plastic changes only in the PL and more specifically, in the right hemisphere.

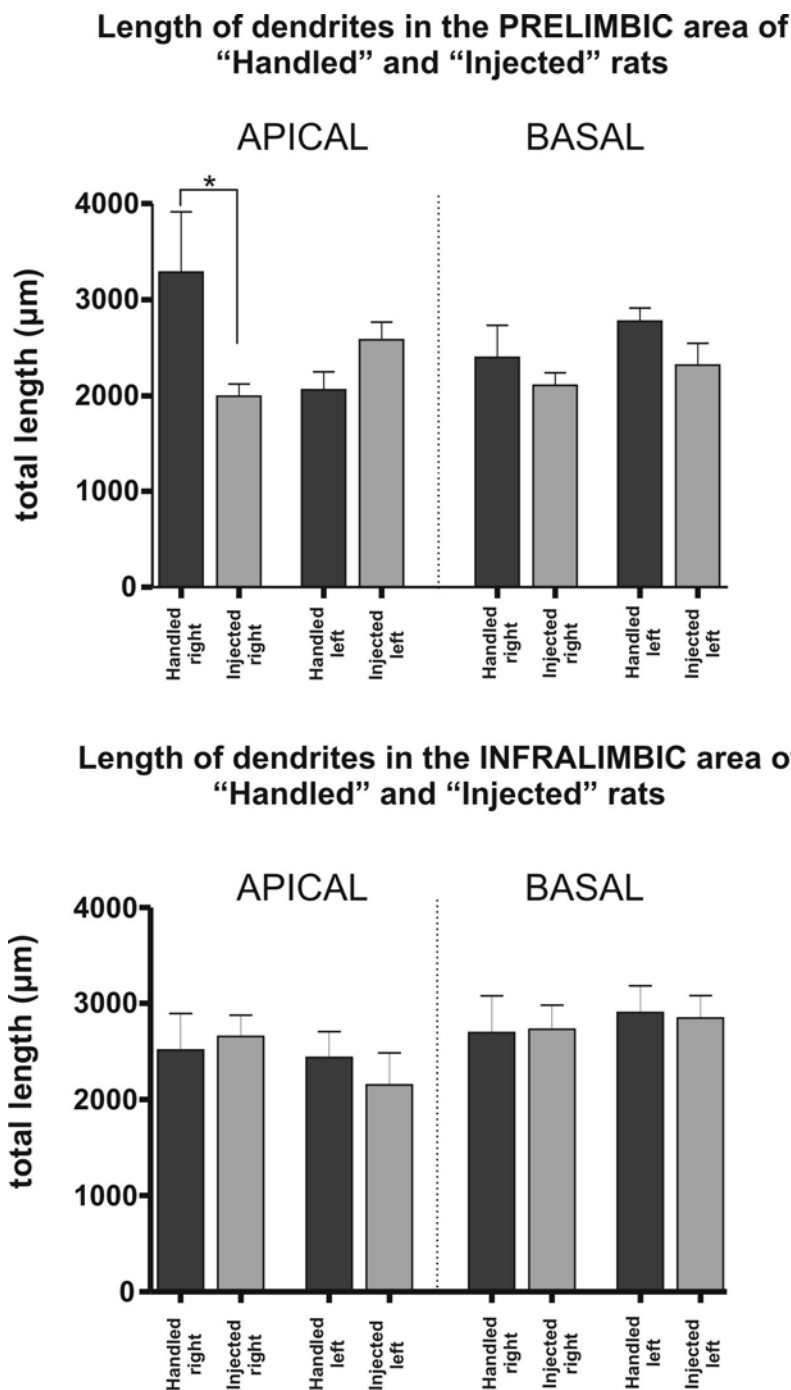


**Figure 26. Effect of daily handling or intraperitoneal injections on the dendritic length of infralimbic and prelimbic areas**

The effects of daily handling or i.p. injections were analyzed in basal and apical dendrites of the prelimbic and infralimbic areas **A**, Prelimbic area: apical dendrites presented significant reductions in the right hemisphere, where rats receiving i.p. injections (injected right) presented shorter dendritic lengths compared to rats that were only handled (handled right) ( $p < 0.05$ ) (left side). No differences were found in basal dendrites. **B**, Infralimbic area: No significant differences were found between handled and injected rats either in basal or apical dendrites. \*,  $P < 0.05$  significant difference as determined by two-way ANOVA with Bonferroni's *post hoc* test. Handled: control rats daily handled for 21-days; Injected: control rats receiving daily i.p. injections of saline for 21 days. Values are presented as means  $\pm$  SEM.

### **8.1.4 Discussion**

In Part IV of this thesis, control rats receiving i.p. injections of saline, presented a slight reduction of the total dendritic length in apical and basal trees in comparison with previous experiments (Part II, where control animals were not injected). The PFC seems to be extremely sensitive to stressful events. Previous studies shown that chronic subcutaneous (s.c.) administration of sesame oil as vehicle in control rats resulted in a reduction in the number of spines in apical dendrites of the PFC (Seib and Wellman 2003). Therefore, it seems that the administration procedure per se might be stressful enough to alter the morphology of dendrites in the PFC. The present study compared the overall morphology of pyramidal neurons of control animals that were only handled for body weight measurements during 21-days (“Handled”), and those that received i.p. injection of saline during same period of time (“Injected”) from previous data of Part II and IV, respectively. Results indicated that mild stress, such as daily i.p. injection with saline, resulted in a retraction of apical dendrites exclusively in the right PL. No changes were observed in basal dendrites of the PL, or in pyramidal cells from the IL. Thus, under these experimental conditions, the right PL seems to be the most sensitive to stress as it was demonstrated by alterations in its dendritic morphology. Recently, Izquierdo et al. (2006) have demonstrated that a single stress episode in mice (swimming stress) caused significant retractions of apical dendrites in the IL. They proposed the IL to be the first PFC area to react to stressful events (by retraction of the apical dendrites) (Izquierdo et al., 2006). When stressors are applied for a longer periods (7- or 21-days of chronic restraint stress) (Part II, Part III; Brown et al., 2005; Radley et al., 2004) other PFC areas, such as PL, can be recruited resulting in plastic changes of their dendritic arbors. Anatomical studies in rats have demonstrated the existence of a “PL loop” involving projections from the PL to the ventral striatum, ventral pallidum, and the mediodorsal nucleus back to the PL (Groenewegen and Uylings, 2000). This loop appears to represent an important circuitry involved in cognitive processing (Vertes, 2006). By contrast, the IL projects to visceromotor centers (Vertes, 2004) and is mainly involved in visceral and autonomic regulation (Heidbreder and Groenewegen, 2003). Thus, specific stress responses of the PL compared to the IL might be linked to the dendritic remodeling in the PL but not in the IL.

The criteria used to select neurons for analysis in this study compared to the previous ones, might also explain the contrasting results with Izquierdo et al. (2006). As

mentioned already in Part II-Part IV of this thesis, previous studies (Cook and Wellman, 2004; Brown et al., 2005; Wellman, 2001) selected neurons located in the border of layer II - III, whereas in the present analysis neurons were located exclusively in layer III (closer to border of layer V). The PFC receives different afferent projections from cortical and subcortical areas, and these projections target specific cells in a layer-specific manner (Gabbott et al., 2005; Vertes, 2004). Most of the medial thalamic input to the PFC is on layer V and deep layer III (Gabbott et al., 2005; Wyss et al., 1990). As the PFC in mammals is defined as the cerebral cortex region that presents reciprocal projections from the medial thalamic nucleus (Uylings et al., 2003), investigating layer III neurons would provide a clearer approach to pathological conditions involving the PFC.

It is concluded that the right PL reacts to stress events in a more sensitive manner than lower PFC areas. Daily i.p. injections with saline caused reductions in the apical dendrites of exclusively in the *right PL*, but not in basal dendrites. These results are in agreement with the hypothesis of a lateralized activation of the PFC to stressful events (Sullivan and Gratton, 1999; Sullivan, 2004) and suggest the use of another route of drug administration to discriminate the drug and treatment effects on stress induced morphological changes in the PFC

## **9 General Discussion**

## 9.1 Prefrontal cortex and stress responses

The aim of present thesis was to contribute to the understanding of the morphological alterations in the PFC caused by repeated stressful experiences. This study illustrated the effects of repeated stressful experiences with a specific regional and hemispheric distinction. Dendritic remodeling was consistently observed in the right hemisphere of the IL and PL sub-areas of the PFC. Moreover, restraint stress applied for one-week leads to the retraction of basal dendrites in proximal distances from the soma in the right PL, and effect accompanied by reductions in spine density. In addition, the exquisite responsiveness of the PL to stress was further demonstrated as intraperitoneal injections *per se* caused dendritic retraction in apical dendrites of the right PL.

At functional level, Schaefer et al. (2003) have demonstrated that branches emerging from distal regions of the apical dendrites diminish coupling (acting as current sinks, reducing the current to the main dendrite), while proximal branches enhance the current transmission (Schaefer et al., 2003). Vetter et al., (2000) provided further clear evidences of a direct correlation between neuronal morphology and propagation of action potentials. Complex dendritic arbors (i.e. high branching points and branch orders) decrease back propagation efficacy leading to a decrease in spike capacity (Vetter et al., 2001). Thus, morphological variations in the dendritic architecture of pyramidal cells might render important adaptive and functional modifications. One can speculate that these dendritic retractions found in apical dendrites of the IL and PL (in proximal and middle distances from the soma, respectively) will result in an enhanced current transmission and permissive excitatory properties.

## 9.2 What are the causes and/or functional consequences of this dendritic remodeling?

Dendritic architecture is a crucial factor that determines the connectivity of neuronal circuits. Several molecular, cellular and physiological components play a role in modulating dendritic morphology. For example, sensory input or environmental enrichment promotes the formation of spines on proximal branches of motor cortex in mice (Turner and Lewis, 2003). Increase innervation by axonal afferents promotes an extensive dendritic sprouting and increases the spine density in hippocampal pyramidal neurons (Kossel et al., 1997). On the other hand, axonal deafferentation decreases the total length and branching points of distal dendrites on giant sensory interneurons from

the cockroach cercal system (Mizrahi and Libersat, 2002). Thus, loss of afferents lead to dendritic retraction (Valverde, 1968; Benes et al., 1977; Deitch and Rubel, 1984) whereas increase of afferents lead to dendritic growth (Goodman and Model, 1988).

As mentioned before, several neurochemical systems are activated by stress (Fuchs and Flugge, 2004). Among others the dopaminergic system is activated by acute stress (Jackson and Moghaddam, 2004) but becomes adapted after repeated stressful situations (Mizoguchi et al., 2000; Jackson and Moghaddam, 2004). Projection neurons from the ventral tegmental area (VTA) target primarily the PFC (Gabbott et al., 2005; Benes et al., 1993). Stimulation of the VTA evokes dopamine overflow in the PFC causing a long-lasting enhancement of long term potentiation (LTP) whereas depletion of cortical dopamine levels generates a dramatic decrease in this LTP (Jay et al., 2004). Decreased spontaneous activity of VTA neurons can be induced by chronic stress (Moore et al., 2001) reducing the dopamine level in the PFC (Mizoguchi et al., 2000) with a final loss of inhibitory input to the PFC generating an final over-excitation of pyramidal neurons of the PFC. The hypothesis of stress-induced dendritic retraction with a concomitant functional impairment (hyperactivation), however, needs to be experimentally tested.

The amygdala is another important structure severely modified by stress (LeDoux, 1994). Contrary to the findings on the PFC, pyramidal cells of the basolateral amygdala revealed an increase in the apical dendritic length after chronic restraint stress (Vyas et al., 2002). This nucleus sends projections to and receives inputs from PL and ACx (Vertes, 2004). Activation of the basolateral amygdala elevates glutamate levels and GABA release in the PL (Del Arco and Mora, 2002) resulting in a net inhibition of the glutamatergic neurons in the PFC (Perez-Jaranay and Vives, 1991). Under normal conditions, the PFC inhibits the basolateral amygdala (Rosenkranz and Grace, 2002) but under stress, this inhibition might be impaired as result of a hyperexcitation of PL neurons, contributing to an over-reactivity of the basolateral amygdala with a resultant dendritic hypertrophy. Thus, afferents from the VTA and from the basolateral amygdala might be implicated in the dendritic alterations observed in the different areas of the PFC. However, it is not yet known which functional consequences can be associated with this morphological remodeling. One might speculated that impairments in learning and memory observed when animals are expose repeatedly to stress events (Miracle et al., 2006; Sousa et al., 2000) are consequence of the regional morphological modifications in different brain structures.



### 9.3 Site-specific dendritic remodeling caused by stress

The majority of synaptic inputs to neocortical pyramidal cells are received in basal dendrites (Larkman, 1991). Same as apical dendrites, basal dendrites can be functionally differentiated in proximal and distal segments. Proximal basal dendrites (located close to the soma) undergo LTP in response to pairing EPSPs with back-after polarization (Gordon et al., 2006). On the other hand, distal basal dendrites (located in neighborhood layers from the soma) typically support initiation of NMDA spikes that in turn are associated with large local calcium influx (Schiller et al., 2000), but fail to undergo LTP when paired with local spikes (Gordon et al., 2006). The same authors postulated that proximal basal dendrites contain synapses that are able to respond to plastic responses, but distal basal dendrites contain synapses that are resistant to plastic changes (Gordon et al., 2006). This previous studies agree with the results of Part III, where stress-induced plastic changes in basal dendrites of the PL were found exclusively in proximal parts but not in distal segments. This might imply that afferents to the PFC alter the dendritic morphology in an exquisite regional manner. Alonso-Nanclares and colleagues (Alonso-Nanclares et al., 2004) described that only symmetrical synapses (which are believed to be inhibitory; Ribak, 1978) can be found in proximal basal dendrites (Alonso-Nanclares et al., 2004) suggesting that proximal portions of basal dendrites receives mostly inhibitory inputs. Moreover, soma and proximal basal dendrites of pyramidal cells located in layer III are in close proximity to the main dopaminergic afferent terminals from the VTA (Gabbott et al., 2005). Reduced dopamine levels in the PFC in chronically stressed rats are highly associated with cognitive (Mizoguchi et al., 2000) and emotional impairments (Sullivan and Dufresne, 2006), thus, dramatic decreases in LTP after depletion of cortical dopamine levels (Jay et al., 2004) might produce inhibitory actions on basal dendrites of the PFC with a resultant plastic changes exclusively on proximal segments, where most of the dopamine terminals are located.

### 9.4 Lateralization and brain function

The correlation between brain asymmetry and functional homeostasis has been described in several human neurological disorders (see Rotenberg, 2004; Davidson et al., 2000). Lateralized functional and anatomical asymmetries of the PFC in healthy subjects is represented by a left-hemisphere dominance that seems to be reversed in

several neurological disorder, such as major depression (Cotter et al., 2005), schizophrenia (Cullen et al., 2006), attention deficit hyperactive disorders (Hill et al., 2003), and autism (Buchsbaum et al., 1992; Haznedar et al., 1997). Not only is a reversed asymmetry linked to pathological conditions, but also reduced functional and morphological asymmetries. Greater right-than left-hemisphere activation mediates the effects of negative affect (Davidson et al., 2000; Rotenberg, 2004). Moreover, damage of the left hemisphere is accompanied by depressed mood whereas right-hemisphere damage is associated with euphoric reactions (see Rotenberg, 2004). In depressed subjects, a relative increase of the electrical activity of the right frontal lobe (Henriques and Davidson, 1990) is accompanied by a relative decrease of the electrical activity of the left hemisphere (Debener et al., 2000). This agrees with the present studies, where the right hemisphere suffered morphological alteration, such as retraction of apical dendrites in the right PL. Electrophysiological studies have explored the relation between dendritic morphology and neuronal function. Vettes et al. (2001) proposed an indirect correlation between higher number of branches or branching points (complex dendritic arbors) and propagation of action potentials. As explained above, stress-induced retraction of apical dendrites of the right PL might exacerbate the spiking capacity of the neuron increasing its further activation in accordance to clinical studies in which the right hemisphere seems hyper-activated in neurological disorders (Rotenberg, 2004).

### **9.5 Regional effects of tianeptine in stress-induced neural plasticity**

Part IV of this thesis tested the antidepressant properties of tianeptine, a well known drug that efficiently blocks stress-induced dendritic remodeling of hippocampal pyramidal neurons (Magarinos et al., 1999). Surprisingly, tianeptine did not abolish the dendritic remodeling caused by chronic stress in the PFC pyramidal neurons, but it causes a further retraction in apical dendrites from the left PL. Beneficial effects on the drug, however, were observed in body and adrenal weight changes. Recently, Vouimba et al. (2006) reported that acute tianeptine treatment blocked the stress-induced suppression of primed burst potentiation in CA1 without affecting the stress-induced enhancement of LTP in the basolateral amygdala nucleus (Vouimba et al., 2006). Moreover, several studies have demonstrated that tianeptine can abolish stress-induced memory impairments (related to hippocampal function, Conrad et al., 1996), but it does not affect fear conditioning (related to amygdala function, Burghardt et al., 2004). Therefore, based on the regional brain distribution of tianeptine (Louilot et al., 1990) and

the site-specific effects the morphology and function of pyramidal neurons of distinct parts of the brain, one can speculate that the hippocampal formation is highly responsive to tianeptine protective effects against stress-induced functional and structural alterations. This hemispheric- and region- specific effect of tianeptine, opens the door for further studies to understand the functional implications of morphological remodeling, as some possible beneficial effects of tianeptine might be linked to dendritic retractions in specific locations of the basal or apical dendrites of pyramidal neurons of the PFC.

## 10 General Summary

This thesis demonstrated that pyramidal neurons of the prelimbic and infralimbic area of the rat prefrontal cortex had an intrinsic morphological asymmetry in that pyramidal neurons in the right hemisphere presented longer apical dendrites compared to the left. Stress induced-morphological alterations in pyramidal neurons were region- and hemispheric dependent, resulting in a final loss of hemisphere lateralization. Stress-induced retraction of apical dendrites in right infralimbic and prelimbic areas; however in anterior cingulate cortex apical dendrites were retracted in the left hemisphere. In addition, stress causes retraction of basal dendrites proximal to soma in the prelimbic area with concomitant reduction in spine density. Furthermore, the right prelimbic area showed reductions in apical dendrites after intraperitoneal injections of vehicle, demonstrating that this sub-area of the prefrontal cortex is highly sensitive to stress.

The effects of diurnal cycle and stress on spine densities in basal dendrites were also investigated. Surprisingly, control rats presented a diurnal variation in the number of spines in the left hemisphere. Chronic stress shifted this circadian variation to the right hemisphere. These alterations were selectively localized in proximal basal dendrites.

The effectiveness of an antidepressant, tianeptine, to abolish the dendritic remodeling caused by stress was evaluated. The drug did not restore the morphological changes induced by stress; however, physiological alterations induced by stress were successfully blocked by tianeptine.

It is hypothesized that these morphological remodeling of pyramidal neurons in the prefrontal cortex may have an important regulatory function in stress responses and might be part of an adaptive strategy to cope with stressful situations. This study offers important information to the field of stress research, as it is the first description of a region- and hemisphere- specific effects of stress in the rat prefrontal cortex.

## 11 Acknowledgments

I would like to thank everybody who helped me directly or indirectly during the realization of this project that finally became a Ph.D. thesis.

I would like to thank my supervisor Prof. Dr. Eberhard Fuchs for his openness, support and trust towards my work. I am also grateful to Prof. Dr. Gabriele Flügge for being the second reader of this thesis, and for her time editing, correcting and discussing the produced manuscript.

I give special thanks to Anna, Heino, Achim, Simone B., Simone L., Andreas K. and Andreas H. for their invaluable help and assistance, and challenging pseudo-conversations in Germlish, with a little taste of Spanish.

I am thankful to Jeanine that we had a common project and for the enjoyable times in Mensa (always on time). To Urs, for many wise discussions about methods and techniques, for the sparkling enthusiasm in science and excitement for patch-clamping cells!

Thanks to JunProf. Dr. Ralf Heinrich for his invaluable support since the very first day I put a step in Göttingen until today! To my committee members: PD Dr. Frank Kirchhoff and PD Dr. Anastasia Stoykova.

I also thank Dr. Gonzalo-Flores from Puebla University in Mexico who gave me the opportunity to visit his laboratory, and to Rubi Martinez for teaching me the Golgi-Cox technique which I applied successfully. For financial support, I have to thank the fellowship council of Mexico, CONACyT.

And who ever though that this academic adventure would permit me to find who I was looking for! Thank you Hans for your emotional support, the nice moments in Göttingen and sharing a future together.

A mi familia, una vez más, ya la tercera tesis, y ojala la última: A mi Mama, que a pesar de estar tan lejos siempre esta muy cerca, ya sea en sueños, en pensamientos, o en la realidad. Porque siempre estas y siempre has estado ahí para apoyarme en todas todas mis aventuras y fantasias. A Isabel por las jaladas de orejas que de alguna manera me despavilan cuando de plano me tiro en la hamaca para tomar el Sol. Gracias por tu responsabilidad, por tu compromiso como doctora, madre, esposa, hermana e hija. A Octavio por su linda vocecita por telefono y los gritos euforicos, a Julio por ser tan chiquito! Gracias a Alex que extraño bastante después de haber

compartido unos buenos años en Canadá y que ahora aprovechamos cuando se puede para regocijarnos un poco y disfrutar de la vida. A la pequeña Sofía por la luz de sus ojos y mágica sonrisa. A Gabo, por ser un súper hermano, por esa ambigüedad extraña entre alburero e intelectual, por su frescura, por todo el cariño y el apoyo. Por invitar las cervezas y las carnes asadas cada vez que se puede.

A mis inolvidables amigas que estaban aquí para encontrarnos. A Tania y Maria por traerme de la realidad al viaje interno, por las ricas comidonas, por los paseitos y las pachangas, por el cariño.

Ich bin meinen deutschen Freundinnen Britta, Petra und Ulrike sehr dankbar für die schöne gemeinsame Zeit und die Erklärung des deutschen Lebensstils. And to my very best friends of the international community in Göttingen: Miguel, Angelina, Lamiae, Mustapha, Mladen, Aniana and many others for unforgettable laughs and weekends together.

## 12 Reference List

Abraham I, Juhasz G, Kekesi KA, Kovacs KJ (1998) Corticosterone peak is responsible for stress-induced elevation of glutamate in the hippocampus. *Stress* 2: 171-181.

Adamec RE, Burton P, Shallow T, Budgell J (1999) Unilateral block of NMDA receptors in the amygdala prevents predator stress-induced lasting increases in anxiety-like behavior and unconditioned startle--effective hemisphere depends on the behavior. *Physiol Behav* 65: 739-751.

al Maskati HA, Zbrozyna AW (1989) Stimulation in prefrontal cortex area inhibits cardiovascular and motor components of the defence reaction in rats. *J Auton Nerv Syst* 28: 117-125.

Alonso-Nanclares L, White EL, Elston GN, DeFelipe J (2004) Synaptology of the proximal segment of pyramidal cell basal dendrites. *Eur J Neurosci* 19: 771-776.

Andersen SL, Teicher MH (1999) Serotonin laterality in amygdala predicts performance in the elevated plus maze in rats. *Neuroreport* 10: 3497-3500.

Aston-Jones G, Bloom FE (1981) Activity of norepinephrine-containing locus coeruleus neurons in behaving rats anticipates fluctuations in the sleep-waking cycle. *J Neurosci* 1: 876-886.

Bagley J, Moghaddam B (1997) Temporal dynamics of glutamate efflux in the prefrontal cortex and in the hippocampus following repeated stress: effects of pretreatment with saline or diazepam. *Neuroscience* 77: 65-73.

Bandyopadhyay S, Gonzalez-Islas C, Hablitz JJ (2005) Dopamine enhances spatiotemporal spread of activity in rat prefrontal cortex. *J Neurophysiol* 93: 864-872.

Benes FM, Parks TN, Rubel EW (1977) Rapid dendritic atrophy following deafferentation: an EM morphometric analysis. *Brain Res* 122: 1-13.

Benes FM, Vincent SL, Molloy R (1993) Dopamine-immunoreactive axon varicosities form nonrandom contacts with GABA-immunoreactive neurons of rat medial prefrontal cortex. *Synapse* 15: 285-295.

Berker EA, Berker AH, Smith A (1986) Translation of Broca's 1865 report. Localization of speech in the third left frontal convolution. *Arch Neurol* 43: 1065-1072.

Berridge CW, Mitton E, Clark W, Roth RH (1999) Engagement in a non-escape (displacement) behavior elicits a selective and lateralized suppression of frontal cortical dopaminergic utilization in stress. *Synapse* 32: 187-197.

Bock J, Gruss M, Becker S, Braun K (2005) Experience-induced changes of dendritic spine densities in the prefrontal and sensory cortex: correlation with developmental time windows. *Cereb Cortex* 15: 802-808.

Bradbury MJ, Cascio CS, Scribner KA, Dallman MF (1991) Stress-induced adrenocorticotropin secretion: diurnal responses and decreases during stress in the evening are not dependent on corticosterone. *Endocrinology* 128: 680-688.

Bremner JD, Narayan M, Anderson ER, Staib LH, Miller HL, Charney DS (2000) Hippocampal volume reduction in major depression. *Am J Psychiatry* 157: 115-118.

Broqua P, Baudrie V, Laude D, Chaouloff F (1992) Influence of the novel antidepressant tianeptine on neurochemical, neuroendocrinological, and behavioral effects of stress in rats. *Biol Psychiatry* 31: 391-400.

Brown SM, Henning S, Wellman CL (2005) Mild, Short-term stress alters dendritic morphology in rat medial prefrontal cortex. *Cereb Cortex* 15: 1714-1722.

Buchsbaum MS, Siegel BV, Jr., Wu JC, Hazlett E, Sicotte N, Haier R, Tanguay P, Asarnow R, Cadorette T, Donoghue D (1992) Brief report: attention performance in autism and regional brain metabolic rate assessed by positron emission tomography. *J Autism Dev Disord* 22: 115-125.

Burghardt NS, Sullivan GM, McEwen BS, Gorman JM, LeDoux JE (2004) The selective serotonin reuptake inhibitor citalopram increases fear after acute treatment but reduces fear with chronic treatment: a comparison with tianeptine. *Biol Psychiatry* 55: 1171-1178.

Cammermeyer J (1978) Is the solitary dark neuron a manifestation of postmortem trauma to the brain inadequately fixed by perfusion? *Histochemistry* 56: 97-115.

Cardinal RN, Parkinson JA, Hall J, Everitt BJ (2002) Emotion and motivation: the role of the amygdala, ventral striatum, and prefrontal cortex. *Neurosci Biobehav Rev* 26: 321-352.

Carlson JN, Fitzgerald LW, Keller RW, Jr., Glick SD (1991) Side and region dependent changes in dopamine activation with various durations of restraint stress. *Brain Res* 550: 313-318.

Carlson JN, Fitzgerald LW, Keller RW, Jr., Glick SD (1993) Lateralized changes in prefrontal cortical dopamine activity induced by controllable and uncontrollable stress in the rat. *Brain Res* 630: 178-187.

Cassano GB, Heinze G, Loo H, Mendlewicz J, Sousa MP (1996) A double-blind comparison of tianeptine, imipramine and placebo in the treatment of major depressive episodes. *European Psychiatry* 11: 254-259.

Ceci A, Fodritto F, Borsini F (1994) Repeated treatment with fluoxetine decreases the number of spontaneously active cells per track in frontal cortex. *Eur J Pharmacol* 271: 231-234.

Cerqueira JJ, Catania C, Sotiropoulos I, Schubert M, Kalisch R, Almeida OF, Auer DP, Sousa N (2005a) Corticosteroid status influences the volume of the rat cingulate cortex - a magnetic resonance imaging study. *J Psychiatr Res* 39: 451-460.



Cerqueira JJ, Pego JM, Taipa R, Bessa JM, Almeida OF, Sousa N (2005b) Morphological correlates of corticosteroid-induced changes in prefrontal cortex-dependent behaviors. *J Neurosci* 25: 7792-7800.

Chrousos GP (1998) Stressors, stress, and neuroendocrine integration of the adaptive response. The 1997 Hans Selye Memorial Lecture. *Ann N Y Acad Sci* 851: 311-335.

Conde F, Maire-Lepoivre E, Audinat E, Crepel F (1995) Afferent connections of the medial frontal cortex of the rat. II. Cortical and subcortical afferents. *J Comp Neurol* 352: 567-593.

Conrad CD, Galea LA, Kuroda Y, McEwen BS (1996) Chronic stress impairs rat spatial memory on the Y maze, and this effect is blocked by tianeptine pretreatment. *Behav Neurosci* 110: 1321-1334.

Conrad CD, LeDoux JE, Magarinos AM, McEwen BS (1999) Repeated restraint stress facilitates fear conditioning independently of causing hippocampal CA3 dendritic atrophy. *Behav Neurosci* 113: 902-913.

Cook SC, Wellman CL (2004) Chronic stress alters dendritic morphology in rat medial prefrontal cortex. *J Neurobiol* 60: 236-248.

Cotter D, Hudson L, Landau S (2005) Evidence for orbitofrontal pathology in bipolar disorder and major depression, but not in schizophrenia. *Bipolar Disord* 7: 358-369.

Couet W, Girault J, Latrille F, Salvadori C, Fourtillan JB (1990) Kinetic profiles of tianeptine and its MC5 metabolite in plasma, blood and brain after single and chronic intraperitoneal administration in the rat. *Eur J Drug Metab Pharmacokinet* 15: 69-74.

Cullen TJ, Walker MA, Eastwood SL, Esiri MM, Harrison PJ, Crow TJ (2006) Anomalies of asymmetry of pyramidal cell density and structure in dorsolateral prefrontal cortex in schizophrenia. *Br J Psychiatry* 188: 26-31.

Czeh B, Michaelis T, Watanabe T, Frahm J, de Biurrun G, van Kampen M, Bartolomucci A, Fuchs E (2001) Stress-induced changes in cerebral metabolites, hippocampal volume, and cell proliferation are prevented by antidepressant treatment with tianeptine. *Proc Natl Acad Sci U S A* 98: 12796-12801.

D'Aquila PS, Newton J, Willner P (1997) Diurnal variation in the effect of chronic mild stress on sucrose intake and preference. *Physiol Behav* 62: 421-426.

Dailey ME, Smith SJ (1996) The dynamics of dendritic structure in developing hippocampal slices. *J Neurosci* 16: 2983-2994.

Dalley JW, Cardinal RN, Robbins TW (2004) Prefrontal executive and cognitive functions in rodents: neural and neurochemical substrates. *Neurosci Biobehav Rev* 28: 771-784.

Davidson RJ, Jackson DC, Kalin NH (2000) Emotion, plasticity, context, and regulation: perspectives from affective neuroscience. *Psychol Bull* 126: 890-909.

de Boer SF, van der Gugten J. (1987) Daily variations in plasma noradrenaline, adrenaline and corticosterone concentrations in rats. *Physiol Behav* 40: 323-328.

de Kloet ER, Vreugdenhil E, Oitzl MS, Joels M (1998) Brain corticosteroid receptor balance in health and disease. *Endocr Rev* 19: 269-301.

Debener S, Beauducel A, Nessler D, Brocke B, Heilemann H, Kayser J (2000) Is resting anterior EEG alpha asymmetry a trait marker for depression? Findings for healthy adults and clinically depressed patients. *Neuropsychobiology* 41: 31-37.

Deitch JS, Rubel EW (1984) Afferent influences on brain stem auditory nuclei of the chicken: time course and specificity of dendritic atrophy following deafferentation. *J Comp Neurol* 229: 66-79.

Del Arco A, Mora F (2002) NMDA and AMPA/kainate glutamatergic agonists increase the extracellular concentrations of GABA in the prefrontal cortex of the freely moving rat: modulation by endogenous dopamine. *Brain Res Bull* 57: 623-630.

Delbende C, Contesse V, Mocaer E, Kamoun A, Vaudry H (1991) The novel antidepressant, tianeptine, reduces stress-evoked stimulation of the hypothalamo-pituitary-adrenal axis. *Eur J Pharmacol* 202: 391-396.

Delbende C, Tranchand BD, Tarozzo G, Grino M, Oliver C, Mocaer E, Vaudry H (1994) Effect of chronic treatment with the antidepressant tianeptine on the hypothalamo-pituitary-adrenal axis. *Eur J Pharmacol* 251: 245-251.

Diorio D, Viau V, Meaney MJ (1993) The role of the medial prefrontal cortex (cingulate gyrus) in the regulation of hypothalamic-pituitary-adrenal responses to stress. *J Neurosci* 13: 3839-3847.

Dolcos F, Rice HJ, Cabeza R (2002) Hemispheric asymmetry and aging: right hemisphere decline or asymmetry reduction. *Neurosci Biobehav Rev* 26: 819-825.

Dresse A, Scuvee-Moreau J (1988) Electrophysiological effects of tianeptine on rat locus coeruleus, raphe dorsalis, and hippocampus activity. *Clin Neuropharmacol* 11 Suppl 2: S51-S58.

Drevets WC, Price JL, Simpson JR, Jr., Todd RD, Reich T, Vannier M, Raichle ME (1997) Subgenual prefrontal cortex abnormalities in mood disorders. *Nature* 386: 824-827.

Dunn J, Scheving L, Millet P (1972) Circadian variation in stress-evoked increases in plasma corticosterone. *Am J Physiol* 223: 402-406.

Fattaccini CM, Bolanos-Jimenez F, Gozlan H, Hamon M (1990) Tianeptine stimulates uptake of 5-hydroxytryptamine in vivo in the rat brain. *Neuropharmacology* 29: 1-8.

Feldman S, Conforti N (1985) Modifications of adrenocortical responses following frontal cortex stimulation in rats with hypothalamic deafferentations and medial forebrain bundle lesions. *Neuroscience* 15: 1045-1047.

Figueiredo HF, Bodie BL, Tauchi M, Dolgas CM, Herman JP (2003) Stress integration after acute and chronic predator stress: differential activation of central stress circuitry and sensitization of the hypothalamo-pituitary-adrenocortical axis. *Endocrinology* 144: 5249-5258.

Frankfurt M, McKittrick CR, McEwen BS, Luine VN (1995) Tianeptine treatment induces regionally specific changes in monoamines. *Brain Res* 696: 1-6.

Fryszak RJ, Neafsey EJ (1991) The effect of medial frontal cortex lesions on respiration, "freezing," and ultrasonic vocalizations during conditioned emotional responses in rats. *Cereb Cortex* 1: 418-425.

Fuchs E, Flugge G (2004) Cellular consequences of stress and depression. *Dial Clin Neurosci* 6: 171-184.

Gabbott PL, Bacon SJ (1996) The organisation of dendritic bundles in the prelimbic cortex (area 32) of the rat. *Brain Res* 730: 75-86.

Gabbott PL, Dickie BG, Vaid RR, Headlam AJ, Bacon SJ (1997) Local-circuit neurones in the medial prefrontal cortex (areas 25, 32 and 24b) in the rat: morphology and quantitative distribution. *J Comp Neurol* 377: 465-499.

Gabbott PL, Warner TA, Jays PR, Salway P, Busby SJ (2005) Prefrontal cortex in the rat: projections to subcortical autonomic, motor, and limbic centers. *J Comp Neurol* 492: 145-177.

Gibb R, Kolb B (1998) A method for vibratome sectioning of Golgi-Cox stained whole rat brain. *J Neurosci Methods* 79: 1-4.

Golding NL, Kath WL, Spruston N (2001) Dichotomy of action-potential backpropagation in CA1 pyramidal neuron dendrites. *J Neurophysiol* 86: 2998-3010.

Goodman LA, Model PG (1988) Superinnervation enhances the dendritic branching pattern of the Mauthner cell in the developing axolotl. *J Neurosci* 8: 776-791.

Gordon U, Polsky A, Schiller J (2006) Plasticity compartments in basal dendrites of neocortical pyramidal neurons. *J Neurosci* 26: 12717-12726.

Gould E, McEwen BS, Tanapat P, Galea LA, Fuchs E (1997) Neurogenesis in the dentate gyrus of the adult tree shrew is regulated by psychosocial stress and NMDA receptor activation. *J Neurosci* 17: 2492-2498.

Gould E, Tanapat P (1999) Stress and hippocampal neurogenesis. *Biol Psychiatry* 46: 1472-1479.

Gray EG (1959) Electron microscopy of synaptic contacts on dendrite spines of the cerebral cortex. *Nature* 183: 1592-1593.

Groenewegen HJ, Uylings HB (2000) The prefrontal cortex and the integration of sensory, limbic and autonomic information. *Prog Brain Res* 126: 3-28.

Gronli J, Murison R, Bjorvatn B, Sorensen E, Portas CM, Ursin R (2004) Chronic mild stress affects sucrose intake and sleep in rats. *Behav Brain Res* 150: 139-147.

Gronli J, Murison R, Fiske E, Bjorvatn B, Sorensen E, Portas CM, Ursin R (2005) Effects of chronic mild stress on sexual behavior, locomotor activity and consumption of sucrose and saccharine solutions. *Physiol Behav* 84: 571-577.

Gulledge AT, Jaffe DB (1998) Dopamine decreases the excitability of layer V pyramidal cells in the rat prefrontal cortex. *J Neurosci* 18: 9139-9151.

Harris KM, Kater SB (1994) Dendritic spines: cellular specializations imparting both stability and flexibility to synaptic function. *Annu Rev Neurosci* 17: 341-371.

Harris RB, Zhou J, Mitchell T, Hebert S, Ryan DH (2002) Rats fed only during the light period are resistant to stress-induced weight loss. *Physiol Behav* 76: 543-550.

Hayes TL, Lewis DA (1993) Hemispheric differences in layer III pyramidal neurons of the anterior language area. *Arch Neurol* 50: 501-505.

Haznedar MM, Buchsbaum MS, Metzger M, Solimando A, Spiegel-Cohen J, Hollander E (1997) Anterior cingulate gyrus volume and glucose metabolism in autistic disorder. *Am J Psychiatry* 154: 1047-1050.

Heidbreder CA, Groenewegen HJ (2003) The medial prefrontal cortex in the rat: evidence for a dorso-ventral distinction based upon functional and anatomical characteristics. *Neurosci Biobehav Rev* 27: 555-579.

Henriques JB, Davidson RJ (1990) Regional brain electrical asymmetries discriminate between previously depressed and healthy control subjects. *J Abnorm Psychol* 99: 22-31.

Hill DE, Yeo RA, Campbell RA, Hart B, Vigil J, Brooks W (2003) Magnetic resonance imaging correlates of attention-deficit/hyperactivity disorder in children. *Neuropsychology* 17: 496-506.

Hill SJ, Oliver DL (1993) Visualization of neurons filled with biotinylated-lucifer yellow following identification of efferent connectivity with retrograde transport. *J Neurosci Methods* 46: 59-68.

Hilz MJ, Dutsch M, Perrine K, Nelson PK, Rauhut U, Devinsky O (2001) Hemispheric influence on autonomic modulation and baroreflex sensitivity. *Ann Neurol* 49: 575-584.

Holtmaat AJ, Trachtenberg JT, Wilbrecht L, Shepherd GM, Zhang X, Knott GW, Svoboda K (2005) Transient and persistent dendritic spines in the neocortex in vivo. *Neuron* 45: 279-291.

Hutsler J, Galuske RA (2003) Hemispheric asymmetries in cerebral cortical networks. *Trends Neurosci* 26: 429-435.

Hutsler JJ (2003) The specialized structure of human language cortex: pyramidal cell size asymmetries within auditory and language-associated regions of the temporal lobes. *Brain Lang* 86: 226-242.

Hutsler JJ, Gazzaniga MS (1996) Acetylcholinesterase staining in human auditory and language cortices: regional variation of structural features. *Cereb Cortex* 6: 260-270.

Izquierdo A, Wellman CL, Holmes A (2006) Brief uncontrollable stress causes dendritic retraction in infralimbic cortex and resistance to fear extinction in mice. *J Neurosci* 26: 5733-5738.

Jackson ME, Moghaddam B (2004) Stimulus-specific plasticity of prefrontal cortex dopamine neurotransmission. *J Neurochem* 88: 1327-1334.

Jay TM, Rocher C, Hotte M, Naudon L, Gurden H, Spedding M (2004) Plasticity at hippocampal to prefrontal cortex synapses is impaired by loss of dopamine and stress: importance for psychiatric diseases. *Neurotox Res* 6: 233-244.

Jedema HP, Moghaddam B (1994) Glutamatergic control of dopamine release during stress in the rat prefrontal cortex. *J Neurochem* 63: 785-788.

Joels M (2001) Corticosteroid actions in the hippocampus. *J Neuroendocrinol* 13: 657-669.

Kalin NH, Larson C, Shelton SE, Davidson RJ (1998) Asymmetric frontal brain activity, cortisol, and behavior associated with fearful temperament in rhesus monkeys. *Behav Neurosci* 112: 286-292.

Kessler RC (1997) The effects of stressful life events on depression. *Annu Rev Psychol* 48: 191-214.

Kitayama I, Yaga T, Kayahara T, Nakano K, Murase S, Otani M, Nomura J (1997) Long-term stress degenerates, but imipramine regenerates, noradrenergic axons in the rat cerebral cortex. *Biol Psychiatry* 42: 687-696.

Kitchener P, Di Blasi F, Borrelli E, Piazza PV (2004) Differences between brain structures in nuclear translocation and DNA binding of the glucocorticoid receptor during stress and the circadian cycle. *Eur J Neurosci* 19: 1837-1846.

Kolb B, Forgie M, Gibb R, Gorny G, Rowntree S (1998) Age, experience and the changing brain. *Neurosci Biobehav Rev* 22: 143-159.

Kole MH, Costoli T, Koolhaas JM, Fuchs E (2004a) Bidirectional shift in the cornu ammonis 3 pyramidal dendritic organization following brief stress. *Neuroscience* 125: 337-347.

Kole MH, Czeh B, Fuchs E (2004b) Homeostatic maintenance in excitability of tree shrew hippocampal CA3 pyramidal neurons after chronic stress. *Hippocampus* 14: 742-751.

Koolhaas JM, Meerlo P, de Boer SF, Strubbe JH, Bohus B (1997) The temporal dynamics of the stress response. *Neurosci Biobehav Rev* 21: 775-782.

Kossel AH, Williams CV, Schweizer M, Kater SB (1997) Afferent innervation influences the development of dendritic branches and spines via both activity-dependent and non-activity-dependent mechanisms. *J Neurosci* 17: 6314-6324.

Krettek JE, Price JL (1977) The cortical projections of the mediodorsal nucleus and adjacent thalamic nuclei in the rat. *J Comp Neurol* 171: 157-191.

Lacroix L, Spinelli S, Heidbreder CA, Feldon J (2000) Differential role of the medial and lateral prefrontal cortices in fear and anxiety. *Behav Neurosci* 114: 1119-1130.

Larkman AU (1991) Dendritic morphology of pyramidal neurones of the visual cortex of the rat: III. Spine distributions. *J Comp Neurol* 306: 332-343.

LeDoux JE (1994) Emotion, memory and the brain. *Sci Am* 270: 50-57.

Liston C, Miller MM, Goldwater DS, Radley JJ, Rocher AB, Hof PR, Morrison JH, McEwen BS (2006) Stress-induced alterations in prefrontal cortical dendritic morphology predict selective impairments in perceptual attentional set-shifting. *J Neurosci* 26: 7870-7874.

Louilot A, Mocaer E, Simon H, Le Moal M (1990) Difference in the effects of the antidepressant tianeptine on dopaminergic metabolism in the prefrontal cortex and the nucleus accumbens of the rat. A voltammetric study. *Life Sci* 47: 1083-1089.

Magarinos AM, Deslandes A, McEwen BS (1999) Effects of antidepressants and benzodiazepine treatments on the dendritic structure of CA3 pyramidal neurons after chronic stress. *Eur J Pharmacol* 371: 113-122.

Magarinos AM, McEwen BS (1995a) Stress-induced atrophy of apical dendrites of hippocampal CA3c neurons: comparison of stressors. *Neuroscience* 69: 83-88.

Magarinos AM, McEwen BS (1995b) Stress-induced atrophy of apical dendrites of hippocampal CA3c neurons: involvement of glucocorticoid secretion and excitatory amino acid receptors. *Neuroscience* 69: 89-98.

Magarinos AM, McEwen BS (2000) Experimental diabetes in rats causes hippocampal dendritic and synaptic reorganization and increased glucocorticoid reactivity to stress. *Proc Natl Acad Sci U S A* 97: 11056-11061.

Magarinos AM, McEwen BS, Flugge G, Fuchs E (1996) Chronic psychosocial stress causes apical dendritic atrophy of hippocampal CA3 pyramidal neurons in subordinate tree shrews. *J Neurosci* 16: 3534-3540.

Mangiavacchi S, Masi F, Scheggi S, Leggio B, De Montis MG, Gambarana C (2001) Long-term behavioral and neurochemical effects of chronic stress exposure in rats. *J Neurochem* 79: 1113-1121.

McEwen BS, Olie JP (2005) Neurobiology of mood, anxiety, and emotions as revealed by studies of a unique antidepressant: tianeptine. *Mol Psychiatry* 10: 525-537.

McKinney RA (2005) Physiological roles of spine motility: development, plasticity and disorders. *Biochem Soc Trans* 33: 1299-1302.

Meijer OC (2006) Understanding stress through the genome. *Stress* 9: 61-67.

Mennini T, Mocaer E, Garattini S (1987) Tianeptine, a selective enhancer of serotonin uptake in rat brain. *Naunyn Schmiedebergs Arch Pharmacol* 336: 478-482.

Miracle AD, Brace MF, Huyck KD, Singler SA, Wellman CL (2006) Chronic stress impairs recall of extinction of conditioned fear. *Neurobiol Learn Mem* 85: 213-218.

Mizoguchi K, Yuzurihara M, Ishige A, Sasaki H, Chui DH, Tabira T (2000) Chronic stress induces impairment of spatial working memory because of prefrontal dopaminergic dysfunction. *J Neurosci* 20: 1568-1574.

Mizrahi A, Libersat F (2002) Afferent input regulates the formation of distal dendritic branches. *J Comp Neurol* 452: 1-10.

Moghaddam B (1993) Stress preferentially increases extraneuronal levels of excitatory amino acids in the prefrontal cortex: comparison to hippocampus and basal ganglia. *J Neurochem* 60: 1650-1657.

Moore H, Rose HJ, Grace AA (2001) Chronic cold stress reduces the spontaneous activity of ventral tegmental dopamine neurons. *Neuropsychopharmacology* 24: 410-419.

Morgan MA, LeDoux JE (1995) Differential contribution of dorsal and ventral medial prefrontal cortex to the acquisition and extinction of conditioned fear in rats. *Behav Neurosci* 109: 681-688.

Mullen RJ, Buck CR, Smith AM (1992) NeuN, a neuronal specific nuclear protein in vertebrates. *Development* 116: 201-211.

Murmu MS, Salomon S, Biala Y, Weinstock M, Braun K, Bock J (2006) Changes of spine density and dendritic complexity in the prefrontal cortex in offspring of mothers exposed to stress during pregnancy. *Eur J Neurosci* 24: 1477-1487.

Nakayama K (2002) Diurnal rhythm in extracellular levels of 5-hydroxyindoleacetic acid in the medial prefrontal cortex of freely moving rats: an in vivo microdialysis study. *Prog Neuropsychopharmacol Biol Psychiatry* 26: 1383-1388.

Neafsey EJ (1990) Prefrontal cortical control of the autonomic nervous system: anatomical and physiological observations. *Prog Brain Res* 85: 147-165.

Neafsey EJ, Hurley-Gius KM, Arvanitis D (1986) The topographical organization of neurons in the rat medial frontal, insular and olfactory cortex projecting to the solitary nucleus, olfactory bulb, periaqueductal gray and superior colliculus. *Brain Res* 377: 561-570.

Nicholson S, Lin JH, Mahmoud S, Campbell E, Gillham B, Jones M (1985) Diurnal variations in responsiveness of the hypothalamo-pituitary-adrenocortical axis of the rat. *Neuroendocrinology* 40: 217-224.

Nimchinsky EA, Sabatini BL, Svoboda K (2002) Structure and function of dendritic spines. *Annu Rev Physiol* 64: 313-353.

Oliver C (1994) Postembedding labeling methods. *Methods Mol Biol* 34: 321-328.

Owens NC, Verberne AJ (2001) Regional haemodynamic responses to activation of the medial prefrontal cortex depressor region. *Brain Res* 919: 221-231.

Paxinos G, Watson G (1997) *The rat brain in stereotaxic coordinates*. San Diego: Academic Press.

Perez-Cruz C, Muller-Keuker J, Heilbronner U, Fuchs E, Flugge G (2007) Morphology of pyramidal neurons in the prefrontal cortex: Lateralized dendritic remodeling by chronic restraint stress. *Neural Plasticity*, in press.

Perez-Jaranay JM, Vives F (1991) Electrophysiological study of the response of medial prefrontal cortex neurons to stimulation of the basolateral nucleus of the amygdala in the rat. *Brain Res* 564: 97-101.

Pillai, A. G., Munoz, C., and Chattarji, S. The antidepressant tianeptine prevents the dendritic hypertrophy in the amygdala and increase in anxiety induced by chronic stress in the rat. *Abstract Viewer/Itinerary Planner*. 2004. Washington, DC, Society for Neurosciences.

Ref Type: Conference Proceeding

Pineyro G, Deveault L, Blier P, Dennis T, de Montigny C (1995) Effect of acute and prolonged tianeptine administration on the 5-HT transporter: electrophysiological, biochemical and radioligand binding studies in the rat brain. *Naunyn Schmiedeberg's Arch Pharmacol* 351: 111-118.

Powell DA, Watson K, Maxwell B (1994) Involvement of subdivisions of the medial prefrontal cortex in learned cardiac adjustments in rabbits. *Behav Neurosci* 108: 294-307.

Purves D, Lichtman JW (1985) Geometrical differences among homologous neurons in mammals. *Science* 228: 298-302.

Pyapali GK, Sik A, Penttonen M, Buzsaki G, Turner DA (1998) Dendritic properties of hippocampal CA1 pyramidal neurons in the rat: intracellular staining in vivo and in vitro. *J Comp Neurol* 391: 335-352.

Quirk GJ, Likhtik E, Pelletier JG, Pare D (2003) Stimulation of medial prefrontal cortex decreases the responsiveness of central amygdala output neurons. *J Neurosci* 23: 8800-8807.

Radley JJ, Morrison JH (2005) Repeated stress and structural plasticity in the brain. *Ageing Res Rev* 4: 271-287.



Radley JJ, Rocher AB, Janssen WG, Hof PR, McEwen BS, Morrison JH (2005) Reversibility of apical dendritic retraction in the rat medial prefrontal cortex following repeated stress. *Exp Neurol* 196: 199-203.

Radley JJ, Rocher AB, Miller M, Janssen WG, Liston C, Hof PR, McEwen BS, Morrison JH (2006) Repeated stress induces dendritic spine loss in the rat medial prefrontal cortex. *Cereb Cortex* 16: 313-320.

Radley JJ, Sisti HM, Hao J, Rocher AB, McCall T, Hof PR, McEwen BS, Morrison JH (2004) Chronic behavioral stress induces apical dendritic reorganization in pyramidal neurons of the medial prefrontal cortex. *Neuroscience* 125: 1-6.

Rajkowska G, Miguel-Hidalgo JJ, Wei J, Dilley G, Pittman SD, Meltzer HY, Overholser JC, Roth BL, Stockmeier CA (1999) Morphometric evidence for neuronal and glial prefrontal cell pathology in major depression. *Biol Psychiatry* 45: 1085-1098.

Ray JP, Price JL (1992) The organization of the thalamocortical connections of the mediodorsal thalamic nucleus in the rat, related to the ventral forebrain-prefrontal cortex topography. *J Comp Neurol* 323: 167-197.

Recabarren MP, Valdes JL, Farias P, Seron-Ferre M, Torrealba F (2005) Differential effects of infralimbic cortical lesions on temperature and locomotor activity responses to feeding in rats. *Neuroscience* 134: 1413-1422.

Reep RL, Goodwin GS, Corwin JV (1990) Topographic organization in the corticocortical connections of medial agranular cortex in rats. *J Comp Neurol* 294: 262-280.

Reppert SM, Weaver DR (2002) Coordination of circadian timing in mammals. *Nature* 418: 935-941.

Retana-Marquez S, Bonilla-Jaime H, Vazquez-Palacios G, Dominguez-Salazar E, Martinez-Garcia R, Velazquez-Moctezuma J (2003) Body weight gain and diurnal differences of corticosterone changes in response to acute and chronic stress in rats. *Psychoneuroendocrinology* 28: 207-227.

Ribak CE (1978) Aspinous and sparsely-spinous stellate neurons in the visual cortex of rats contain glutamic acid decarboxylase. *J Neurocytol* 7: 461-478.

Robinson RG, Kubos KL, Starr LB, Rao K, Price TR (1984) Mood disorders in stroke patients. Importance of location of lesion. *Brain* 107 ( Pt 1): 81-93.

Robinson TE, Kolb B (1997) Persistent structural modifications in nucleus accumbens and prefrontal cortex neurons produced by previous experience with amphetamine. *J Neurosci* 17: 8491-8497.

Rocher C, Spedding M, Munoz C, Jay TM (2004) Acute stress-induced changes in hippocampal/prefrontal circuits in rats: effects of antidepressants. *Cereb Cortex* 14: 224-229.

Rosenkranz JA, Grace AA (2002) Cellular mechanisms of infralimbic and prelimbic prefrontal cortical inhibition and dopaminergic modulation of basolateral amygdala neurons in vivo. *J Neurosci* 22: 324-337.

Rotenberg VS (2004) The peculiarity of the right-hemisphere function in depression: solving the paradoxes. *Prog Neuropsychopharmacol Biol Psychiatry* 28: 1-13.

Rueter LE, Jacobs BL (1996) Changes in forebrain serotonin at the light-dark transition: correlation with behaviour. *Neuroreport* 7: 1107-1111.

Rybkin II, Zhou Y, Volaufova J, Smagin GN, Ryan DH, Harris RB (1997) Effect of restraint stress on food intake and body weight is determined by time of day. *Am J Physiol* 273: R1612-R1622.

Sacchetti G, Bonini I, Waeterloos GC, Samanin R (1993) Tianeptine raises dopamine and blocks stress-induced noradrenaline release in the rat frontal cortex. *Eur J Pharmacol* 236: 171-175.

Sage D, Maurel D, Bosler O (2001) Involvement of the suprachiasmatic nucleus in diurnal ACTH and corticosterone responsiveness to stress. *Am J Physiol Endocrinol Metab* 280: E260-E269.

Schaefer AT, Larkum ME, Sakmann B, Roth A (2003) Coincidence detection in pyramidal neurons is tuned by their dendritic branching pattern. *J Neurophysiol* 89: 3143-3154.

Schiller J, Major G, Koester HJ, Schiller Y (2000) NMDA spikes in basal dendrites of cortical pyramidal neurons. *Nature* 404: 285-289.

Seib LM, Wellman CL (2003) Daily injections alter spine density in rat medial prefrontal cortex. *Neurosci Lett* 337: 29-32.

Seldon HL (1981) Structure of human auditory cortex. I. Cytoarchitectonics and dendritic distributions. *Brain Res* 229: 277-294.

Seldon HL (1982) Structure of human auditory cortex. III. Statistical analysis of dendritic trees. *Brain Res* 249: 211-221.

Selye H (1973) The evolution of the stress concept. *Am Sci* 61: 692-699.

SHOLL DA (1953) Dendritic organization in the neurons of the visual and motor cortices of the cat. *J Anat* 87: 387-406.

Simic G, Bexheti S, Kelovic Z, Kos M, Grbic K, Hof PR, Kostovic I (2005) Hemispheric asymmetry, modular variability and age-related changes in the human entorhinal cortex. *Neuroscience* 130: 911-925.

Slopsema JS, Van der GJ, de Bruin JP (1982) Regional concentrations of noradrenaline and dopamine in the frontal cortex of the rat: dopaminergic innervation of the prefrontal subareas and lateralization of prefrontal dopamine. *Brain Res* 250: 197-200.

Sousa N, Lukoyanov NV, Madeira MD, Almeida OF, Paula-Barbosa MM (2000) Reorganization of the morphology of hippocampal neurites and synapses after stress-induced damage correlates with behavioral improvement. *Neuroscience* 97: 253-266.

Stein-Behrens BA, Lin WJ, Sapolsky RM (1994) Physiological elevations of glucocorticoids potentiate glutamate accumulation in the hippocampus. *J Neurochem* 63: 596-602.

Sternberger LA, Sternberger NH (1983) Monoclonal antibodies distinguish phosphorylated and nonphosphorylated forms of neurofilaments in situ. *Proc Natl Acad Sci U S A* 80: 6126-6130.

Stewart CA, Reid IC (2000) Repeated ECS and fluoxetine administration have equivalent effects on hippocampal synaptic plasticity. *Psychopharmacology (Berl)* 148: 217-223.

Sullivan RM (2004) Hemispheric asymmetry in stress processing in rat prefrontal cortex and the role of mesocortical dopamine. *Stress* 7: 131-143.

Sullivan RM, Dufresne MM (2006) Mesocortical dopamine and HPA axis regulation: role of laterality and early environment. *Brain Res* 1076: 49-59.

Sullivan RM, Gratton A (1998) Relationships between stress-induced increases in medial prefrontal cortical dopamine and plasma corticosterone levels in rats: role of cerebral laterality. *Neuroscience* 83: 81-91.

Sullivan RM, Gratton A (1999) Lateralized effects of medial prefrontal cortex lesions on neuroendocrine and autonomic stress responses in rats. *J Neurosci* 19: 2834-2840.

Sullivan RM, Gratton A (2002) Behavioral effects of excitotoxic lesions of ventral medial prefrontal cortex in the rat are hemisphere-dependent. *Brain Res* 927: 69-79.

Terreberry RR, Neafsey EJ (1987) The rat medial frontal cortex projects directly to autonomic regions of the brainstem. *Brain Res Bull* 19: 639-649.

Thiel CM, Schwarting RK (2001) Dopaminergic lateralisation in the forebrain: relations to behavioural asymmetries and anxiety in male Wistar rats. *Neuropsychobiology* 43: 192-199.

Torrellas A, Guaza C, Borrell J, Borrell S (1981) Adrenal hormones and brain catecholamines responses to morning and afternoon immobilization stress in rats. *Physiol Behav* 26: 129-133.

Turner CA, Lewis MH (2003) Environmental enrichment: effects on stereotyped behavior and neurotrophin levels. *Physiol Behav* 80: 259-266.

Ushijima K, Morikawa T, To H, Higuchi S, Ohdo S (2006) Chronobiological disturbances with hyperthermia and hypercortisolism induced by chronic mild stress in rats. *Behav Brain Res* 173: 326-330.

Uylings HB, Groenewegen HJ, Kolb B (2003) Do rats have a prefrontal cortex? *Behav Brain Res* 146: 3-17.

Uylings HB, Jacobsen AM, Zilles K, Amunts K (2006) Left-right asymmetry in volume and number of neurons in adult Broca's area. *Cortex* 42: 652-658.

Valverde F (1968) Structural changes in the area striata of the mouse after enucleation. *Exp Brain Res* 5: 274-292.

van Eden CG, Hoorneman EM, Buijs RM, Matthijssen MA, Geffard M, Uylings HB (1987) Immunocytochemical localization of dopamine in the prefrontal cortex of the rat at the light and electron microscopical level. *Neuroscience* 22: 849-862.

Vertes RP (2004) Differential projections of the infralimbic and prelimbic cortex in the rat. *Synapse* 51: 32-58.

Vertes RP (2006) Interactions among the medial prefrontal cortex, hippocampus and midline thalamus in emotional and cognitive processing in the rat. *Neuroscience* 142: 1-20.

Vetter P, Roth A, Hausser M (2001) Propagation of action potentials in dendrites depends on dendritic morphology. *J Neurophysiol* 85: 926-937.

Vouimba RM, Munoz C, Diamond DM (2006) Differential effects of predator stress and the antidepressant tianeptine on physiological plasticity in the hippocampus and basolateral amygdala. *Stress* 9: 29-40.

Vyas A, Mitra R, Shankaranarayana Rao BS, Chattarji S (2002) Chronic stress induces contrasting patterns of dendritic remodeling in hippocampal and amygdaloid neurons. *J Neurosci* 22: 6810-6818.

Wall PM, Blanchard RJ, Yang M, Blanchard DC (2004) Differential effects of infralimbic vs. ventromedial orbital PFC lidocaine infusions in CD-1 mice on defensive responding in the mouse defense test battery and rat exposure test. *Brain Res* 1020: 73-85.

Watanabe Y, Gould E, Cameron HA, Daniels DC, McEwen BS (1992a) Phenytoin prevents stress- and corticosterone-induced atrophy of CA3 pyramidal neurons. *Hippocampus* 2: 431-435.

Watanabe Y, Gould E, Daniels DC, Cameron H, McEwen BS (1992b) Tianeptine attenuates stress-induced morphological changes in the hippocampus. *Eur J Pharmacol* 222: 157-162.

Watanabe Y, Gould E, McEwen BS (1992c) Stress induces atrophy of apical dendrites of hippocampal CA3 pyramidal neurons. *Brain Res* 588: 341-345.

Wellman CL (2001) Dendritic reorganization in pyramidal neurons in medial prefrontal cortex after chronic corticosterone administration. *J Neurobiol* 49: 245-253.

Whitton PS, Sarna GS, O'Connell MT, Curzon G (1991) The effect of the novel antidepressant tianeptine on the concentration of 5-hydroxytryptamine in rat hippocampal dialysates in vivo. *Neuropharmacology* 30: 1-4.

Wilson CJ, Groves PM, Kitai ST, Linder JC (1983) Three-dimensional structure of dendritic spines in the rat neostriatum. *J Neurosci* 3: 383-388.

Wood GE, Young LT, Reagan LP, Chen B, McEwen BS (2004) Stress-induced structural remodeling in hippocampus: prevention by lithium treatment. *Proc Natl Acad Sci U S A* 101: 3973-3978.

Wyss JM, van Groen T, Sripanidkulchai K (1990) Dendritic bundling in layer I of granular retrosplenial cortex: intracellular labeling and selectivity of innervation. *J Comp Neurol* 295: 33-42.

Yoon BW, Morillo CA, Cechetto DF, Hachinski V (1997) Cerebral hemispheric lateralization in cardiac autonomic control. *Arch Neurol* 54: 741-744.

Yuste R, Bonhoeffer T (2004) Genesis of dendritic spines: insights from ultrastructural and imaging studies. *Nat Rev Neurosci* 5: 24-34.

Zhou Q, Homma KJ, Poo MM (2004) Shrinkage of dendritic spines associated with long-term depression of hippocampal synapses. *Neuron* 44: 749-757.

Zilles K, Wree A (1995) Cortex: areal and laminar structure. In: *The rat nervous system* (Paxinos G, ed), pp 649-685. San Diego: Academic Press.

Zuo Y, Lin A, Chang P, Gan WB (2005) Development of long-term dendritic spine stability in diverse regions of cerebral cortex. *Neuron* 46: 181-189.

# 13 Curriculum vitae

## EDUCATION

- German Primate Center and Georg-August-Universität Göttingen, Germany  
Ph.D. in Systems and Cognitive Neurosciences  
Thesis: Morphological consequences of chronic stress on the pyramidal cells of the rat prefrontal cortex. Clinical Neurobiology Laboratory, German Primate Center, Göttingen, Germany.

- University of Toronto, Canada  
M.Sc. in Pharmacology and Collaborative Program in Neuroscience (Graduation Nov. 2003).  
Thesis: Anticonvulsant actions of deoxycorticosterone and its metabolites in infant rats.  
Department of Pharmacology, University of Toronto.

- National University of Mexico (UNAM), Mexico  
B.Sc. in Biological Science (Graduation July, 2000).  
Thesis: Mu-opioid receptor levels in rats treated with kainic acid at different ages.  
Neuropharmacology Laboratory CINVESTAV Sede Sur, Mexico City.

## AWARD, SCHOLARSHIPS & PRIZES

IBRO-CEER Summer School. Debrecen, Hungary  
*First prize in seminar presentation* (July 11–22, 2005)

Scholarship awarded for Ph.D. studies by National Council for Sciences and Technology (CONACyT) of the Mexican Government (Jan 2004-Dec 2006)

Visions in Pharmacology Research Symposium. University of Toronto, Canada.  
*3<sup>rd</sup> prize winner in poster presentation* (May 22, 2003)

Academic Excellence Award by the University of Toronto (Jan 2003)

Scholarship awarded for M.Sc. studies by CONACyT of the Mexican Government (Sept. 2001-Sept. 2003)

Scholarship awarded for B.Sc. studies by CONACyT of the Mexican Government (Nov. 2000-June 2001)

## INTERNATIONAL CONGRESS AND MEETINGS

7<sup>th</sup> Meeting of the German Society of Neuroscience. Göttingen, Germany (March 29 - April 02, 2007) Poster: T13-3B

28<sup>th</sup> Annual Meeting of the Society of Neuroscience, Atlanta, USA. (October 14-18, 2005) Poster: W13

27<sup>th</sup> Annual Meeting of the Society of Neuroscience, Washington D.C. USA. (November 12-16, 2005) Poster: EE10

6<sup>th</sup> Meeting of the German Society of Neuroscience. Göttingen, Germany (February 17-20, 2005) Poster: 209B

26<sup>th</sup> Annual Meeting of the Society of Neuroscience. San Diego, California, USA. (October 23-27, 2004): Attendance

25<sup>th</sup> Annual Meeting of the Society of Neuroscience. New Orleans, USA. (November 8-12, 2003)  
Poster: QQ5

Southern Ontario Neuroscience Association Meeting (SONA), London University, Ontario, Canada (July 21, 2003) Poster: 20

Visions in Pharmacology Research Symposium. University of Toronto, Canada. (May 22, 2003)  
Poster

XLIV Congress of Mexican Society of Physiological Sciences Monterrey, N.L. Mexico (August 26-30, 2001) Poster C108

24<sup>th</sup> International Epilepsy Congress, Buenos Aires, Argentina. (May 13-18, 2001) Poster E0323

## **CURRICULAR COURSES**

IBRO-CEER Summer School "Research strategies for the study of complex neural networks: From synaptic transmission to seeing the brain in action" Debrecen, Hungary (July 11–22, 2005)

"Short course in Animal Care" University of Toronto, Canada (October 2001)

"Radiation Protection Training Course" University of Toronto, Canada (March 2002)

"Actualisation in Pharmacobiology" Pre-congress course in the XLIV National Congress of Physiological Science, Monterrey, N.L. Mexico (August 26-30, 2001)

"Latin-American Course of Microdialysis and Capillar Electrophoresis", Mexican Society of Physiological Sciences, Faculty of Medicine at the National University of Mexico (UNAM) (August 28 – September 1, 2000)

## **EXTRACURRICULAR COURSES**

**German Language:** Grundstufe 1 Goethe Institute (December 2002). Toronto Canada. Grundstufe 2, Volkshochschule Göttingen, Germany (January-July 2004). Grundstufe 3, Lectorate, University of Göttingen (February- July 2005).

**English Language:** Intermediate level, London Capital College, Candem, London, England UK (September-December 1997). TOEFL 247, Essay 4.5

**French Language,** Frances Alliance, 2<sup>nd</sup> level. Col. Del Valle, México, City (June-August 1993) – Lecture Compressive Test

## LIST OF PUBLICATIONS

### Peer-review journals:

**Perez-Cruz C.**, Flugge G., Fuchs E. Effects of diurnal cycle and stress on the morphology of basal dendrites and spine densities in the prelimbic area (in preparation)

**Perez-Cruz C.**, Muller-Keuker J., Heilbronner U., Fuchs E., Flugge G. (2007) Morphology of pyramidal cells in the left and the right prefrontal cortex and sub-area specific dendritic remodeling after chronic restraint stress. *Neural Plasticity* (in press)

**Perez-Cruz C.**, Lonsdale D., Burnham W.M. (2007) Anticonvulsant actions of deoxycorticosterone in infant rats. *Brain Res* 1145: 81-89

**Perez-Cruz C.**, Burnham W.M., Likodii S. (2006) Anticonvulsant actions of deoxycorticosterone are blocked by finasteride, but not by indomethacine in 15-day-old rats" *Exp Neurol*. 200:283-289.

**Pérez-Cruz C.**, Rocha L. (2002) Kainic acid modifies mu receptor binding in young, adult and elderly rats. *Cell Mol Neurobiol* 22: 745-749.

### Books:

Burnham W.M., Lonsdale D., Shahzamani A., **Perez-Cruz C.**, Edwards H.E. (2005) Development of new anticonvulsants using the kindling model. In: Corcoran M.E., Moshe S.L. (Eds.), *Kindling* 6, Plenum Press, New York. USA. pp. 325-332.

**Perez-Cruz C.** 2003. Anticonvulsant actions of deoxycorticosterone. Thesis (M.Sc.) University of Toronto.

### Abstracts:

**Perez-Cruz C.**, Flügge G., Fuchs E. Stress induced regional and hemispheric morphological modifications of pyramidal cells in the rat prefrontal cortex. Proceedings of the 7<sup>th</sup> Meeting of the German Neuroscience Society. March 28-31, 2007. Suppl.:T13-3B

**Perez-Cruz C.**, Fuchs E. Chronic tianeptine treatment prevents stress-induced dendritic remodeling of piramidal cells in the prelimbic area of the rat. Annual Meeting Society for Neuroscience, Atlanta, USA, Oct 14-18, 2006. Poster W13

Heilbronner U., **Perez-Cruz C.**, Muller-Keuker J., Flugge G., Fuchs E. Left- right differences in pyramidal cells of the rat infralimbic area. Annual Meeting Society for Neuroscience, Washington, DC, Nov 12-16, 2005. Program No. 872.20

**Perez-Cruz C.**, Heilbronner U., Muller-Keuker J., Flugge G., Fuchs E. Boundary definition and neuronal morphology of sub-areas of the rat prefrontal cortex. Proceedings of the 6<sup>th</sup> Meeting of the German Neuroscience Society / 30<sup>th</sup> Göttingen Neurobiology Conference 2005. Eds. Zimmermann, H., Kriegstein, K. *Neuroforum* 2005, 1 Suppl.:209B

**Perez-Cruz C.**, Burhnam M.W. The anticonvulsant action of deoxycorticosterone is mediated by dihydrodeoxycorticosterone in infant rats. Annual Meeting Society for Neuroscience, New Orleans, USA. Nov 8-12, 2003



Rocha, L., **Perez-Cruz, C.**, Briones, M. Evaluation of mu receptors in rats treated with kainic acid at different ages. J. Int League against Epilepsy. 42: Suppl. 2, 2001. Abstracts from the 24<sup>th</sup> International Epilepsy Congress

**Perez-Cruz, C.**, Briones M., Rocha-Arrieta, L. Evaluacion de los niveles de receptores mu en ratas tratadas con acido kainico a diferentes edades” RESPYN (Revista de la Facultad de Salud Publica y Nutricion) Edicion Especial No. 2, 2001



Seasonal changes in a tree located in the garden of the Medical School, University of Göttingen, Germany (2006). Drawings of neurons by Ramon y Cajal (1852-1934).